CARBON FIBER REINFORCED POLYMER, LIGHT GAUGE HIGH TENSILE STEEL AND STEEL PLATE ON STRENGTHENING CONCRETE BEAMS

By
Omar M. Malkawi

Supervisor
Dr. Yasser Hunaiti, Prof

This Thesis was Submitted in Partial Fulfillment of the Requirements for the Master's Degree of Science in Civil Engineering

Faculty of Graduate Studies
The University of Jordan

April, 2011

This Thesis (Carbon Fiber Reinforced Polymer, Light Gauge Steel and Steel Plate on Strengthening Concrete Beams) was successfully defended and approved on March 10, 2011.

<u>**Examination Committee**</u>	<u>**Signature**</u>
Dr. Yasser Hunaiti (Supervisor). Prof. of Civil Engineering	....
Dr. Samih Qaqish (Member). Prof. of Civil Engineering	....
Dr. Mutasim Soud Abdel – Jaber (Member). Assoc. Prof. of Civil Engineering	....
Dr. Ghazi A. Abu – Farsakh (Member). Prof. of Civil Engineering. (Jordan University of Science and Technology).	....

ACKNOWLEDGEMENTS

I would like to thank my parents for making me believe in my dreams and supporting me to achieve my goals. I would like to extend my deepest regards to my brothers and sister for being there with me throughout.

Also, I would like to make an especial thank to my advisor Professor Yasser Hunaiti for his efforts in assisting and guiding me to complete this work.

Finally, My deepest thank goes to my friends in Saudi Arabia and United Arab Emirate for helping me by providing the carbon fiber reinforced polymer that were used to strengthen the laboratory specimens.

Table of Contents

LIST OF TABLES

LIST OF FIGURES

Figure **page**

Figure **page**

Figure **page**

Notation

A_f Area of FRP external reinforcement (mm^2).

A_s Area of nonprestressed steel reinforcement (mm^2)

A_{sp} Area of external steel plate (mm^2)

b Width of rectangular cross section (mm)

c Depth of the neutral axis (mm)

C_E Environmental-reduction factor

d Effective depth (mm)

E_c Modulus of elasticity of concrete (MPa)

E_{CFRP} Tensile modulus of elasticity of carbon fiber reinforced polymer (MPa)

E_s Modulus of elasticity of steel (MPa)

f_c Compressive stress in concrete (MPa)

f_{CFRP} Stress in the CFRP reinforcemen (MPa)

f_{fu}* Ultimate tensile strength of the CFRP material as reported by manufacture (MPa)

f_s Stress in non pre stressed steel reinforcement (MPa)

$f_{s,s}$ Stress level in non pre stressed steel reinforcement at service loads (MPa)

f_y Yield strength of non pre stressed steel reinforcement (MPa)

h Overall depth of a beam (mm)

I_{cr} Moment of inertia of cracked concrete section (mm^4)

I_g Moment of inertia of gross concrete section (mm^4)

k Ratio of the depth of the neutral axis to the effective depth

L Clear span (mm)

M_{cr} Cracking moment (N-mm)

M_n Nominal moment strength (N-mm)

Mu Ultimate unit resisting moment (N-mm)

n Number of plies of CFRP external strengthening material

R_n Nominal strength of a member

t_f Thickness of one ply of the FRP reinforcement (mm)

β Ratio of the depth of the equivalent rectangular stress block to the depth of the neutral axis

ε_{bi} Initial strain in the CFRP due to dead load (mm/mm)

ε_c Stain level in the concrete (mm/mm)

ε_{cu} Compressive strain of concrete (mm/mm)

ε_{CFRP} Strain in the CFRP (mm/mm)

ε_{fu} Design rupture strain of CFRP (mm/mm)

$\varepsilon_{fu}*$ Ultimate rupture strain of the CFRP (mm/mm)

ε_s Strain in the nonprestessed steel reinforcement (mm/mm)

ε_{sy} Strain yield of nonprestressed steel reinforcement (mm/mm)

ϕ Strength reduction factor

κ_m Bond-dependent coefficient for flexure

ρ_s Ratio of nonprestressed reinforcement

ψ_f Additional CFRP strength-reduction factor

CARBON FIBER REINFORCED POLYMER, LIGHT GAUGE HIGH TENSILE STEEL AND STEEL PLATE ON STRENGTHENING CONCRETE BEAMS

By
Omar M. Malkawi

Supervisor
Dr. Yasser Hunaiti, Prof

ABSTRACT

Strengthening structures is still challenge. To overcome this problem different external composite materials are used. The purpose of this research was to investigate the performance of three different external composite materials (carbon fiber reinforced polymer, light gauge high tensile steel and steel plate) in strengthening reinforced concrete beams and to improve and develop designing procedures of strengthening system. Fifteen rectangular reinforced concrete beams dividing into four different groups. The first group contains two rectangular reinforced concrete beams without strengthening material used as control beams. The second group contains five rectangular concrete beams strengthened by two types of carbon fiber reinforced polymer laminates and wrap. The third group contains four rectangular beams strengthened by light gauge high tensile steel. The last group has four rectangular beams strengthened by steel plate. The carbon fiber reinforced polymer laminate system was a sufficient material for increasing the flexural capacity of reinforced concrete beams (high strength-to-weight ratio).

Keywords Beams, Strengthen, CFRP, Light Gauge High Tensile Steel, Steel Plate

Chapter 1 Introduction

1.1 General

The traditional material used in the strengthening of structure is steel because of low resistance corrosion, large size and large weight there is a need to develop economic and efficient method to strengthen existing reinforced concrete. The motivation to strengthen an existing reinforced concrete comes from two sources: increase the strength of existing reinforced concrete elements to prevent failure from additional weight on the design and repair deterioration that has taken place over the years of operation.

An alternative to reinforced concrete replacement is strengthening using well-established methods. Casting additional elements, increasing cross-section size, and bonding steel plates are techniques that have been used in the past. These solutions can be expensive and difficult to implement, therefore our goal is developing economic and efficient methods to strengthen existing reinforced concrete [Foster DC 2000].

The use of Carbon Fiber Reinforced Polymer (CFRP) composite materials in the repair and retrofit of concrete elements increased flexural and shear capacity of elements. Moreover increased the ductility and stiffness. To reduce the deflection under service loads the CFRP materials were identified as a possible alternative material on strengthening reinforced concrete elements.

1.2 Objectives

The objective of this research is to investigate the effectiveness of different composite materials to strengthen reinforced concrete beams. This general goal is divided into three distinct aims. Firstly, the thesis aims to clarify strengthening of reinforced concrete beams by three different external composite materials (carbon fiber reinforced polymer, light gauge high tensile steel and steel plate). Secondly, the thesis aims at studying stress strain diagram for strengthening reinforced concrete beams to evaluate the behavior of the materials under applied load. Finally, the thesis aims to present flexural design guidelines (ultimate and serviceability) for strengthening reinforced concrete beams.

1.3 Thesis Layouts

This work is organized into six main chapters. Chapter 1 is the introduction, which provides a brief introduction and objective of this work. Chapter 2 of this work provides a discussion of the material necessary for the study of FRP bond in the flexural retrofit and a literature review of relevant material. Chapter 3 presents more details on the mechanical and material properties of Carbon Fiber Reinforced Polymer, light gauge high tensile steel and adhesive material in addition to concrete and steel reinforcement. Chapter 4 gives theoretical design and guidelines for structural reinforced concrete strengthened by different groups of composite materials. Chapter 5 presents the description of the laboratory tests of beams strengthened by carbon fiber reinforced polymer, light gauge high tensile steel and steel plates and discussion of the failure sequence of different groups of strengthened beams. Chapter 6 covers a summary, conclusion and recommendations for the results of theoretical and experimental results.

Chapter 2 Literature review

2.1 Introduction

A structural member is strengthened when the strength or stiffness of the existing member is insufficient, whether from increased traffic loads or errors in construction.

The use of carbon fiber reinforced polymer (CFRP) materials is needed for deteriorated or damaged structures to recover their strength and serviceability and to extend their service life depending on structural types (flexural, shear, or compression members) [Han Tae Choi 2008]. In this thesis, literature review of CFRP strengthened members are discussed focusing on the flexural strengthening of reinforced concrete (RC) members.

2.2 Historical Background

The concept of composite materials can be traced back to the use of straw as reinforcement in bricks used by ancient civilizations (e.g. Egyptians in 800 B. C.) [Tang 1997]. Recently in the United States, short glass fiber reinforcement was used in the early 1930's to reinforce concrete. FRPs are the latest version of this very old idea of making better composite material by combining two different materials [Nanni 1999].

The development of FRP reinforcement can be found in the expanded use of composites after World War II: the automotive industry first introduced composites in early 1950's and since then many components of today's vehicles are being made out of composites. The aerospace industry began to use FRP composites as lightweight material with acceptable strength and stiffness which reduced the weight of aircraft structures , pressure vessels and containers.

In civil engineering, the use of composites is only beginning to gain acceptance because composite materials have not been economically competitive with traditional building materials such as steel or concrete [ASCE, 1984]. The use of these materials for the repair and strengthening of the aging infrastructure provides an interesting alternative to traditional methods, because of their high strength-to-weight ratio, corrosion resistance, and excellent fatigue performance.

2.3 Flexural Strengthening

The main concept of flexural strengthening is to improve the strength and stiffness of concrete flexural members by adding reinforcement to the concrete tensile surface. Traditionally, steel reinforcement has been widely used as a strengthening material. For example, section enlargement using steel reinforced concrete as shown in Figure 2.1. Steel plate bonding as shown in Figure 2.2, and external steel post-tensioning technique Figure 2.3 have been widely applied. Recently, flexural strengthening by fiber reinforced polymer material (FRP) Figure 2.4 has been investigated and applied because of its many advantages compared to steel reinforcement.



Figure 2.1 Steel reinforcment


Figure 2.2 Steel plate bonding

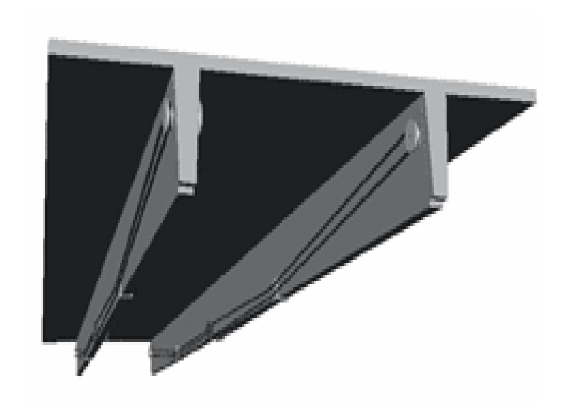

Figure 2.3 External steel post-tensioning


Figure 2.4 External FRP

2.4 Experimental studies

2.4.1 Mohd Zamin Jumaat and Ashraful Alam (2008).

Experimental studies involving strengthening of R.C. beams using externally bonded plates and anchorages. The research consisted of five rectangular beams. All beams had span length of 2000mm and cross sectional dimensions of 125X250mm.

The different external composite materials and test results are summarized in Table 2.1 and Table 2.2.

Table 2.1 External composite materials

Serial No	Specimen	Strengthening Materials			Anchor	
		Type	Thickness (mm)	Width (mm)	End(200 mm)	Intermediate (40 mm @110 mm c/c)
1	A1	-----	-------	------	---------	
2	B1	Steel Plate	2.73	73		
3	B4	Steel Plate	2.73	73	L shape	L shape
4	C1	CFRP	1.2	80		
5	C4	CFRP	1.2	80	L shape	L shape

Table 2.2 Test results

Specimen	1st Crack Load in kN (% Increase over control)	Failure Load in kN (% Increase over control)	Failure mode
A1	14	80.59	*Flexural*
B1	35 (150)	104.3 (29)	*Debonding*
B4	35 (150)	125.4 (56)	*Flexural*
C1	27 (93)	123.9 (54)	*Debonding*
C4	25 (79)	157.8 (96)	*Concrete compression*

2.4.2 O. Gunes, E. Karaca, and B. Gunes (2006).

Design of FRP retrofitted flexural members against debonding failures were investigated by O. Gunes, E. Karaca, and B. Gunes (2006).

The geometry and reinforcement details of the control specimen (CM1) is shown in Figure 2-5 and the strengthening configurations of the tested beams are shown in Figure 2-6.All specimens shown in this figures were strengthened with 1270 mm long, 38.1 mm wide, and 1.2 mm thick FRP plates. For FRP shear strengthening, 40-mm wide straight and L-shaped plates were used. For comparison with external shear strengthening, the shear capacity of a beam was increased through larger internal shear reinforcement (see beam S2PF7M in Figure 2-6).

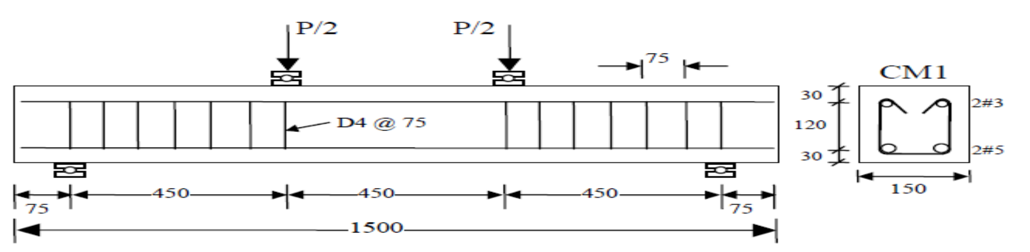


Figure 2-5 Control specimen

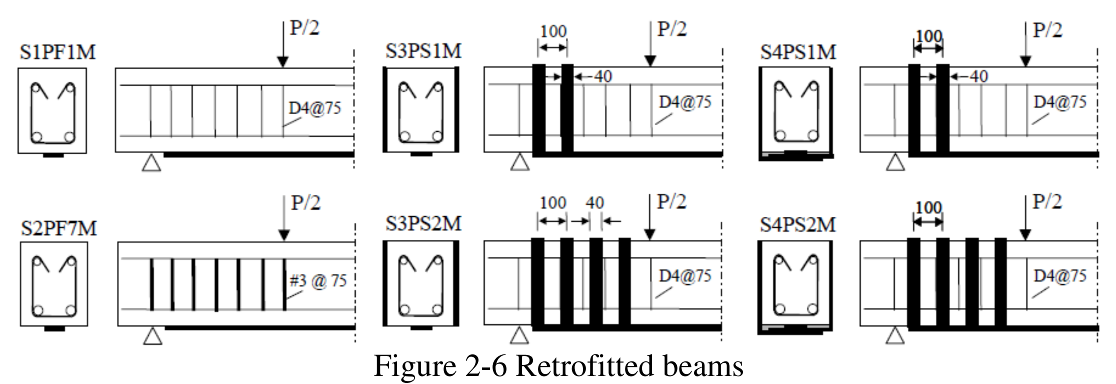


Figure 2-6 Retrofitted beams

Table 2-3 Properties of materials

Material	Compressive strength (MPa)	Yield strength (MPa)	Tensile strength (MPa)	Tensile modulus (MPa)	Ult. tensile strain (%)
Concrete	41.4	-	-	-	-
#3 and #5 rebars	-	440	-	200,000	-
D4 deformed bars	-	620	-	200,000	-
CFRP plate	-	-	2800.0	165,000	1.69
Epoxy adhesive	-	-	24.8	4,482	1.00

The Figure 2-7 showed the experimental load - deflection of control and retrofitted beams.

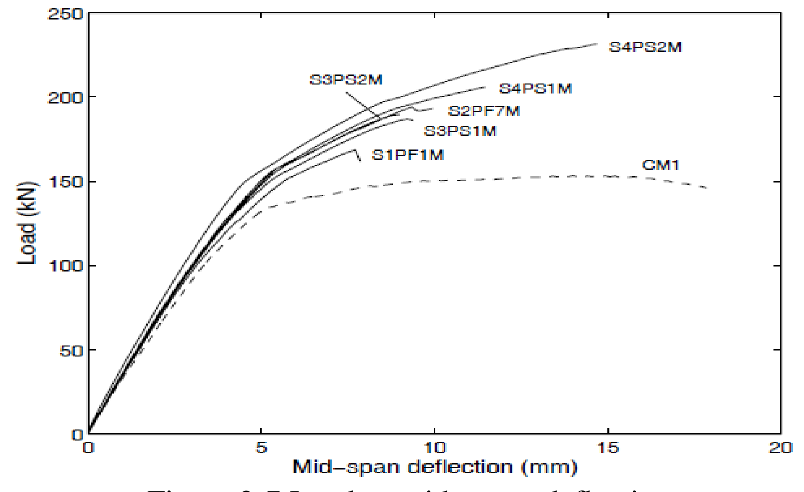


Figure 2-7 Load vs mid - span deflection

2.5 Fiber reinforced polymer

2.5.1 Properties of FRP

The mechanical properties of FRP bars are typically quite different from those of steel bars and depend mainly on both matrix and fibers type, as well as their volume fraction. Generally FRP bars have lower weight, lower Young's modulus but higher strength than steel. The most commonly available fiber types are the carbon (CFRP), glass (GFRP) and aramid (AFRP) fibers.

Fibers

The composite materials properties are mainly influenced by the choice of fibers and matrix. In civil engineering, three types of fibers dominate. These are carbon, glass, and aramid fibers and the composite is often named by the reinforcing fiber, e.g. CFRP for Carbon Fiber Reinforced Polymer. They have different properties and have different prices, which make one more suitable than the other for different purposes.

For strengthening purposes carbon composites are the most suitable. All fibers have generally higher stress capacity than ordinary steel and are linear elastic until failure. The most important properties that differ between the fiber types are strength, stiffness and ultimate strains.

Carbon

Carbon fibers have a high modulus of elasticity, 200 – 800 GPa. The ultimate elongation is (0.3 - 2.5) % where the lower elongation corresponds to the higher stiffness.

Carbon fibers do not absorb water and are resistant to many chemical solutions. They withstand fatigue properly, do not stress corrode and don't show any creep or relaxation. Moreover, they have less relaxation compared to low relaxation of high tensile pre stressing steel strands. Carbon fibers are electrically conductive and, therefore, might give galvanic corrosion in direct contact with steel.

The types of carbon fibers are as follows:

- **UHM** (ultra high modulus): Modulus of elasticity > (450GPa).
- **HM** (high modulus): Modulus of elasticity is in the range (350-450GPa).
- **IM** (intermediate modulus): Modulus of elasticity is in the range (200-350GPa).
- **HT** (high tensile, low modulus). Tensile strength > (3 GPa) and modulus of elasticity < (100 GPa).
- **SHT** (super high tensile). Tensile strength > (4.5GPa) and modulus of elasticity < (100 GPa).

Table (2.4) Advantages and Disadvantages of FRP Reinforcement [Anders (2003)]

Advantages of FRP Reinforcement	**Disadvantages of FRP reinforcement**
High longitudinal tensile strength	No yielding before brittle rupture
Corrosion resistance	Low modulus of elasticity
Lightweight (1/5 to 1/4 density of steel)	Low transverse strength
Nonmagnetic	High coefficient of thermal expansion
High fatigue endurance	

One of the earliest research programs that investigated the use of CFRP composites to strengthen reinforced concrete elements was conducted at the Swiss Federal Institute of Technology [Meier et al., 1992]. In the late 1980s bridges that had been strengthened using steel plates were showing signs of corrosion after only a few years in service. Alternatively carbon fiber composites were selected instead of steel plates. A qualitative

comparison of the performance of carbon, glass, and aramid composites is presented in Table 2.2 [Meier and Winistörfer, 1995].

Table (2.5) Qualitative Comparison of Various Fibers used in Composites [Meier and Winistörfer, 1995].

	CFRP	GFRP	AFRP
Tensile strength	Very good	Very good	Very good
Compressive strength	Very good	Inadequate	Good
Young's Modulus	Very good	Good	Adequate
Long – term behavior	Very good	Good	Adequate
Fatigue behavior	Excellent	Good	Adequate
Bulk Density	Good	Excellent	Adequate
Alkaline resistance	Very good	Good	Inadequate
Price	Adequate	Adequate	Very good

2.6 Debonding

Failures in FRP-strengthened reinforced concrete (RC) members may occur by flexural failures of critical sections, such as FRP rupture and crushing of compressive concrete, or by debonding of FRP plate from the RC beams. Debonding in FRP strengthened RC members occurs in regions of high stress concentrations, which are often associated with material discontinuities and with the presence of cracks [Gunes, 2004].

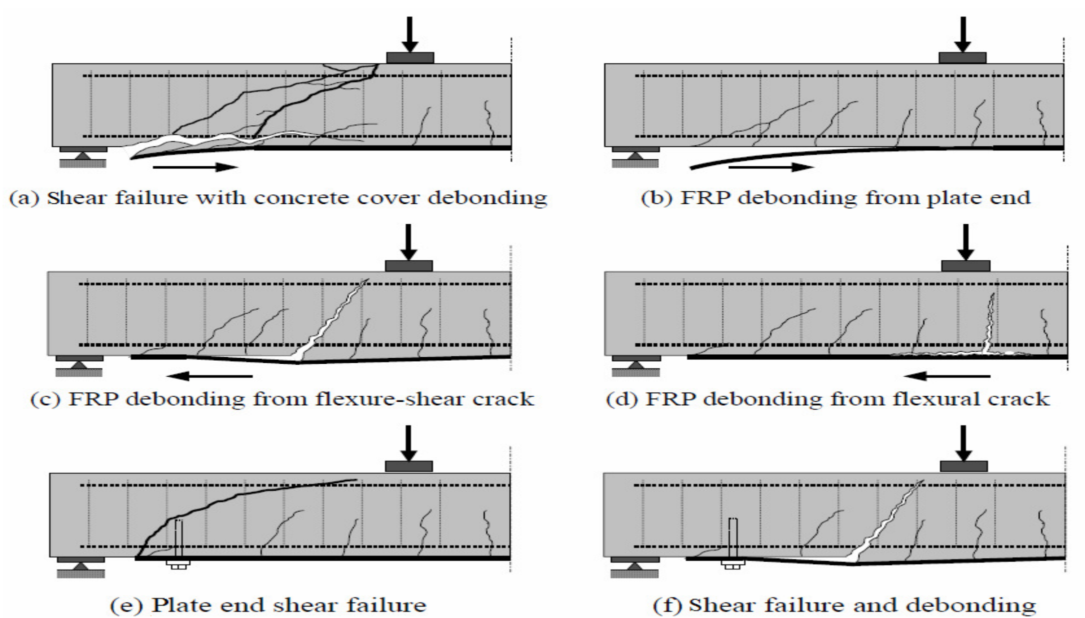


Figure 2.8 Debonding failure mechanisms [Gunes, 2004].

Chapter 3 Materials

3.1 Concrete

The concrete was prepared by a ready mix plant. The specified 28-day compressive strength of concrete was 25.3 MPa as the average of concrete cylinders.



Figure 3.1 Beams specimens formwork prior to placing concrete.



Figure 3.2 Concrete Casting.



Figure 3.3 Finished set of beams.

3.2 Reinforcing steel

Because concrete is weak in tension the bars are placed near their tension faces. The yield strength of steel bars used in this experimental program was determined by performing the tensile test on two specimens of each bar diameter. The average tensile strength of steel bars was found to be 415 MPa for both Φ12 and Φ 10 mm bars.



Figure 3.4 Steel Reinforcement.

3.3 Carbon fiber reinforced polymer

- **Sika CarboDur S512/80**



Figure 3.5 Carbon fiber reinforced polymer(S512/80).

- **V-Wrap C100 high strength Carbon Fiber**



Figure 3.6 Carbon fiber wrap (C 100).

Mechanical / Physical Properties of material

Table (3.1) Properties of Reinforcing CFRP Sheets

Type	Width (mm)	Thickness (mm)	Cross sectional area (mm^2)	Density
Sika S512/80	50	1.20	60	1.6 g/cm^3
V-Wrap C100	-	0.65	-	0.462 g/cm^3

Type	E-modulus	Tensile strength	Strain%
Sika S512/80	165GPa	3100MPa	0.85
V-Wrap C100	38.6GPa	650MPa	1.68

3.4 Light-Gauge Steel (G 550) - Thin sheets of galvanized 0.89 mm thickness (to prevent oxidation and corrosion) with tensile strength 550 MPa

Advantages

Strength-to-Weight ratio is defined as the relationship between a material strength and its weight. Also, known as specific strength, it is the material's strength, which is defined as the force per unit area at failure, divided by its density. Materials that are light but are also very strong have a high strength-to-weight ratio.

Thermal conductivity is defined as the ability of a material to conduct heat. The formula is Fourier's Law, which is defined as the quantity of heat transmitted during time through a thickness of material in a direction normal to the surface area due to a temperature difference under a steady state of conditions and when the heat transfer is dependent only on the temperature gradient.

Light gauge steel framing generates minimal waste. All light gauge steel construction materials are 100% recyclable.



Figure 3.7 Light gauge high tensile steel

3.5 Adhesives

The selection of adhesive material depends on many properties such as strength, elastic modulus and elongation percentage. The adhesive materials are commonly used as concrete epoxies. The selection of an epoxy type is to be used in a particular application is governed by various factors including the environment and the required speed of fabrication. In this research, the adhesives materials are concresive 2200 and concresive 1414.

Concresive 2200 is anon slumping epoxy bedding compound and adhesive. It is a two pack fine aggregate filled fast curing material ideal for a variety of bedding, gap filling and concrete repair applications.





Figure 3.8 Concrete epoxy

Typical Properties

Table (3.2) Properties of Concrete Epoxy (concresive 2200)

Property	Concresive 2200
Mixed density @ 25° C	1700 kg/m³
Compressive Strength @ 7days	60 MPa
Pot life 25° C	1 hour 45 minutes

Application procedure

- Mixing 3 kg pack has been designed to be readily mixed by a trowel
- Knife or trowel concresive 2200 to the required level using the minimum solvent on the trowel to aid workability
- The surface finished smoothly by using a paint brush

Concresive 1414 is a permanent epoxy adhesive for internal or external bonding of renderings, granolithic toppings and concrete to concrete.

Typical Properties

Table (3.3) Properties of Concrete Epoxy (concresive 1414)

Property	Concresive 1414
Mixed density @ 25° C	1485 kg/m³
Compressive Strength @ 7days	60 MPa
Pot life 25° C	2 hours

Application procedure

- Carefully transfer the entire contents of the smaller container of concresive 1414 reactor component to the larger concresive 1414 base component tin and thoroughly mix.
- Using a stout palette knife with a paint mixing paddle until uniformity is achieved.

Chapter 4 Theoretical Studies

4.1 Design Guidelines

The American Concrete Institute (ACI 440) design guidelines for structural concrete reinforced with FRP Bars (ACI 440.1R-06, 2006) are primarily based on modifications of the ACI-318 steel code of practice (ACI 318-02, 2002).

The ACI 440.1R design philosophy is based on the concept that “the brittle behavior of both CFRP reinforcement and concrete allows consideration to be given to either CFRP rupture or concrete crushing as the mechanisms that control failure so the margin of safety suggested by this guide against failure is therefore higher than that used in traditional steel reinforced concrete design".

4.2 Basis of Design of Strengthening RC Beam

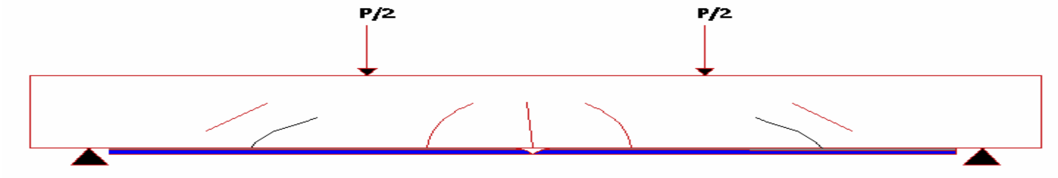
This research provides the necessary guidance to carry out the design of CFRP, Steel Plate and Light Gauge High Tensile Steel Plate strengthening system for concrete structures.

1) The design of concrete structures strengthening using all systems above should satisfy strength and serviceability requirement.
2) Special care is required in the case of structural analysis where almost complete lack of ductility of the CFRP shall be taken into account.
3) Specific fire resistance analysis of the structural elements will be performed according to fire regulations.

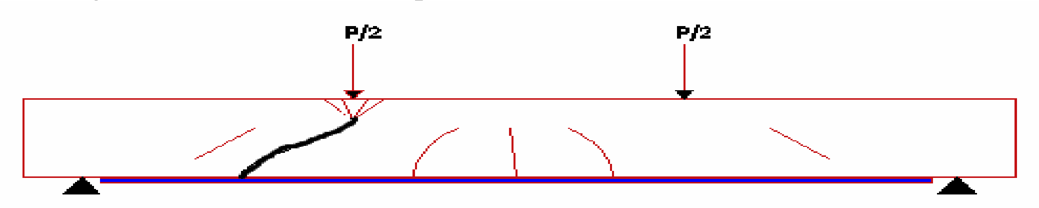
4.3 Failure Modes

Normally five flexural failure modes are possible with externally strengthened reinforced concrete beams:

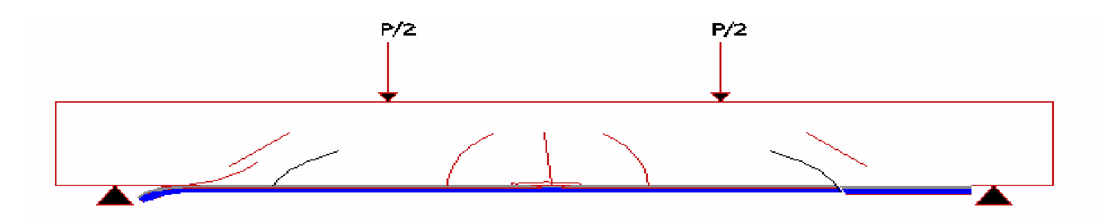
1) Rupture of the strengthening material on the bottom of the beam.



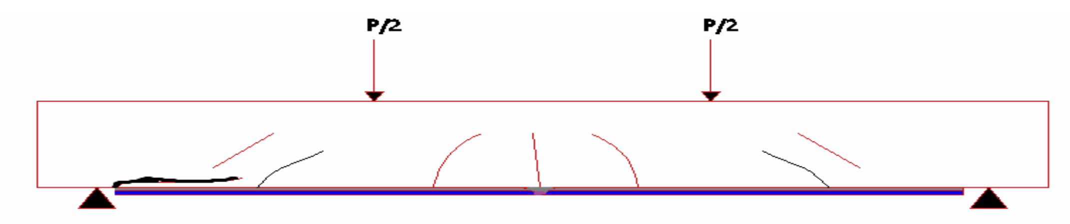
2) Crushing of the concrete at the top of the beam.



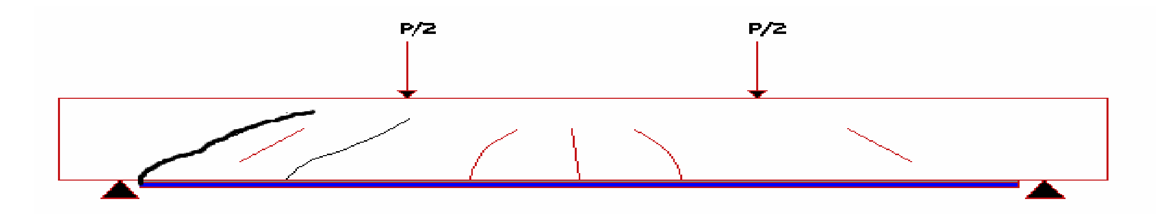
3) Debonding of the strengthening material from the concrete (end, shear crack and flexural crack).



4) Shear/tension delimitation of the concrete cover (cover delimitation).



5) Plate end shear failure



4.4 Recommendations of Design of FRP Systems

American Concrete Institute (ACI) Committee 440 has developed guide specifications for the design and construction of externally bonded FRP systems [ACI 440.2R-02].

To prevent debonding of FRP recommended limiting the strain in the FRP by multiplying the rupture strain of the FRP fabric (ε_{fu}) with a bond-dependent factor(K_m) as given by Equation 4.1:

Where
ε_{fu} is the FRP design rupture strain
K_m is:

$$K_m = \begin{cases} \frac{1}{60\varepsilon_{fu}}\left(1 - \frac{n\,E_f\,t_f}{360{,}000}\right) \leq 0.9 & \text{for } n\,E_f\,t_f \leq 180{,}000 \text{ N/mm} \\ \frac{1}{60\varepsilon_{fu}}\left(1 - \frac{90{,}000}{n\,E_f\,t_f}\right) \leq 0.9 & \text{for } n\,E_f\,t_f > 180{,}000 \text{ N/mm} \end{cases} \quad (4.1)$$

The design ultimate strength (f_{fu}) and rupture strain (ε_{fu}) are obtained by the product of the corresponding ultimate tensile strength (f_{fu}*) and strain (ε_{fu}*) of the FRP material as reported by the manufacturer with appropriate environmental reduction factors (C_E) suggested by ACI 440.2R-02.

$$f_{fu} = C_E\, f_{fu}^{*} \quad (4.2)$$

$$\varepsilon_{fu} = C_E\, \varepsilon_{fu}^{*} \quad (4.3)$$

$$E_f = \frac{f_{fu}}{\varepsilon_{fu*}} \quad (4.4)$$

Environmental reduction factors (C_E) for different environmental exposure conditions are shown in Table 4.1 [ACI 440 -02 Table 8.1].

Environmental reduction factor (C_E) for different FRP

Table (4.1) Environmental Reduction Factor (C_E)

Exposure Condition	Fiber and Resin Type	Environmental Reduction
Interior exposure	Carbon / epoxy	0.95
	Glass / epoxy	0.75
	Aramid / epoxy	0.85
Exterior exposure	Carbon / epoxy	0.85
	Glass / epoxy	0.65
	Aramid / epoxy	0.75
Aggressive environment	Carbon / epoxy	0.85
	Glass / epoxy	0.5
	Aramid / epoxy	0.7

4.5 Strain and Stress in CFRP

The maximum strain or the effective strain (ε_{fe}) in the CFRP at the ultimate can be determined from Equation

$$\varepsilon_{fe} = \varepsilon_{cu} \frac{(h-c)}{c} - \varepsilon_{bi} \leq K_m \ \varepsilon_{fu} \qquad (4.5)$$

Where
ε_{bi} is the initial substrate strain in CFRP due to dead load

$$f_{fe} = E_f \varepsilon_{fe}$$

4.6 Flexural Forces in CFRP Strengthened Beams

Idealized strain and stress distributions in a CFRP strengthened concrete beams and the force equilibrium at ultimate load conditions are shown in Figure 4.1.

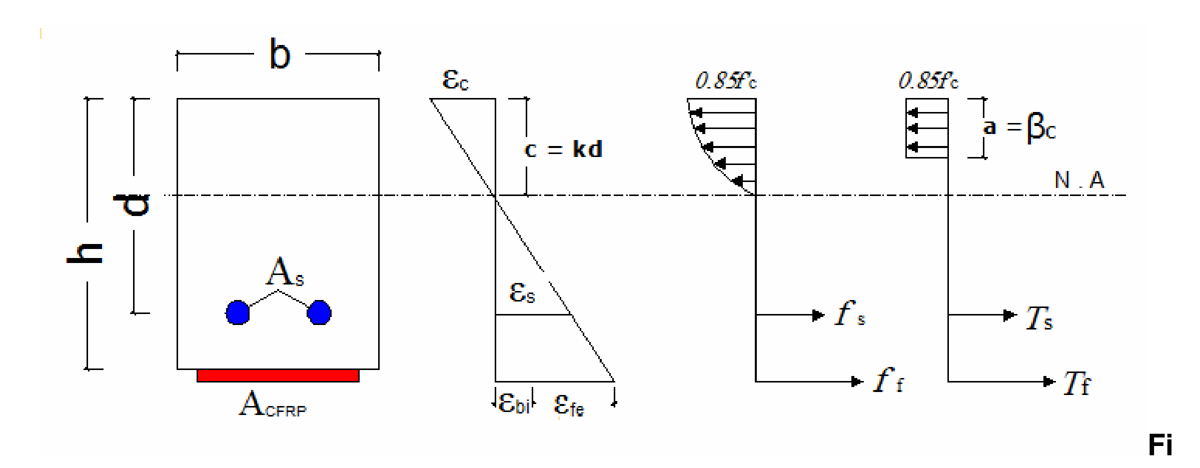


Figure 4.1 Strain distribution and force equilibrium conditions for beam strengthened by CFRP at the ultimate load conditions in a reinforced concrete beam with CFRP (a) beam cross-section, (b) strain distribution, (c) Nonlinear stress distribution, and (d) Stress distribution equivalent.

4.7 Flexural Strain and Stress in CFRP Strengthened Beams

The fundamental assumptions made in deriving the nominal strength of CFRP strengthened beam are the same as those for conventional concrete beams [MacGregor and ACI 318].

The strain distribution is assumed linear and the stress distribution is assumed uniform over the compression zone of concrete. And due to additional CFRP the following assumption are made:

1- No relative slip or deformation exists between the CFRP and concrete substrate to which it is bonded.
2- CFRP follows a linear stress strain relation up to failure.

The derivation of moment capacities of CFRP beams is based on satisfying two basic conditions: the static equilibrium of forces in concrete, steel, and CFRP and the compatibility of strains in concrete, steel, and CFRP.

The maximum usable strain in concrete is assumed to be 0.003 ($\varepsilon_c = \varepsilon_{cu} = 0.003$). The strain in steel reinforcement at yield is based on Hooke's law, i.e., the yield stress f_y of the reinforcing steel is equal to E_s times the steel yield strain, where E_s is the modulus of elasticity of steel. Assuming E_s = 204 GPa, the following values of yield strains are obtained for Grade 40 and Grade 60 reinforcement:

- **Grade 40 (280MPa) reinforcement**

$$\varepsilon_y = f_y / E_s = 280/204{,}000 = 0.0014 \tag{4.6}$$

- **Grade 60 (420MPa) reinforcement**

$$\varepsilon_y = f_y / E_s = 420/204{,}000 = 0.0021 \tag{4.7}$$

For design purposes, the maximum (ultimate) tensile stress in a conventional reinforced beam corresponds to steel yield strain value, whereas for a CFRP strengthened beam, the maximum tensile stress corresponds to CFRP rupture strain.

Carbon fiber fabric (rupture) ($\varepsilon_{cfrp} = \varepsilon_{cfrpu} \approx (0.01\text{-}0.015)$).

Strain Compatibility

Referring to similar triangles in Figure 4.2, the following relations are established:

$$\frac{\varepsilon_c}{c} = \frac{\varepsilon_s}{(d - c)} = \frac{\varepsilon_f}{(h - c)} \tag{4.8}$$

Force Equilibrium

The compressive force in concrete (**C_c**) is

$$C_c = 0.85\, f'_c ab \tag{4.9}$$

The tensile force in steel ($\mathbf{T}_s$) is

$T_s = A_s f_s = A_s E_s \varepsilon_s$ (before steel yielding, $\varepsilon_s < \varepsilon_y$) (4.10)

$T_s = A_s f_y = A_s E_s \varepsilon_y$ (after steel yielding, $\varepsilon_s \geq \varepsilon_y$) (4.11)

The tensile force in CFRP (T_{cfrp}) before or at rupture ($\varepsilon_{cfrp} < \varepsilon_{cfrpu}$) is

$T_{cfrp} = A_{cfrp} f_{cfrp} = A_{cfrp} E_{cfrp} \varepsilon_{cfrp}$ (4.12)

The tensile force in CFRP ($\mathbf{T}_{cfrp}$) after rupture

$$\mathbf{T}_{cfrp} = 0 \quad (4.13)$$

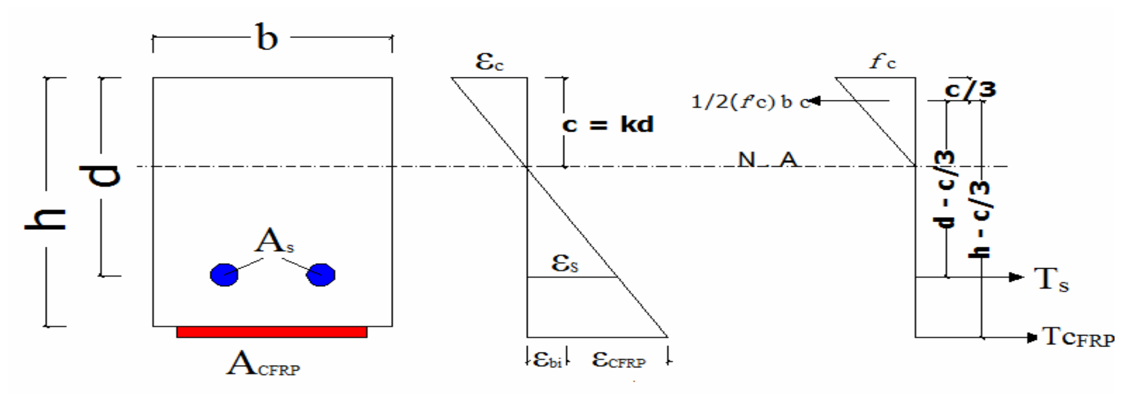


Figure 4.2 Strain distribution and force equilibrium at the service loads for beam strengthened by CFRP

Neutral axis factor (k) without CFRP is given as:

$$k = \sqrt{(\rho_s n_s)^2 + 2(\rho_s n_s)} - (\rho_s n_s) \quad (4.14)$$

Neutral Axis Factor (k) with CFRP :

$f_s = E_s \varepsilon_s$ $f_{cfrp} = E_{cfrp} \varepsilon_{cfrp}$ $f_c = E_c \varepsilon_c$ (4.15)

From equilibrium of forces:

$$A_s f_s + A_{cfrp} f_{cfrp} = \frac{(b \text{X} c)}{c} (f_c)$$

$$A_s (E_s \varepsilon_s) + A_{cfrp} (E_{cfrp} \varepsilon_{cfrp}) = \frac{(b X c)}{c} E_c \varepsilon_c \quad (4.16a)$$

From compatibility equation

$$\varepsilon_s = \varepsilon_c \frac{(d-c)}{c} \quad (4.17)$$

$$\varepsilon_{cfrp} = \varepsilon_c \frac{(h-c)}{c} \quad (4.18)$$

Substitute Equation (4.17) and (4.18) in Equation (4.16a)

$$A_s (E_s \varepsilon_c \frac{(d-c)}{c}) + A_{cfrp} (E_{cfrp} \varepsilon_c \frac{(h-c)}{c}) = \frac{(b X c)}{c} E_c \varepsilon_c \quad (4.16b)$$

Dividing equation (4.16b) by ε_c

$$A_s (E_s \frac{(d-c)}{c}) + A_{cfrp} (E_{cfrp} \frac{(h-c)}{c}) = \frac{(b X c)}{c} (E_c) \quad (4.16c)$$

Simplify the Equation 4.16c

$$A_s (E_s (d-c)) + A_{cfrp} (E_{cfrp} (h-c)) = \frac{(b X c^2)}{2} E_c \quad (4.16d)$$

$$A_s \frac{E_s}{E_c} (d-c) + A_{cfrp} \frac{E_{cfrp}}{E_c} (h-c) = \frac{(b X c^2)}{2} \quad (4.16e)$$

Substitute $\frac{E_s}{E_c} = n_s$ & $\frac{E_f}{E_c} = n_f$ in Equation 4.16e

$$A_s (n_s (d-c)) + A_{cfrp} (n_{cfrp} (h-c)) = \frac{(b X c^2)}{2} \quad (4.16f)$$

$$2 \frac{A_s}{b X d} (n_s (d-c)) + 2 \frac{A_{cfrp}}{b X d} (n_f (h-c)) = \frac{c^2}{d} \quad (4.17g)$$

Rearrange Equation by substitute $\frac{A_s}{b X d} = \rho_s$ and $\frac{A_{cfrp}}{b X d} = \rho_f$

$$2 \rho_s (n_s (d-c)) + 2 \rho_{cfrp} (n_{cfrp} (h-c)) = \frac{c^2}{d} \quad (4.17h)$$

Rearrange various terms in Equation

$$\frac{c^2}{d} + 2 (\rho_s n_s + \rho_{cfrp} n_{cfrp}) c - 2 (\rho_s n_s d + \rho_{cfrp} n_{cfrp} h) = 0 \quad (4.18i)$$

Solving quadratic Equation c = kd

$$k = \sqrt{\left(\rho_s n_s + \rho_{cfrp} n_{cfrp}\right)^2 + 2(\rho_s n_s + \rho_{cfrp} n_{cfrp} \frac{h}{d})} - (\rho_s n_s + \rho_{cfrp} n_{cfrp}) \qquad (4.19)$$

4.8 Nominal Moment Capacity

Based on the new definitions of flexural behavior cases [ACI 318-02 Section 10.3.2 through 10.3.5] and [ACI 440-02] five different failure modes controlled nominal flexural strength in terms of stresses and strains in concrete, steel, and CFRP as following :-

1- Tension controlled failure without CFRP rupture

2- Tension controlled failure with CFRP rupture

3- Tension and compression controlled failure with steel yielding

4- Compression controlled failure without steel yielding and without CFRP rupture

5- Balanced failure

4.8.1 Tension controlled failure without CFRP rupture

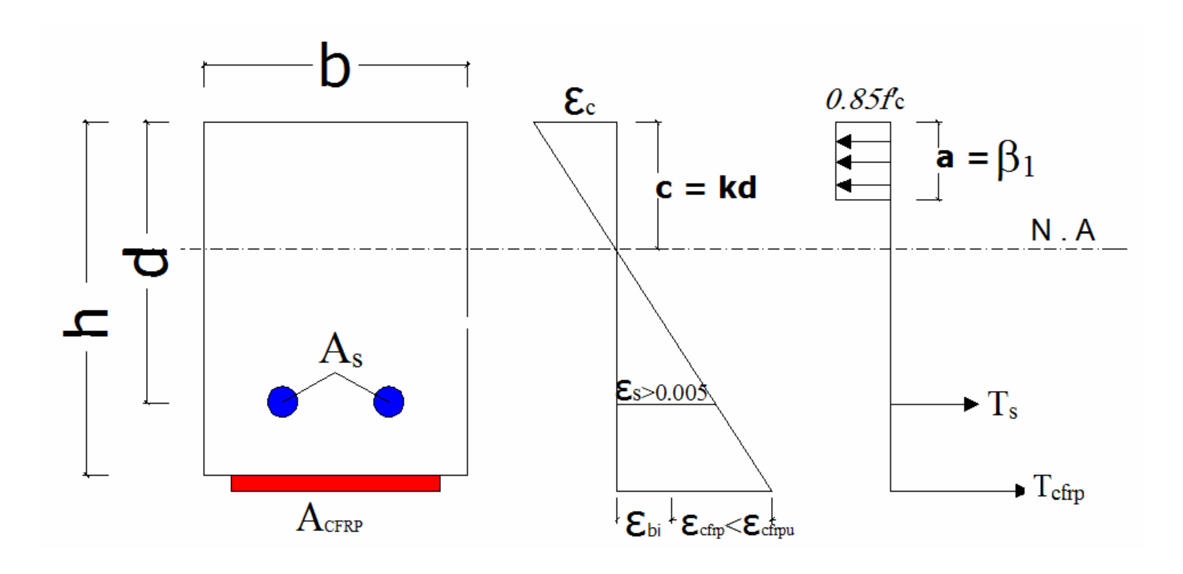


Figure 4.3 Force distribution in a tension controlled failure without CFRP rupture

Tension-controlled failure without CFRP rupture means steel yielding ($\varepsilon_s \geq 0.005$) without CFRP rupture ($\varepsilon_{cfrp} < \varepsilon_{cfrpu}$) this failure mode eventually leads to crushing of the concrete beam in the compression zone.

Due to secondary compression failure, assuming that the full usable strain in concrete has occurred is reasonable (i.e., concrete has crushed) so that $\varepsilon_c = \varepsilon_{cu} = 0.003$.

Strain of Steel (ε_s)

$$\frac{\varepsilon_s}{d-c} = \frac{\varepsilon_{cu}}{c} \quad (4.20a)$$

Where $c = a/\beta_1$ and β_1 is defined by [ACI 318-05 section 10.2.7.3]

$$\varepsilon_s = \frac{\varepsilon_{cu}}{c}(d-c) = \frac{\varepsilon_{cu}}{a}(\beta_1 d - a) \quad (4.20b)$$

CFRP Strain (ε_{cfrp})

$$\frac{\varepsilon_{cfrp} + \varepsilon_{bi}}{h-c} = \frac{\varepsilon_{cu}}{c} \quad (4.21a)$$

Rearrange Equation (4.21a)

$$\varepsilon_{cfrp} = \frac{\varepsilon_{cu}}{c}(h-c) - \varepsilon_{bi} = \frac{\varepsilon_{cu}}{a}(\beta_1 d - a) - \varepsilon_{bi} \quad (4.21b)$$

Force Equilibrium

$$0.85\, f_c' ab = A_s f_y + A_{cfrp}\, E_{cfrp}\, \varepsilon_{cfrp} \quad (4.22a)$$

Substitute Equation 4.21b in Equation 3.22a and simplify the Equation

$$0.85\, f_c' ab = A_s f_y + A_{cfrp}\, E_{cfrp} \left(\frac{\varepsilon_{cu}}{a}(\beta_1 d - a) - \varepsilon_{bi} \right) \quad (4.22b)$$

$$0.85\, f_c' ab = A_s f_y + A_{cfrp}\, E_{cfrp} \frac{\varepsilon_{cu}}{a}\beta_1 h - A_{cfrp}\, E_{cfrp}\,(\varepsilon_{cu} + \varepsilon_{bi}) \quad (4.22c)$$

$$0.85\, f_c' ba^2 - A_s f_y\, a - A_{cfrp}\, E_{cfrp}\, \varepsilon_{cu}\beta_1 h + A_{cfrp}\, E_{cfrp}\, a(\varepsilon_{cu} + \varepsilon_{bi}) = 0 \quad (4.22d)$$

Rearrange various term

$$0.85\, f_c' ba^2 - (A_s f_y - A_{cfrp}\, E_{cfrp}(\varepsilon_{cu} + \varepsilon_{bi}))\, a - A_{cfrp}\, E_{cfrp}\, \varepsilon_{cu}\beta_1 h = 0 \quad (4.22e)$$

Solving a from quadratic Equation.

Nominal strength

$M_n = A_s f_y(d - \frac{a}{2}) + \psi_f \ A_{cfrp} \ E_{cfrp} \ \varepsilon_{cfrp} (h - \frac{a}{2})$

$$\phi M_n = \phi \left[A_s f_y(d - \frac{a}{2}) + \psi_f A_{cfrp} \ E_{cfrp} \ \varepsilon_{cfrp} (h - \frac{a}{2}) \right] \quad (4.23)$$

Where

ϕ (strength reduction factor)

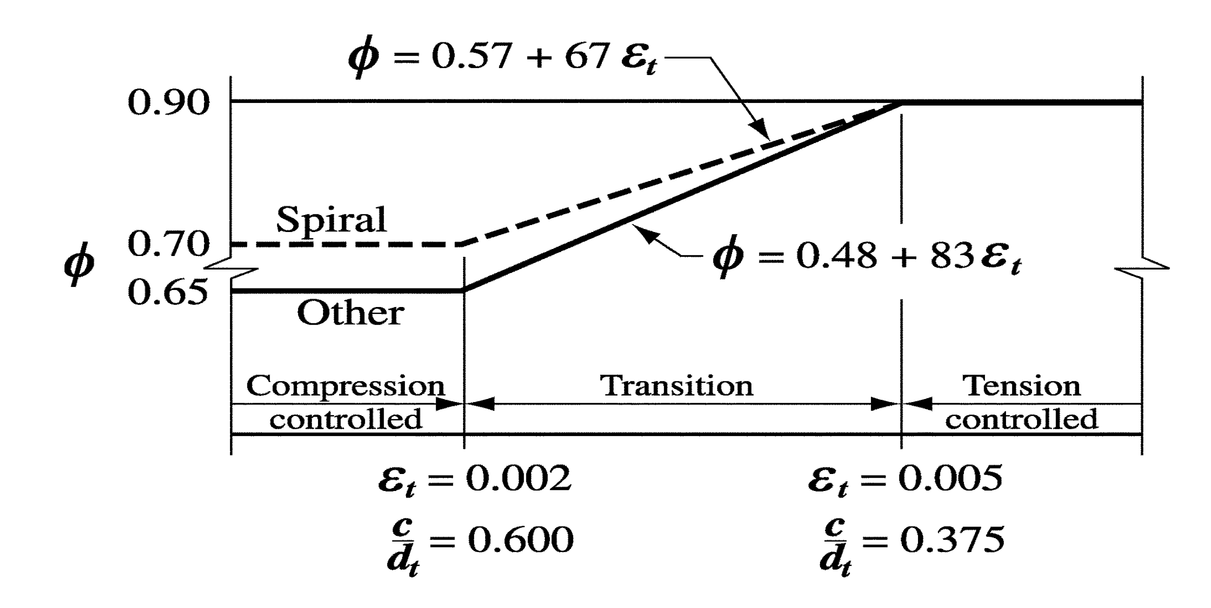


Figure 4.4 Strength reduction factor [ACI 318-05]

The strength reduction factor additional by FRP $\psi_f = 0.85$ [ACI 440].

4.8.2 Tension controlled failure with CFRP rupture

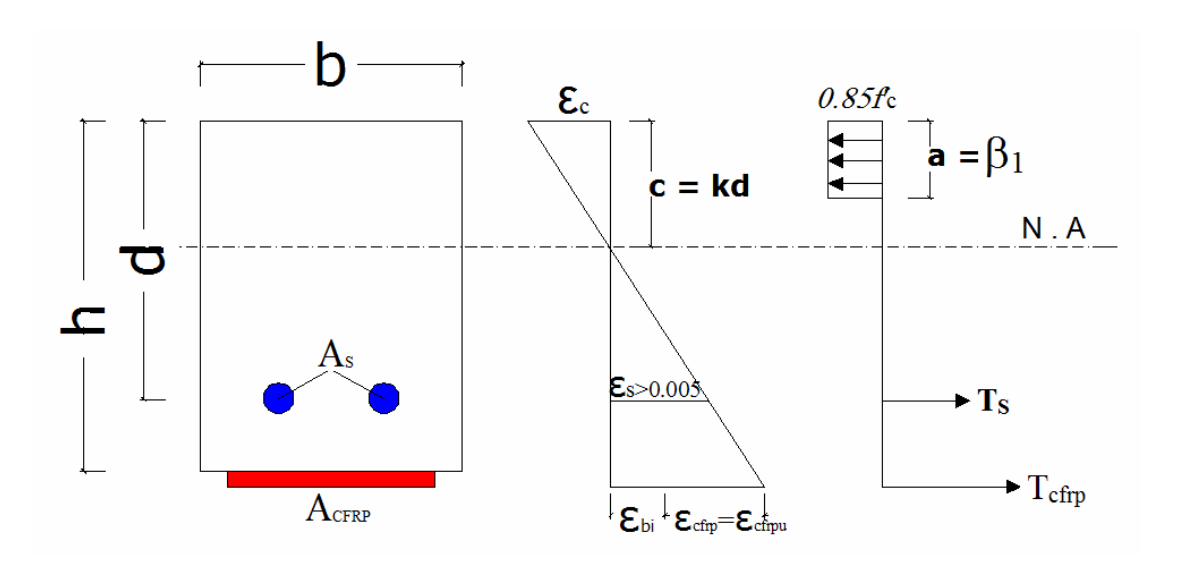


Figure 4.5 Force distributions in a tension controlled failure with CFRP rupture

Strain of Concrete (ε_c)

$$\frac{\varepsilon_c}{c} = \left(\frac{\varepsilon_{cfrp}+\varepsilon_{bi}}{h-c}\right) \tag{4.24a}$$

$$\varepsilon_c = \left(\frac{\varepsilon_{cfrp}+\varepsilon_{bi}}{h-c}\right) c \tag{4.24b}$$

Strain of Steel (ε_s)

$$\varepsilon_s = \left(\frac{\varepsilon_{cfrp}+\varepsilon_{bi}}{h-c}\right)(d-c) = \frac{\varepsilon_{cfrp}+\varepsilon_{bi}}{\beta_1 h - a}(\beta_1 d - a) \tag{4.25}$$

Strain of CFRP (ε_{cfrp})

$$\varepsilon_{cfrp} = \varepsilon_{cfrpu} \tag{4.26}$$

Force Equilibrium

$$0.85\, f_c' ab = A_s f_y + A_{cfrp}\, E_{cfrp}\, \varepsilon_{cfrp}$$

$$a = \frac{A_s f_y + A_{cfrp}\, E_{cfrp}\, \varepsilon_{cfrp}}{0.85\, f_c' b}$$

Flexural Capacity

$$M_n = A_s f_y(d - \frac{a}{2}) + \psi_f \; A_{cfrp} \; E_{cfrp} \; \varepsilon_{cfrp} \, (h - \frac{a}{2})$$

$$\phi M_n = \phi \left[A_s f_y(d - \frac{a}{2}) + \psi_f A_{cfrp} \; E_{cfrp} \; \varepsilon_{cfrp} \, (h - \frac{a}{2}) \right] \qquad (4.27)$$

4.8.3 Tension- and Compression-Controlled Failure with Steel Yielding and without CFRP Rupture

Strain in concrete: $\varepsilon_c = \varepsilon_{cu} = 0.003$

Strain in steel: $\varepsilon_{sy} \le \varepsilon_s < 0.005$

Strain in CFRP: $\varepsilon_{cfrp} < \varepsilon_{cfrpu}$

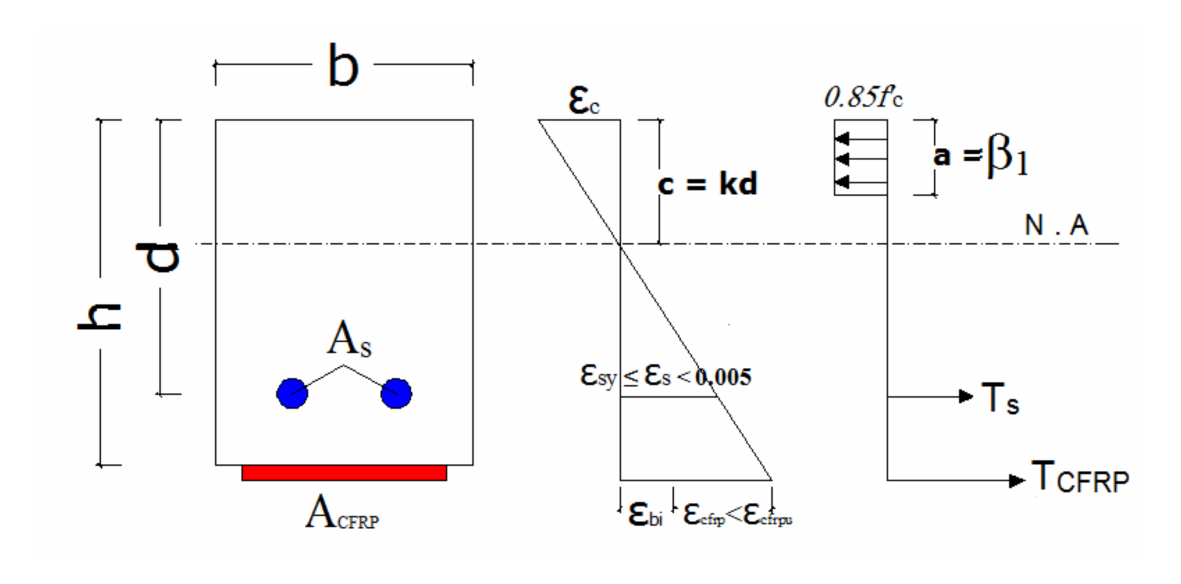


Figure 4.6 Force distributions in a tension- and compression controlled failure with steel yielding and without CFRP rupture

Tension and compression controlled failure with steel yielding and without CFRP rupture as same as of tension controlled failure without CFRP rupture (Section 4.8.1).

4.8.4 Compression-Controlled Failure Without Steel Yielding and without CFRP Rupture

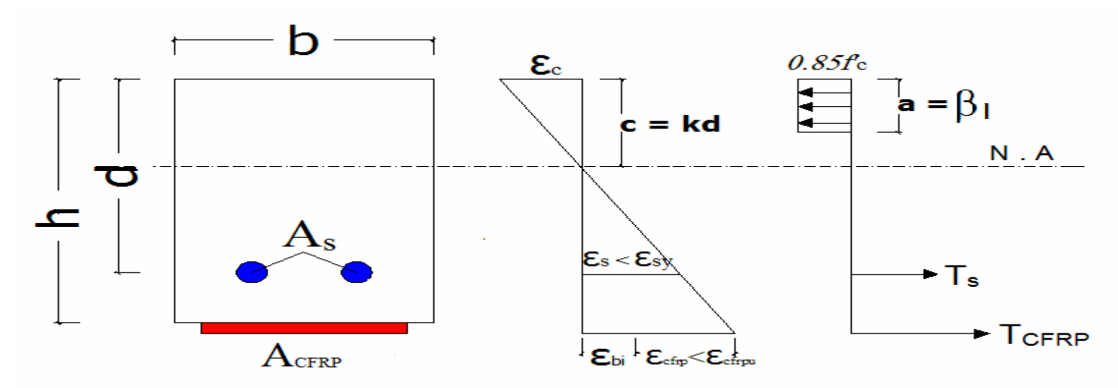


Figure 4.7 Force distributions in a compression controlled failure without steel yielding and without CFRP rupture

Strain in concrete: $\varepsilon_c = \varepsilon_{cu} = 0.003$

Strain in steel: $\varepsilon_s < \varepsilon_{sy}$

Strain in CFRP: $\varepsilon_{cfrp} < \varepsilon_{cfrpu}$

Flexural Capacity

$$M_n = A_s f_y(d - \frac{a}{2}) + \psi_f \ A_{cfrp} \ E_{cfrp} \ \varepsilon_{cfrp} \ (h - \frac{a}{2})$$

$$\square M_n = \square \left[A_s E_s \varepsilon_s (d - \frac{a}{2}) + \psi_f A_{cfrp} \ E_{cfrp} \ \varepsilon_{cfrp} (h - \frac{a}{2} \right]$$
(4.28)

4.8.5 Balanced Failure

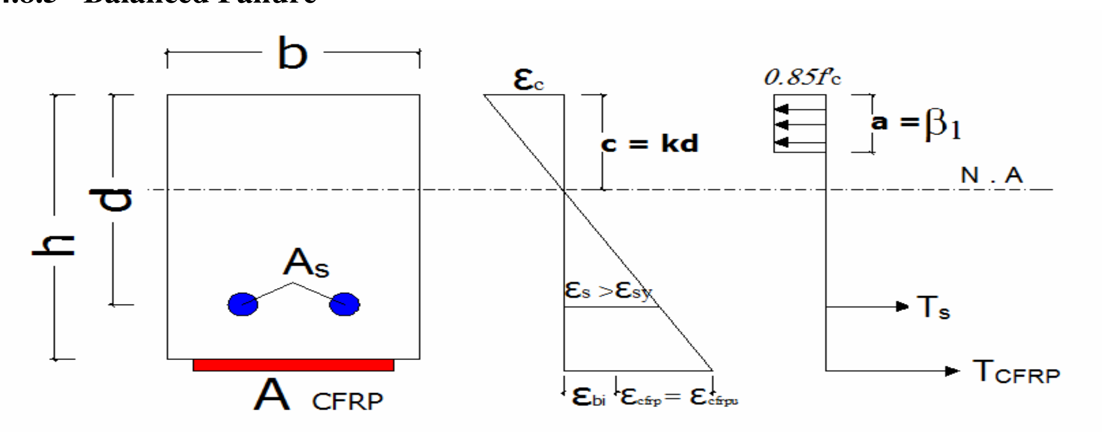


Figure 4.8 Force distributions in a balanced failure

Strain in concrete: $\varepsilon_c = \varepsilon_{cu} = 0.003$

Strain in steel: $\varepsilon_s > \varepsilon_{sy}$

Strain in CFRP: $\varepsilon_{cfrp} = \varepsilon_{cfrpu}$

$$\frac{\varepsilon_{cu} + \varepsilon_{cfrpu} + \varepsilon_{bi}}{h} = \frac{\varepsilon_{cu}}{c} \tag{4.29}$$

$$0.85\, f_c'ab = A_s f_y + A_{cfrp}\, E_{cfrp}\, \varepsilon_{cfrp}$$

$$M_n = A_s f_y(d - \frac{a}{2}) + \psi_f A_{cfrp}\, E_{cfrp}\, \varepsilon_{cfrp}\,(h - \frac{a}{2})$$

$$\square M_n = \square \left[A_s f_y(d - \frac{a}{2}) + \psi_f A_{cfrp}\, E_{cfrp}\, \varepsilon_{cfrp}\,(h - \frac{a}{2}) \right] \tag{4.30}$$

4.9 Flexural Forces of Steel Plate Strengthened Beams

Idealized strain and stress distributions in a steel plate strengthened concrete beam and the force equilibrium at ultimate load conditions are shown in Figure 4.8. Forces in various elements of the beam cross-section are expressed in terms of stresses in concrete, steel reinforcement, and steel plate.

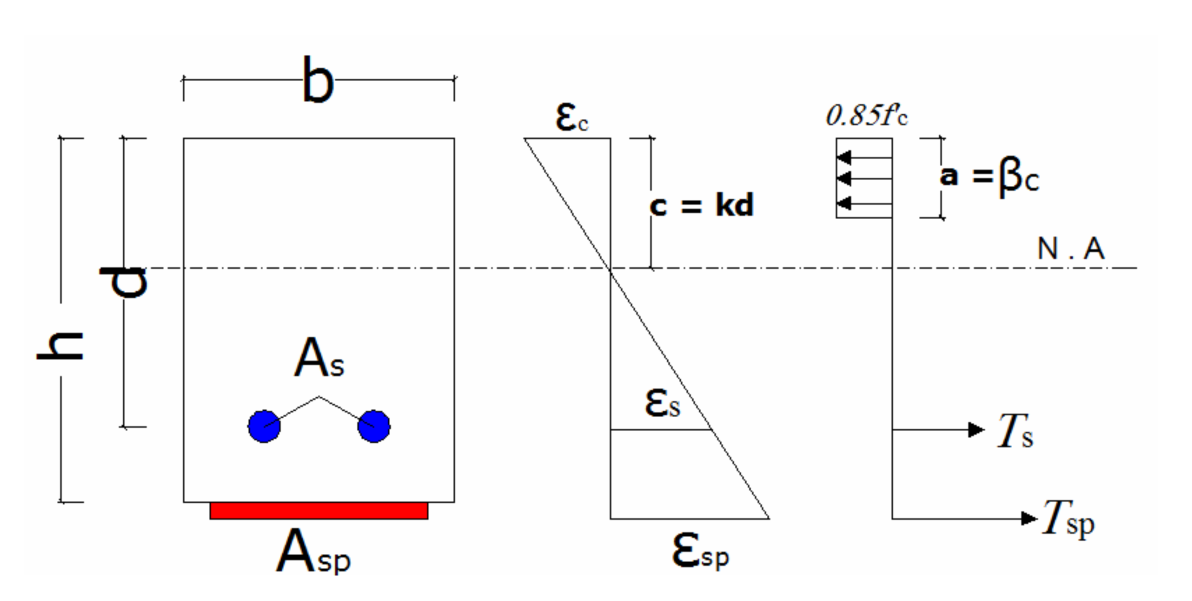


Figure 4.9 Strain distribution and force equilibrium for beam strengthened by steel plate at the ultimate loads

Strain Compatibility

Referring to similar triangles in figure4.8, the following relations are established.

$$\frac{\varepsilon_c}{c} = \frac{\varepsilon_s}{d-c} = \frac{\varepsilon_{sp}}{(h-c)} \quad (4.31)$$

Force Equilibrium

The compressive force in concrete (**C_c**) is

$C_c = 0.85\, f_c'ab$

The tensile force in steel (**T_s**) is

$T_s = A_s f_s = A_s E_s \varepsilon_s$ (before steel yielding, $\varepsilon_s < \varepsilon_y$) (4.32)

$T_s = A_s f_y = A_s E_s \varepsilon_y$ (after steel yielding, $\varepsilon_s \geq \varepsilon_y$) (4.33)

The tensile force in Steel plate (T_{sp})

$$T_{sp} = A_{sp} f_{sp} = A_{sp} (E_{sp}\, \varepsilon_{sp}) \quad (4.34)$$

Nominal Flexural Strength

$$\square M_n = \square \left[A_s f_y \left(d - \frac{a}{2}\right) + A_{sp} f_y'\left(h - \frac{a}{2}\right) \right] \quad (4.35)$$

4.10 Serviceability

4.10.1 Deflection

The design of a reinforced concrete member is based on two criteria: strength and serviceability. The mandate of strength is based on ultimate strength of the member to withstand the factored loads during its predicted lifetime.

Serviceability is taken to ensure that the structural members behave in a manner acceptable to the society under the effect of service loads. Four major considerations affect the serviceability of concrete structures:

1. Deflection

2. Crack width

3. Creep-rupture

4. Fatigue

In the present work we will discuss the deflections

The deflection in concrete structures must be controlled for a variety of reasons. The most obvious reason is that an excessive deflection would convey a sense of impending failure.

Excessive deflection in a concrete beam or a slab can lead to bonding and cracking, which is highly undesirable as these can lead to structural damage. Two types of deflections should be considered to ensure the serviceability of concrete members: immediate deflection (also called short-term) and long-term deflection. Immediate deflection occurs during the normal service life of a member as a result of a percent of the live loads. Long-term deflection occurs as a result of sustained loads.

4.10.2 Deflection Design Guideline (ACI-318)

Two methods for the control of deflections of one-way flexural members:

1) **Limit Span/Depth or Indirect method [ACI-318 Table 9.5a].**

TABLE 9.5(a)—MINIMUM THICKNESS OF NONPRESTRESSED BEAMS OR ONE-WAY SLABS UNLESS DEFLECTIONS ARE CALCULATED

	minimum thickness h			
	Simply Supported	One End Continous	Both End Continous	Cantilever
Member	Member not Supporting or attached to partions or other construction likely to be damaged by large deflections			
Solid one way span	l/20	l/24	l/28	l/10
Beams or Ribbed one way slab	l/16	l/18.5	l/21	l/8

2) Calculate the deflection value and compare with limits (Direct Method)

Deflections are inversely proportional to the moment of inertia where as determination of the moment of inertia of a homogeneous uncracked section is simple ($I=bh^3/12$ for a rectangular section, where b is the width and h is the overall depth). Moment of inertia of a reinforced concrete section is complex, because of the cracking that occurs under service loads.

As long as a concrete section remains uncracked, its moment of inertia I_{unc} equals the sum of the moment of inertia of the gross section I_g and the moment of inertia of the transformed area of steel reinforcement taken about the centroidal axis of the transformed uncracked section.

When the applied moment (M_a) exceeds the cracking moment (M_{cr}) , the beam cracks at several locations along the span, resulting in reduced stiffness of the beam as a whole (also called the overall flexural stiffness of the beam). Under this condition, the moment of inertia must be based on the properties of the cracked section (I_{cr}) .

To determine the deflection of a beam intermittently cracked along the span, the effective moment of inertia (I_e) must be used, which is a function of (I_{cr}) . Noting that the extent of cracking depends also on the applied moment and the cracking moment, the effective moment of inertia is a complex function of I_g ,I_{cr} ,M_a , and M_{cr}.

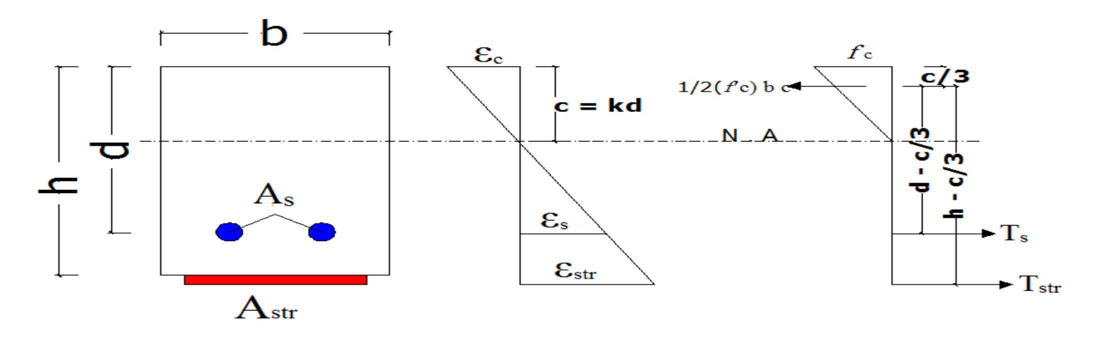


Figure 4.10 Strain distribution and force equilibrium for the strengthened beam

$$I_{cr} = (\frac{1}{3})\, b(kd)^3 + n_s A_s\,(d - kd)^2 + n_f A_f\,(h - kd)^2 \quad (4.36)$$

Where

$$k = \sqrt{\left(\rho_s\, n_s + \rho_{cfrp}\, n_{cfrp}\right)^2 + 2(\rho_s\, n_s + \rho_{cfrp}\, n_{cfrp}\, \frac{h}{d})} - (\rho_s\, n_s + \rho_{cfrp}\, n_{cfrp})$$

$$\frac{E_s}{E_c} = n_s \qquad\qquad \frac{E_f}{E_c} = n_f$$

ACI 318 adapted equation to determine the effective moment of inertia (Ie) of a steel-reinforced section

$$I_e = (\frac{M_{cr}}{M_a})^3\, I_g + \left[1 - (\frac{M_{cr}}{M_a})^3\right] I_{cr} \quad (4.37)$$

Where

M_{cr} = the cracking moment

$$M_{cr} = \frac{f_r\, I_g}{y_t}. \quad (4.38)$$

f_r = modulus of rupture of concrete, MPa $(0.6\sqrt{f'c})$

M_a = the applied service load moment where deflection is being considered

The serviceability of a member (deflections, crack widths) under service loads should satisfy applicable provisions of ACI-318.

The effect of the FRP external reinforcement on the serviceability can be assessed using the transformed section analysis.

To avoid inelastic deformations of the reinforced concrete members strengthened with external CFRP reinforcement, the existing internal steel reinforcement should be prevented from yielding under service load levels. The stress in the steel under service load should be limited to 80% of the yield strength.

$f_{s,s} \leq 0.80 f_y$ (4.39)

According to ACI 318, Section 9.5.2.5, the long-term deflection due to creep and shrinkage, Δcp+sh, can be determined by multiplying the immediate deflection caused by sustained loads by a factor (ACI 440, Equation 8-13a):

$$\Delta_{cp}+sh = \lambda(\Delta_i)_{sus}. \quad (4.40)$$

Where

$(\Delta_i)_{sus}$. is the immediate deflection under sustained loads.

The value of the coefficient λ is a function of the time-dependent factor ξ that accounts

$$\lambda = \frac{\xi}{1+50\rho'} \quad (4.41)$$

5 years or more.. 2.0

12 months... 1.4

6 months... 1.2

3 months... 1.0

Where

ξ = time-dependent factor for sustained loads (ξ_{CFRP}/ξ_{steel})

ρ′ = steel compression reinforcement ratio

Chapter 5 Description of Laboratory Specimens

5.1 Scope

The main objectives of this part of research are to determine the flexural strength and deflection of beams (with or without composite material).

5.2 Experimental program

The fifteen rectangular reinforced concrete beams (200X250) mm cross section were tested under mid-point bending over a clear span of 1500mm to evaluate the flexural behavior of strengthened beams.

All beams were reinforced with two 3Φ12 bars (A_s = 339 mm²) and had an effective depth of 220 mm. The beams were adequately reinforced for shear using Φ 10 mm diameter stirrups, placed at 150 mm spacing.

1) **Two of the specimens was used as a control specimen, and were not retrofitted with any strengthening materials.**



Figure 5.1 Control beam specimens

2) **Four of specimens were retrofitted with Steel Plate strengthening materials.**





Figure 5.2 beam specimens strengthened by steel plate

3) **Four of specimens were retrofitted with light gauge high tensile steel as a strengthening material.**



Figure 5.3 beam specimen strengthened by light gauge steel plate

4) **Five of specimens were retrofitted with CFRP strengthening materials (laminates and wrap).**



Figure 5.4 beam specimen strengthened by CFRP wrap system



Figure 5.5 beam specimen strengthened by CFRP laminate system

All of the specimens were tested monotonically under increasing midspan displacement to failure.

5.3 Test Setup and Instrumentation

1) Beam specimens were tested in two-point bending over a 1,700 mm span, using a 1000 kN testing machine, as shown in Figure 5.6. The load was applied at a 1 kN/s rate of loading. Steel plates, 50 mm wide, were positioned at the supports and a 120 mm wide plate was positioned at the loading point to distribute the loads and to avoid local crushing of concrete.

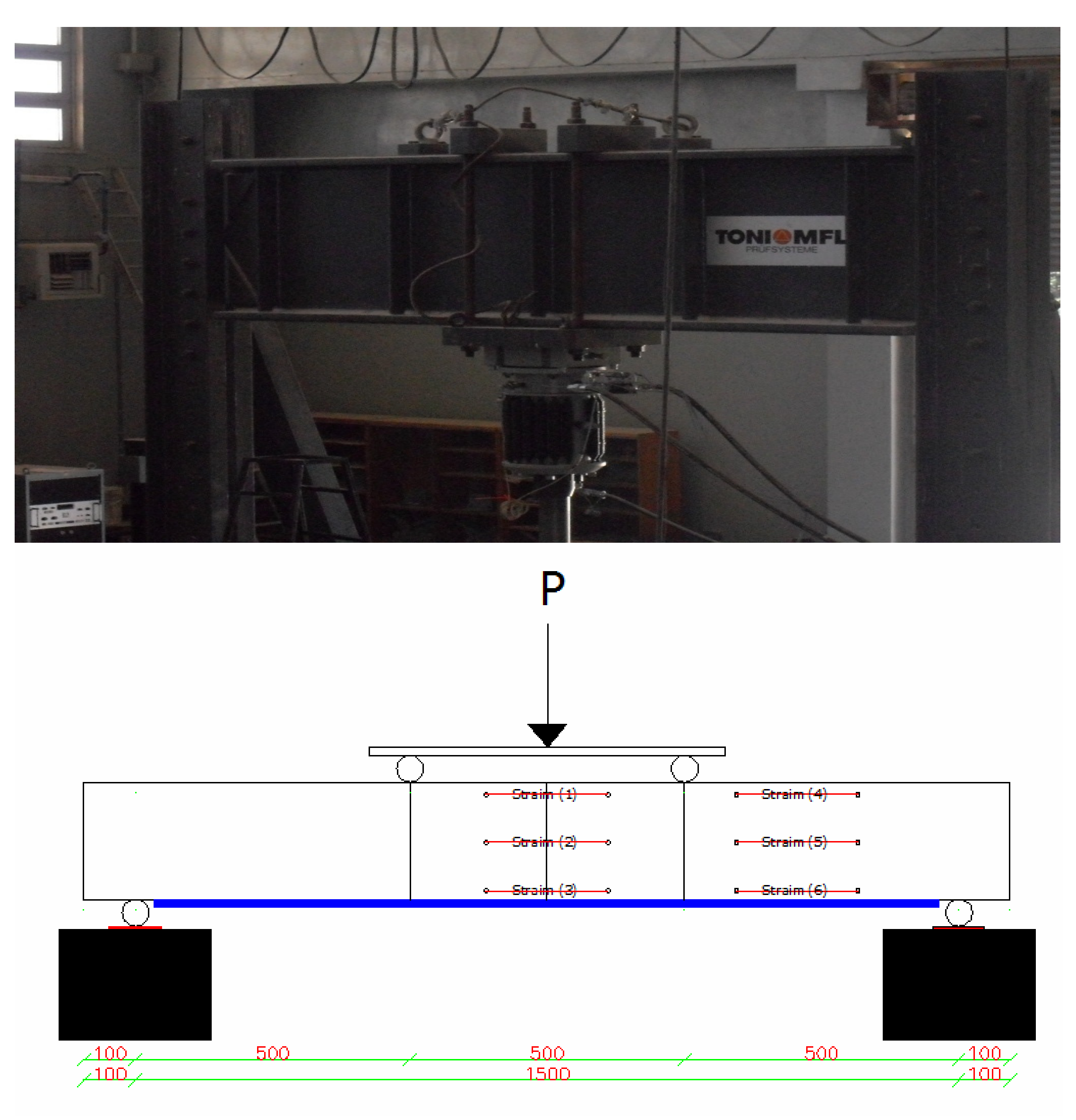


Figure 5.6 Test setup for rectangular beam specimens and position of displacement strain gauge transducers

2) Dial gage was used to monitor the mid-span deflection.



Figure 5.7 Dial gage

3) Displacement strain gauge transducers were installed on the compression, middle and tension sides at mid-span and right side of the beams, where the tension gauge was located at the same elevation of the internal reinforcement to establish the strain distribution along the length of steel plate under increased loads.

5.4 Experimental Beams Behavior

5.4.1 Control Beams (1500 X 200 X 250) mm

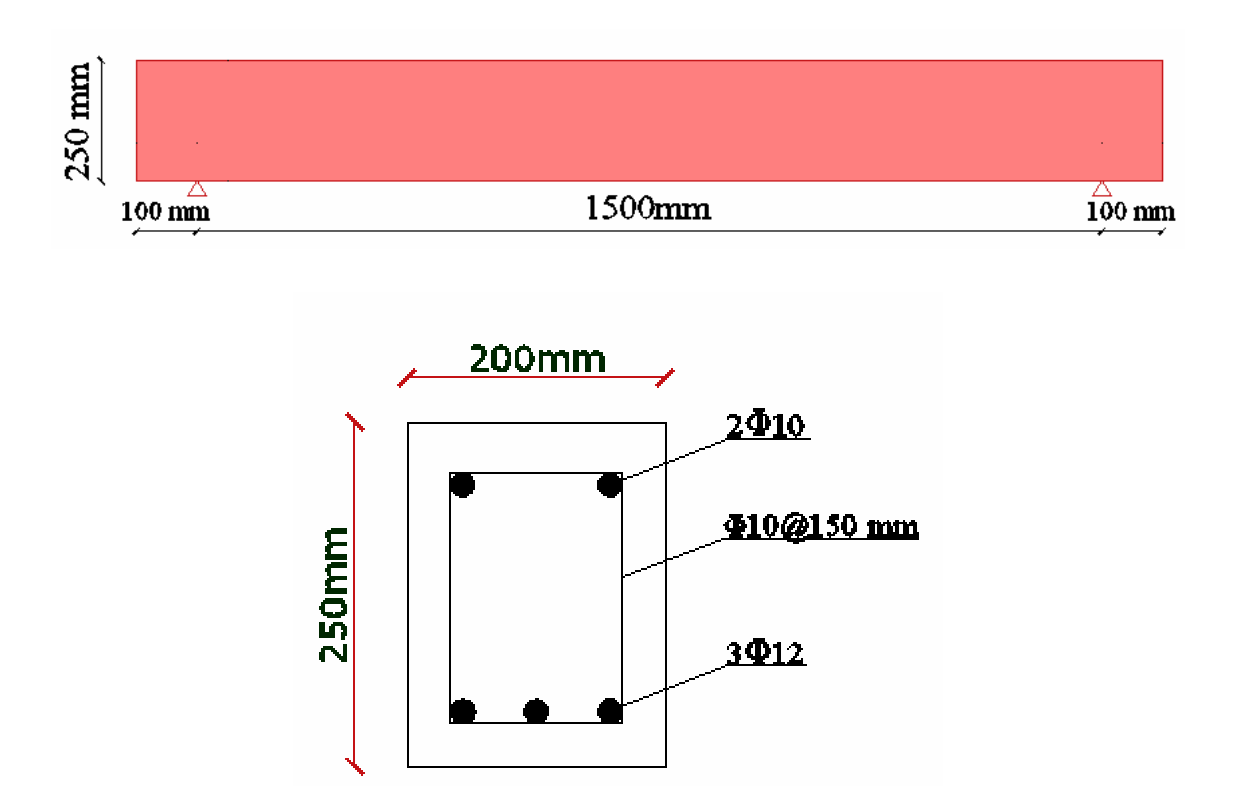


Figure 5.8 Control beam specimens without strengthening materials

Load – deflection curve of specimens CB 01 and CB 02 are shown in Figure 5.9. The deflection at load failure was approximately 11 mm for both specimens.

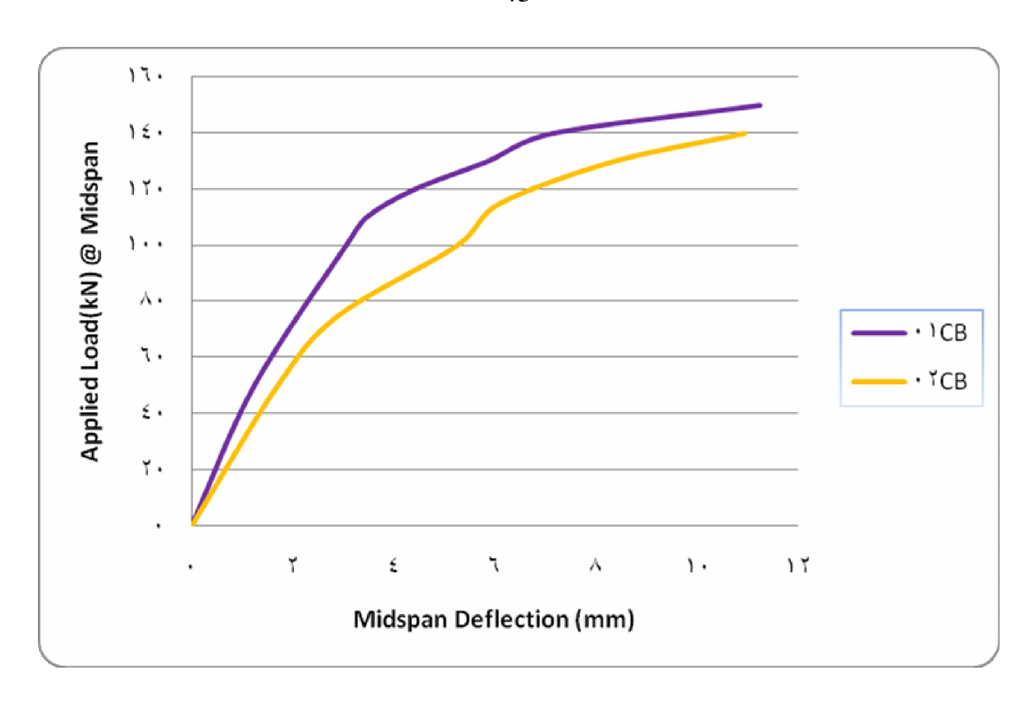


Figure 5.9 Load - versus – midspan deflection for control beams

CB01 and CB02: during loading of beams to failure, when the load was approximately two thirds or more a clicking sound was occasionally emitted from the beams. After the clicking sound the beams exhibited large deflections. Besides, this sound was a significant warning sign preceding the sudden failure of the beams. Average control beam, failure load was 145 kN. First crack appeared at 100 kN, 69 % of the ultimate load. Crack pattern showed that failure mode was tension failure as shown in Figure 5.9.

5.4.1.1 Measured Strain and Strain Profiles

The analytical model was based on several assumptions that are commonly used in the design of reinforced concrete flexural members.

Similar to most analytical methods used to calculate the flexural response of reinforced concrete elements, the cross section was divided into horizontal slices. The total response of the cross section is obtained by adding the contribution of each slice. Separate slices were used for the different materials; therefore, the idealized behavior of each slice is controlled by the stress-strain relationship for a given material.

The following assumptions, which are consistent with current design practice of reinforced concrete sections, were used in the model:

• Strains increase proportionally with distance from the neutral axis.

• No slip occurs between the steel reinforcement and concrete surrounding it.

• Perfect bond exists between composite material and concrete surface.

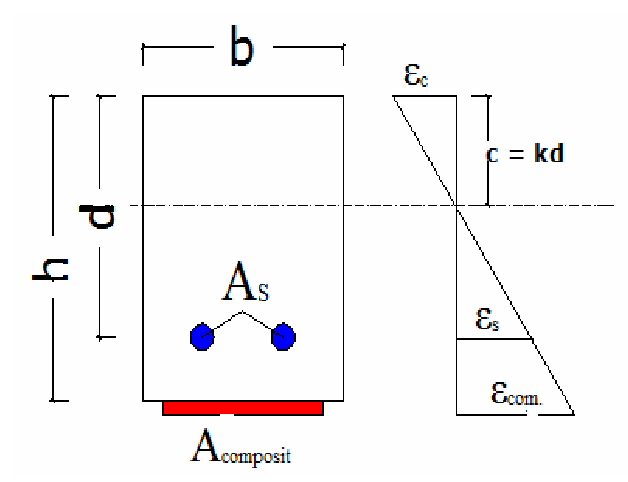


Figure 5.10 Strain distributions for the strengthened beam

Figure 5.10 shows the load – strain curve on the surface of the concrete at middle of span of specimen CB 01. In this Figure, compressive strain (strain 1) is plotted as a negative strain.

The strain gage was bonded 30mm below the top surface of the beam and the compressive strain at a load, approximately equal 150 kN is -0.00122 while the strain gage on tension side (strain 3) was bonded at 220 mm below the top surface of the beam where the strain at failure load is 0.0147.

Figure 5.11 shows the load – strain curves on the surface of the concrete at right side of span of specimen CB 01. Compressive strain (strain 4) at failure load is -0.0016, while tensile strain (strain 6) is 0.00729.

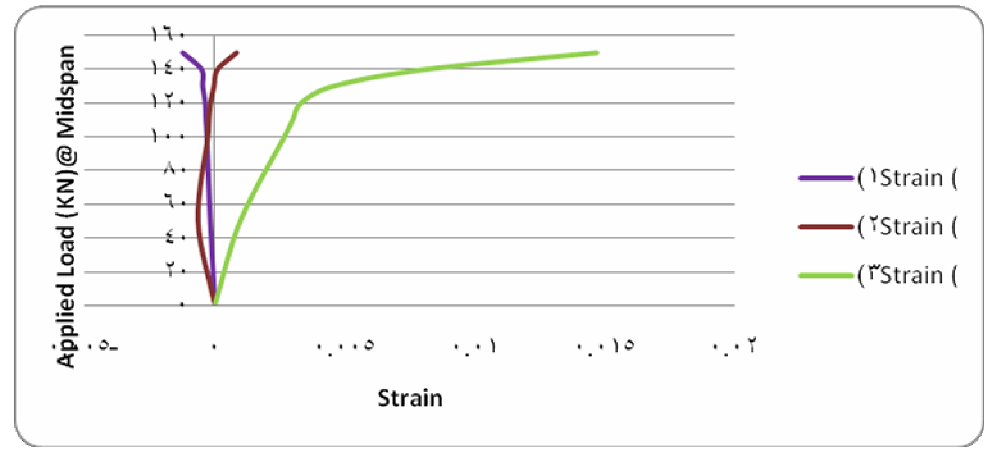


Figure 5.11 Test specimens (CB01) - showing strain gauges (1),(2) and (3)

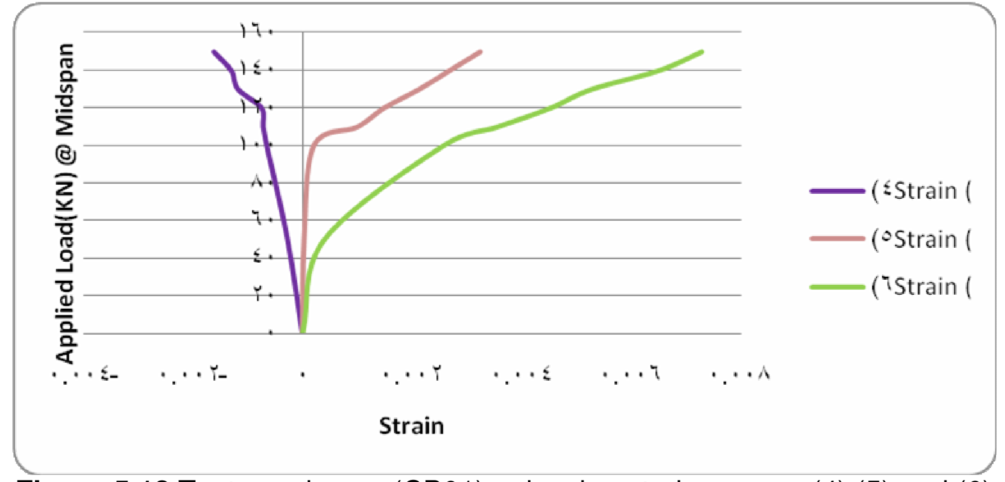


Figure 5.12 Test specimens (CB01) - showing strain gauges (4),(5) and (6)

According to, the load – strain curves Figure 5.12 on the surface of the concrete at middle of span of specimen CB 02. Compressive strain (strain 1) at failure load, approximately, equals 140 kN is -0.0015. On other hand, the strain at tension side (strain 3) at failure load is 0.009.

Figure 5.13 shows the load – strain curve on the surface of the concrete at right side of span of specimen CB 02 in this Figure the compressive strain (strain 4) at failure load is -0.0005, while tensile strain (strain 6) is 0.005.

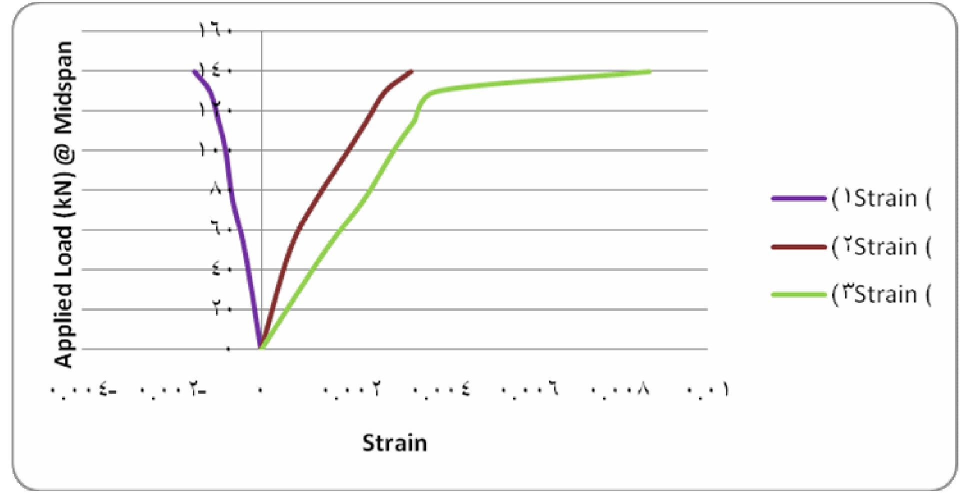


Figure 5.13 Test specimens (CB02) – showing strain gauges (1),(2) and (3)

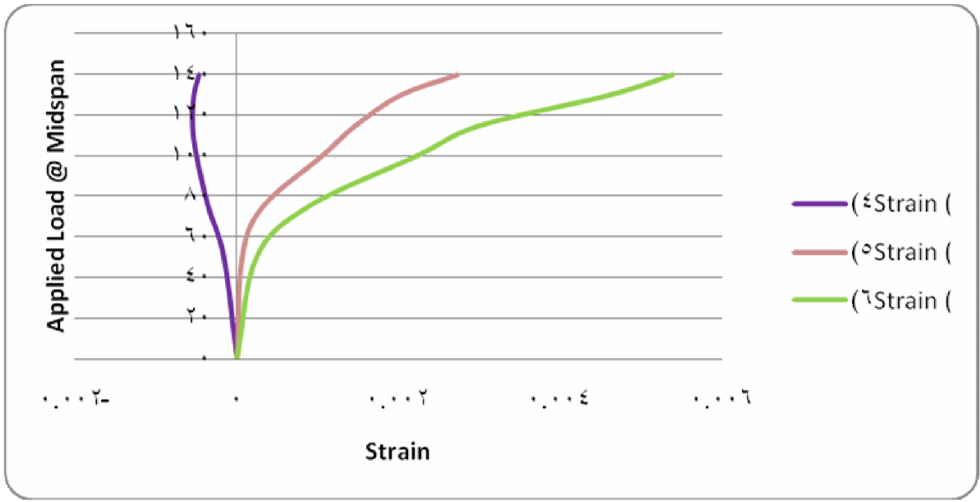


Figure 5.14 Test specimens (CB02) - showing strain gauges (4), (5) and (6)

Figures 5.14 and 5.15 show the strain distribution with depth for the CB 01 and CB 02 beams at the middle of span and at right side respectively. Tensile strains are plotted as positive values in these Figures the average measured strains were considered to vary linearly within the reinforced concrete section.

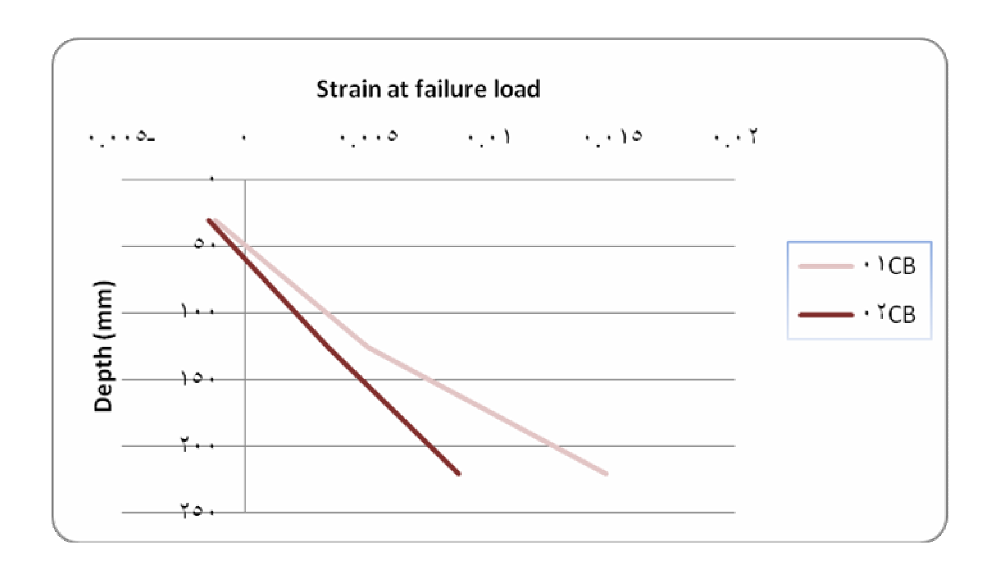


Figure 5.15 Strain profile for CB 01 and CB 02 at middle of span

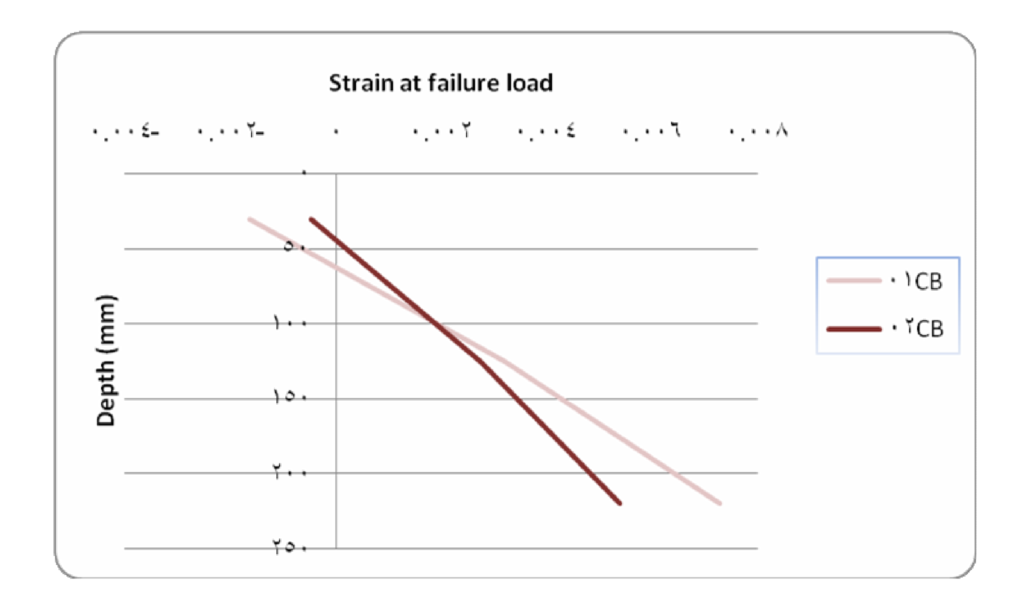
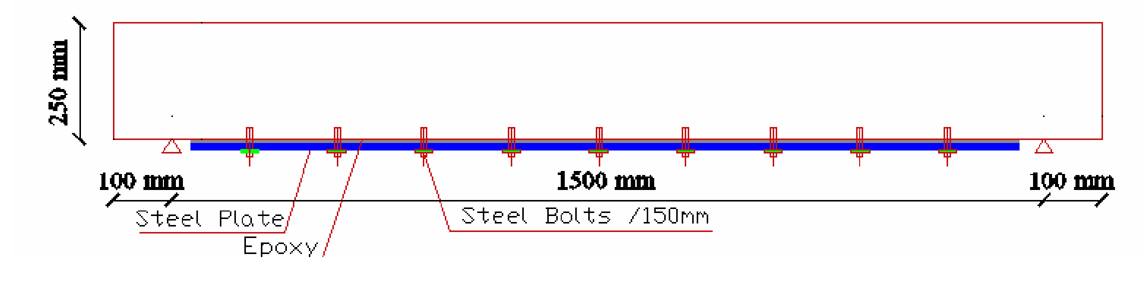


Figure 5.16 Strain profile for CB 01 and CB 02 at right side of span

5.4.2 Rectangular beam with steel plate strengthening materials

Properties of Steel Plate					
Beam	L(mm)	b(mm)	t(mm)	Ultimate tensile strength (MPa)	Modulus of elasticity (GPa)
ST01	1500	150	3.0	420	204
ST02	1500	120	3.0	420	204
ST03	1500	100	3.0	420	204
ST04	1500	80	3.0	420	204



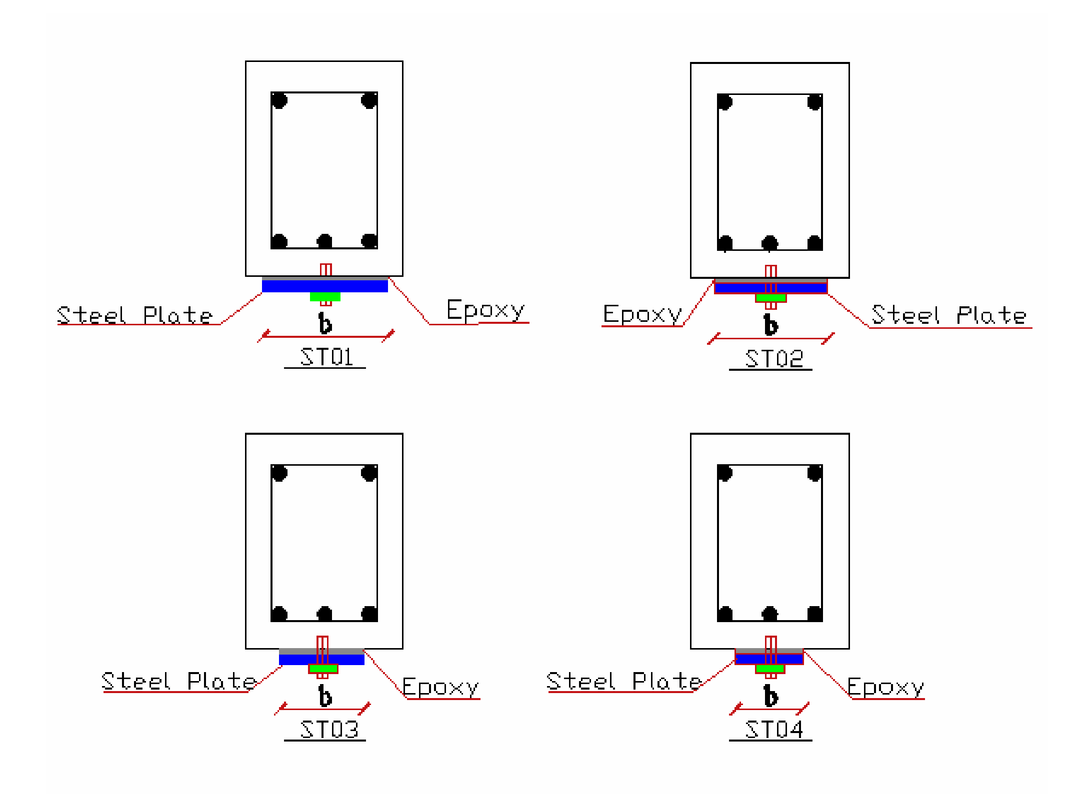


Figure 5.17 Details of beams strengthened by steel plate

Load – deflection curves of specimens STP 01, STP 02, STP 03, STP 04 and control beam is shown in Figure 5.17. The load deflection curves for beams are strengthened by steel plate are clearly affected by composite material.

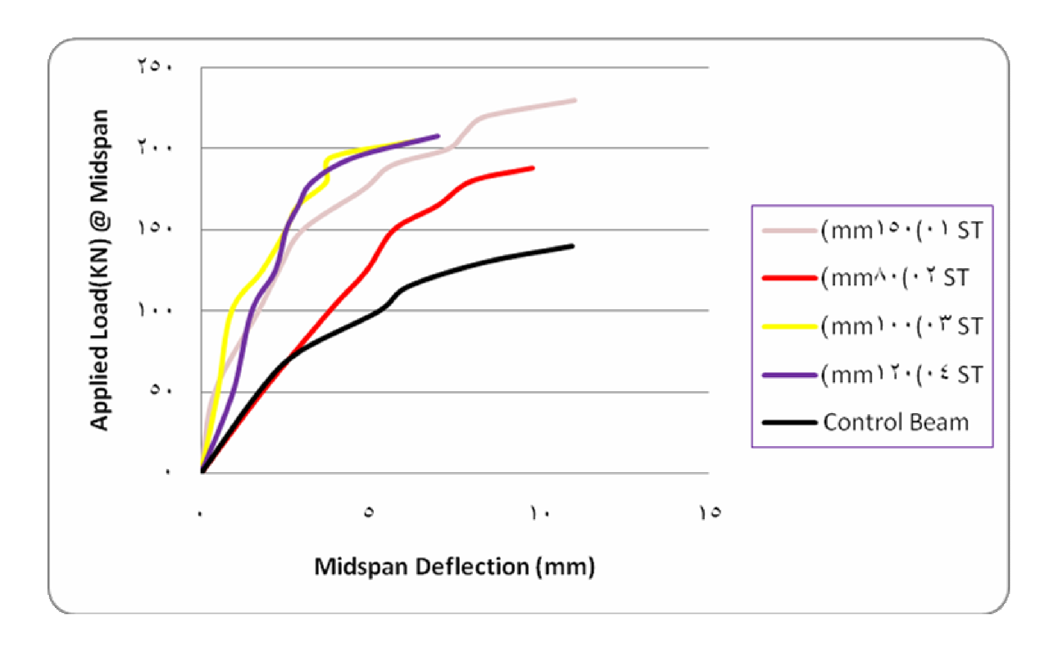


Figure 5.18 Load - versus – midspan deflection for steel plate system with control beam.

Figure 5.18 shows the load – strain curves on the surface of the concrete at middle of span of specimen ST 01. Compressive strain (strain 1) at failure load, approximately, equals 230 kN is -0.002, while the strain at tension side (strain 3) at failure load is 0.003.

Figure 5.19 shows the load – strain curves on the surface of the concrete at right side of span of specimen ST 01. Compressive strain (strain 4) at failure load is -0.0008, while tensile strain (strain 6) is 0.014.

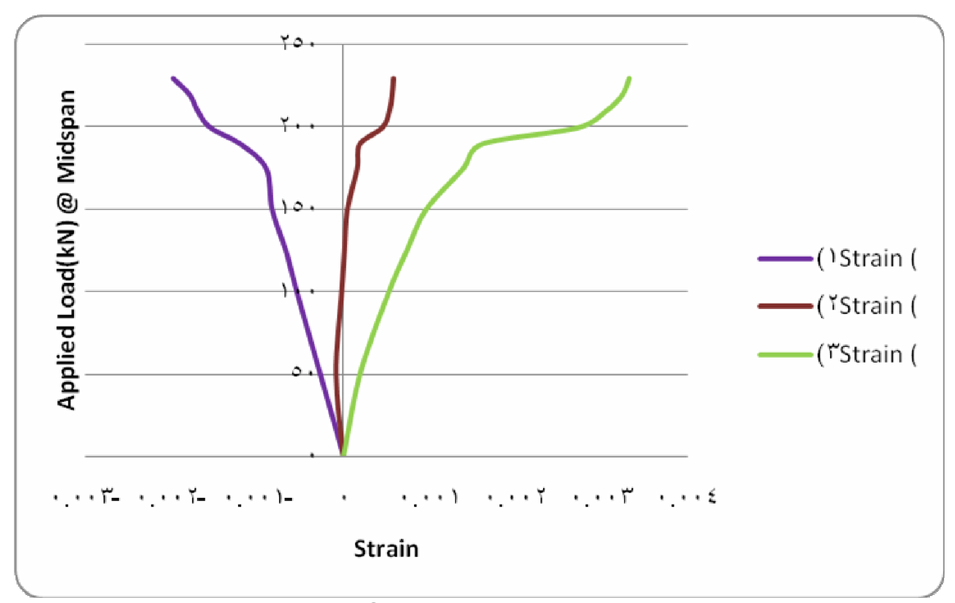


Figure 5.19 Test specimen (ST01) – showing strain gauges (1), (2) and (3)

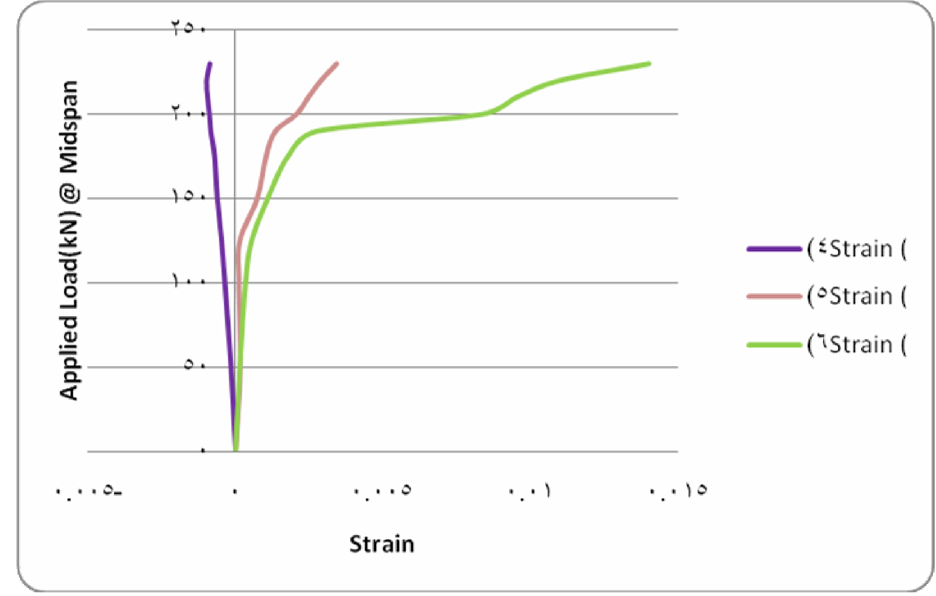


Figure 5.20 Test specimen (ST01) – showing strain gauges (4), (5) and (6)

The measured load – strain curves at the middle of span of ST 02 are presented in Figure 5.20. Compressive strain (strain 1) at failure load, approximately, equals 188 kN is -0.0027, while the strain at tension side (strain 3) at failure load is 0.003.

On other hand Figure 5.21 shows the load – strain curves on the surface of the concrete at right side of span of specimen ST 02. Compressive strain (strain 4) at failure load is -0.0014, while tensile strain (strain 6) is 0.018.

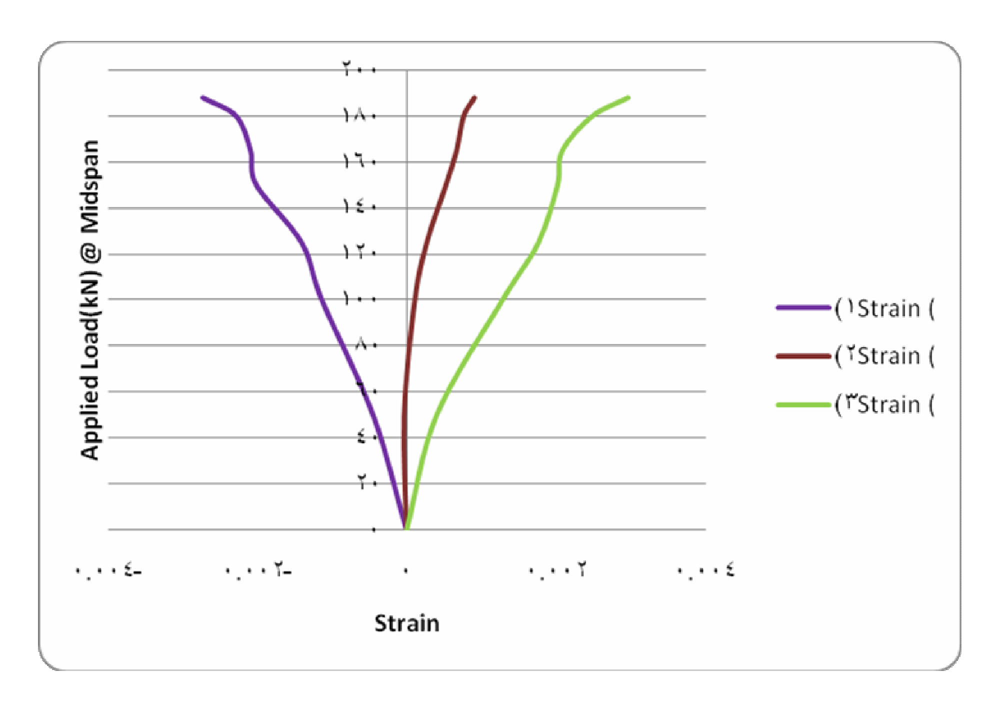


Figure 5.21 Test specimen (ST02) – showing strain gauges (1), (2) and (3)

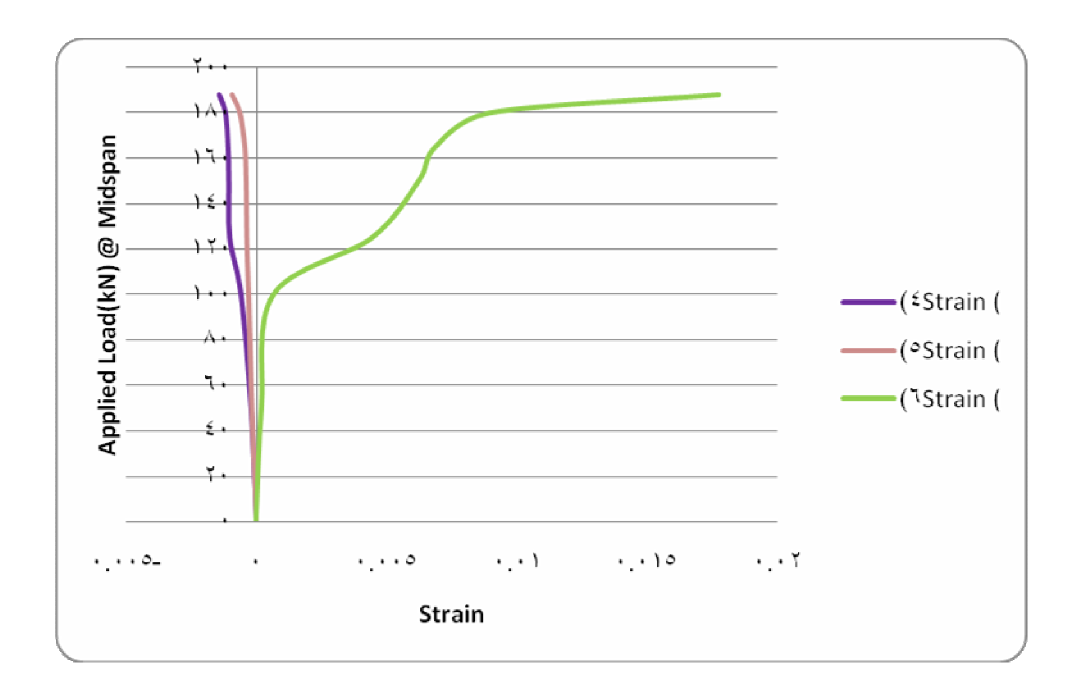


Figure 5.22 Test specimen (ST02) – showing strain gauges (4), (5) and (6)

Figure 5.22 shows the load – strain curves on the surface of the concrete at middle of span of specimen ST 03. Compressive strain (strain 1) at failure load, approximately, equals 205 kN is -0.0014, while the strain at tension side (strain 3) at failure load is 0.0067.

Figure 5.23 shows the load – strain curves on the surface of the concrete at right side of span of specimen ST 03. Compressive strain (strain 4) at failure load is -0.0013, while tensile strain (strain 6) is 0.014.

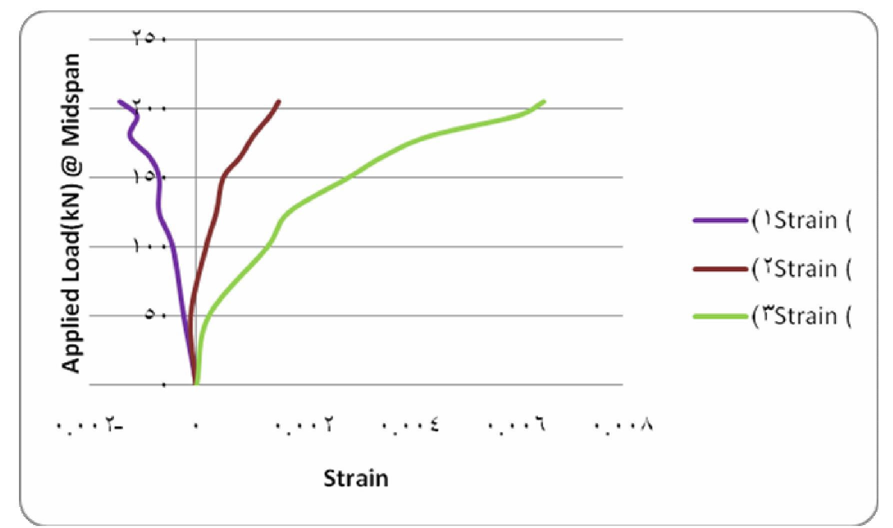


Figure 5.23 Test specimen (ST03) - showing strain gauges (1),(2) and (3)

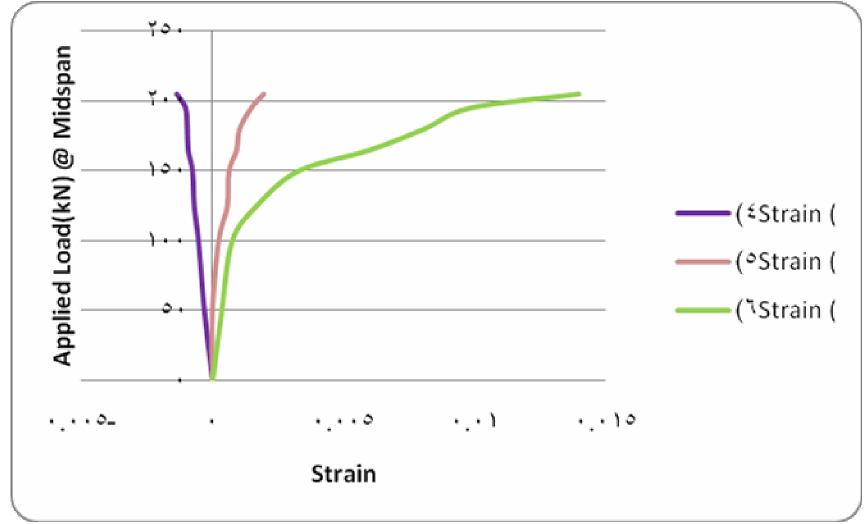


Figure 5.24 Test specimen (ST03) – showing strain gauges (4),(5) and (6)

The measured load – strain curves on the surface of the concrete at middle of span of specimen ST 04 is shown in Figure 5.24. Compressive strain (strain 1) at failure load, approximately, equals 208 kN is -0.0015, while the strain at tension side (strain 3) at failure load is 0.007.

Figure 5.25 shows the load – strain curves on the surface of the concrete at right side of span of specimen ST 04. Compressive strain (strain 4) at failure load is -0.0010, while tensile strain (strain 6) is 0.018.

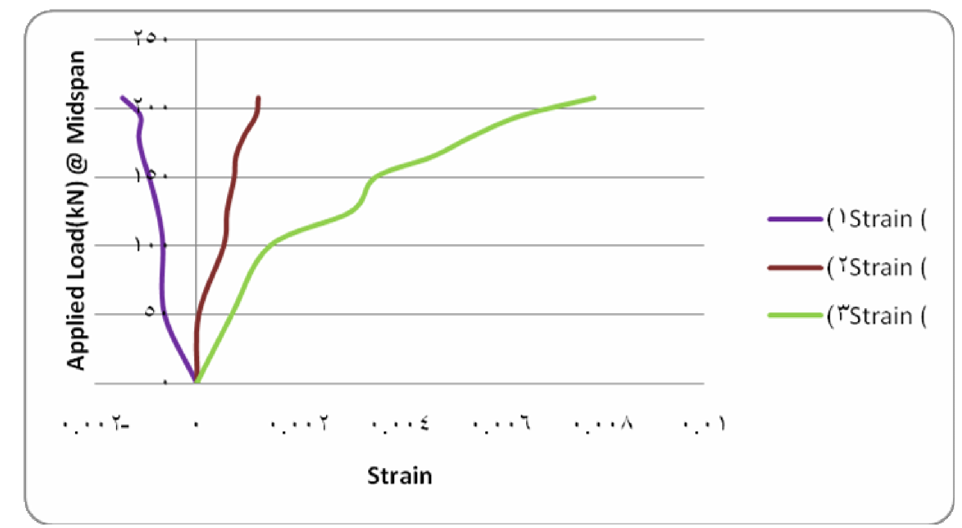


Figure 5.25 Test specimen (ST04) - showing strain gauges (1),(2) and (3)

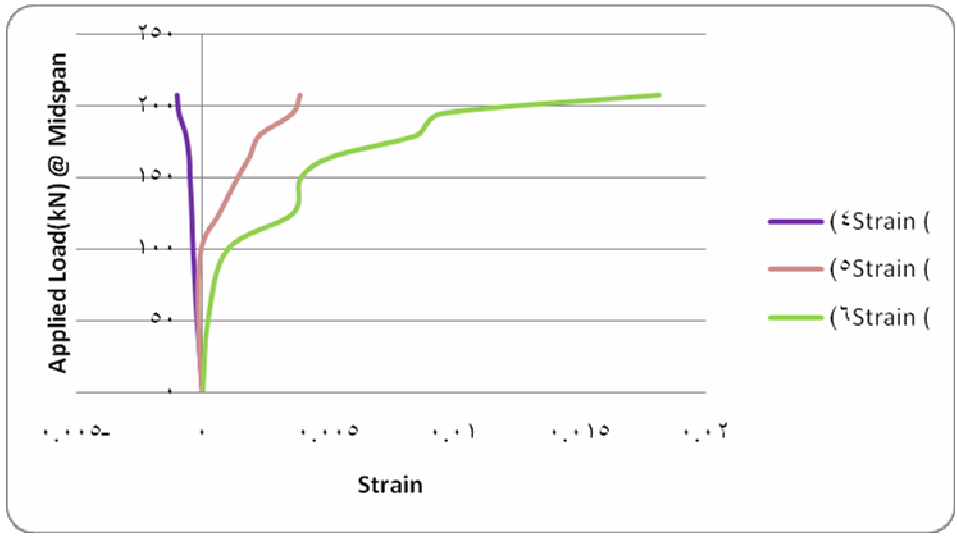


Figure 5.26 Test specimen (ST04) - showing strain gauges (4),(5) and (6)

Figure 5.26 shows the strain profile distributions with depth for the ST 01, ST 02, ST 03 and ST 04 beams at the middle of span.

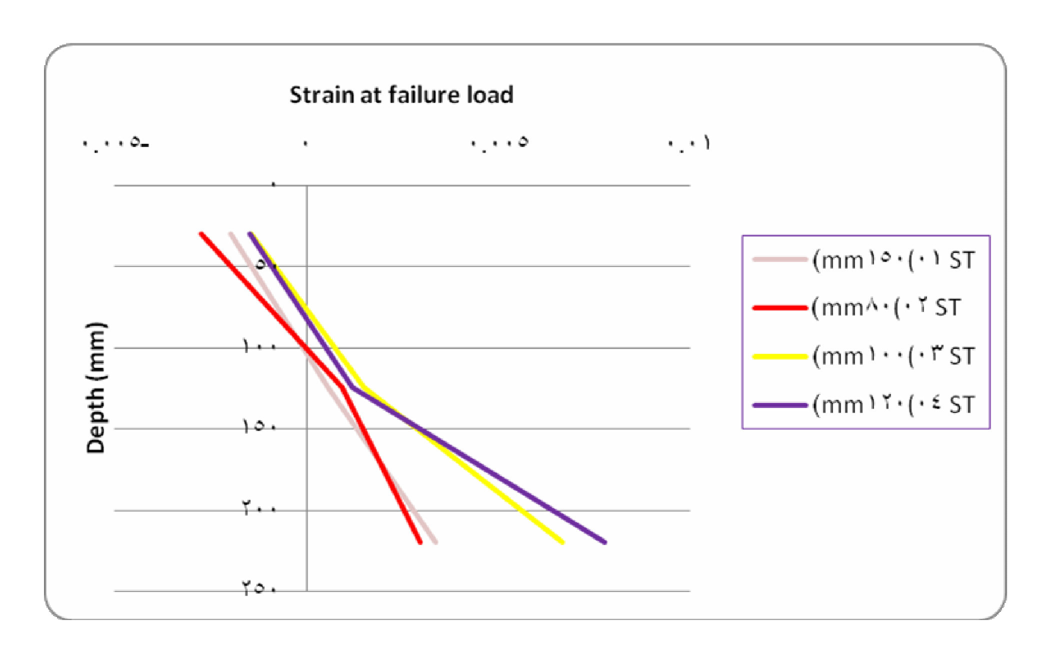


Figure 5.27 Strain profile at middle of span for ST 01, ST 02, ST 03 , and ST 04

The strain profiles distributions with depth for the ST 01, ST 02, ST 03 and ST 04 beams at right side of span are presented in Figure 5.27.

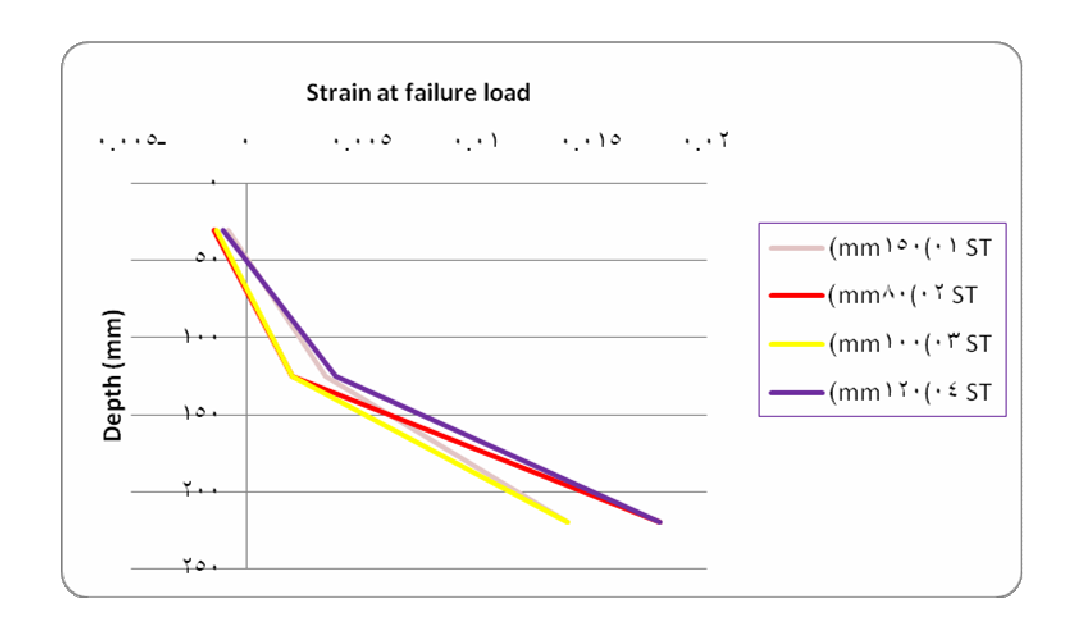


Figure 5.28 Strain profile at right side of span for ST 01, ST 02, ST 03 , and ST 04

All loads – strain curves and strain profiles were given an indication of failure mode of beams strengthened by steel was shear cracks failure. The Figures (5.28, 5.29 and 5.30) show the failure mode of beams strengthened by steel plates.



Figure 5.29 Beam ST 02 at failure



Figure 5.30 Beam ST 03 at failure

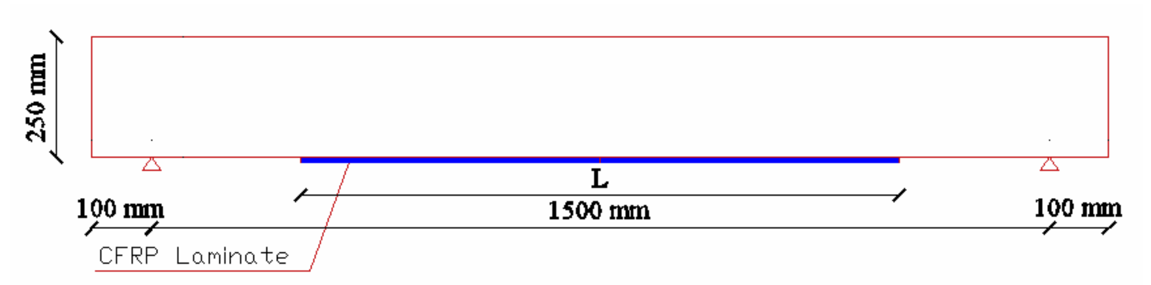


Figure 5.31 Beam ST 04 at failure

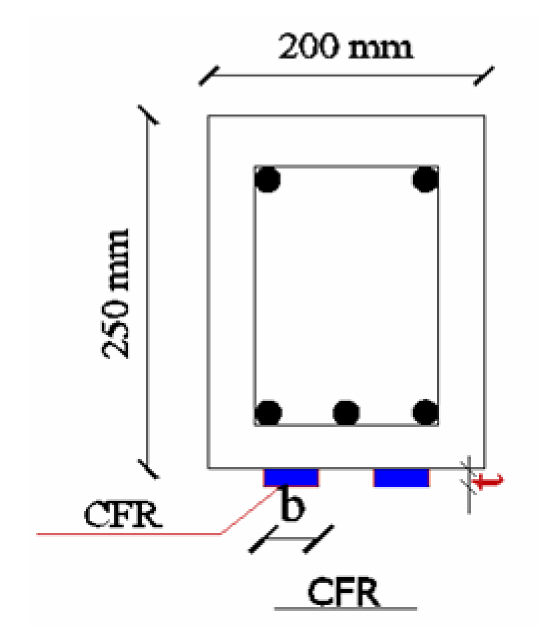
5.4.3 Rectangular beam with CFRP strengthening materials (laminate & Wrap).

5.4.3.1 Reinforced concrete beam (1500mm X 200mm X 250mm) strengthened by CFRP laminate system.

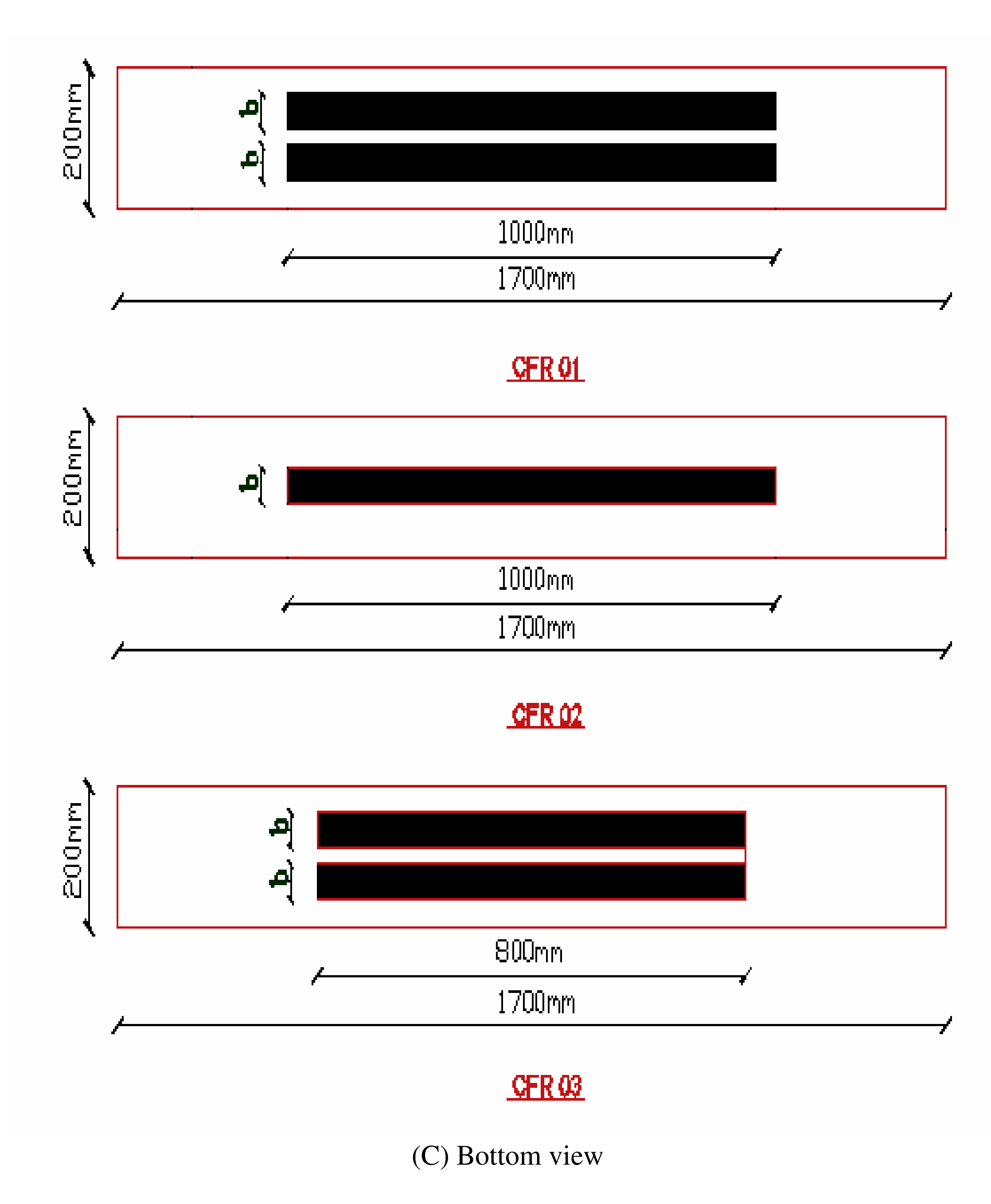
Properties of CFRP						
	Beam	L *(mm)*	b (mm)	t (mm)	Ultimate tensile strength (MPa)	Modulus of elasticity (GPa)
1	CFR01	1000	2X50	1.21	3000	165
2	CFR02	1000	1X50	1.21	3000	165
3	CFR03	800	2X50	1.21	3000	165



(a) Side view beam



(b) Cross section view



(C) Bottom view

Figure 5.32 Details of beams strengthened by carbon fiber laminates

The load – deflection curves of specimens CFR 01, CFR 02 and CFR 03 with control Beam are described in Figure 5.32. The load deflection curves of the strengthened specimens indicated that stiffness of the beams is increased by the carbon fiber reinforced polymer composite material.

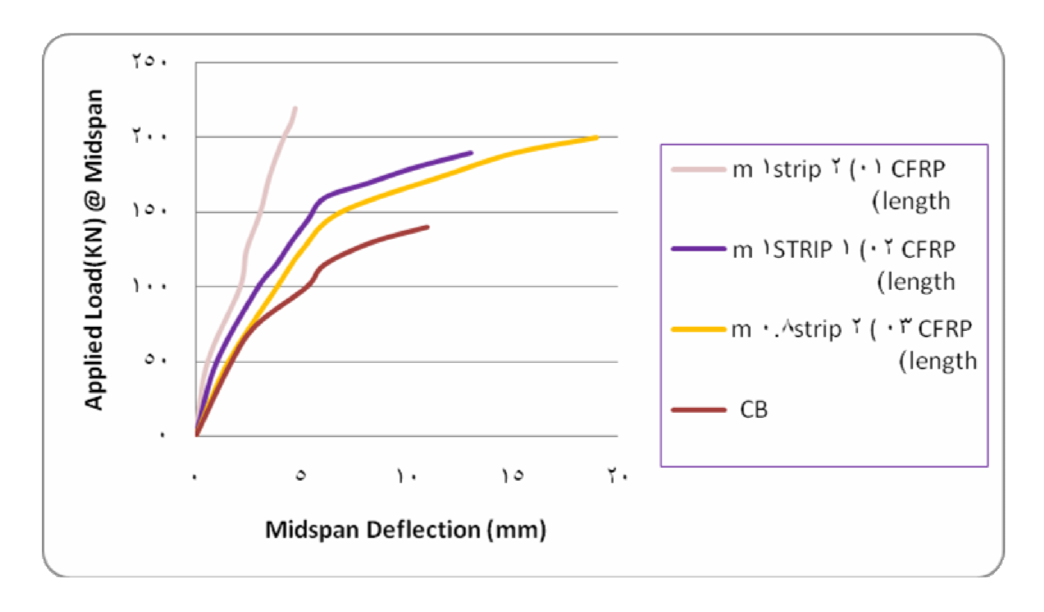


Figure 5.33 Load – versus – midspan deflection for CFRP laminate system with control beam

The load – strain curves on the surface of the concrete at middle of span of specimen CFR 01 are described in Figure 5.33. Compressive strain (strain 1) at failure load, approximately, equals 220 kN is -0.0021, while the strain at tension side (strain 3) at failure load is 0.005.

Figure 5.34 shows the load – strain curves on the surface of the concrete at right side of span of specimen CFR 01. Compressive strain (strain 4) at failure load is -0.0010, while tensile strain (strain 6) is 0.0135.

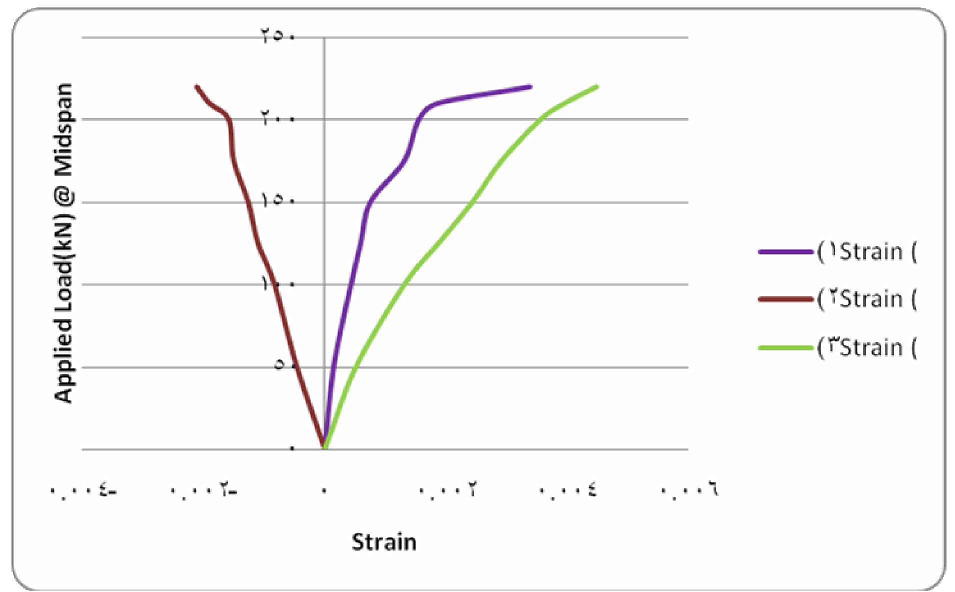


Figure 5.34 Test specimens (CFR 01) – showing strain gauges (1), (2) and (3)

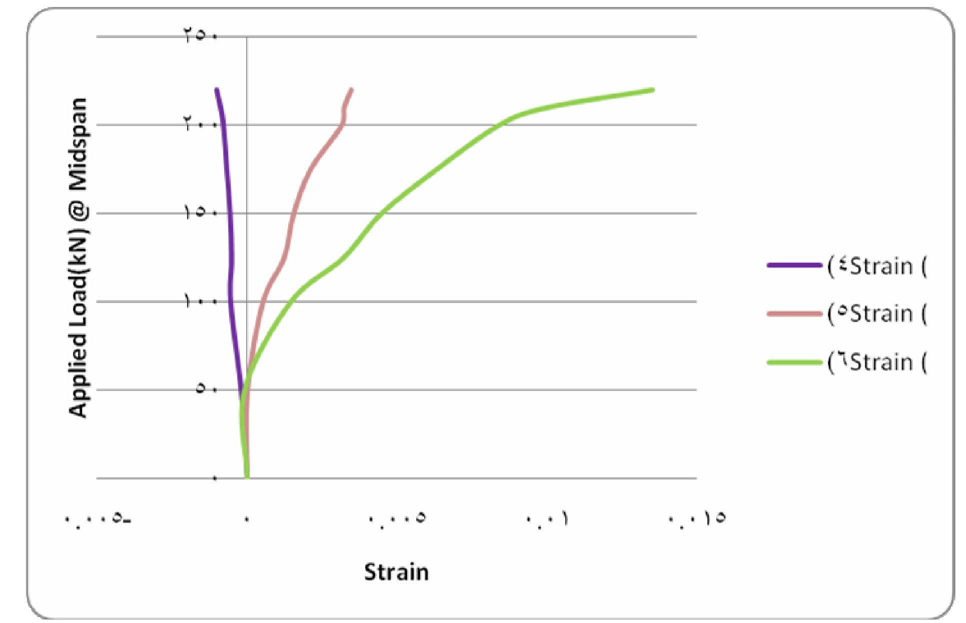


Figure 5.35 Test specimens (CFR01) – showing strain gauges (4), (5) and (6)

Figure 5.35 shows the load – strain curves on the surface of the concrete at middle of span of specimen CFR 02. Compressive strain (strain 1) at failure load, approximately, equals 190 kN is -0.0028, while the strain at tension side (strain 3) at failure load is 0.0064.

The load – strain curves on the surface of the concrete at right side of span of specimen CFR 02 are shown in Figure 5.36. Compressive strain (strain 4) at failure load is -0.0014, while tensile strain (strain 6) is 0.02.

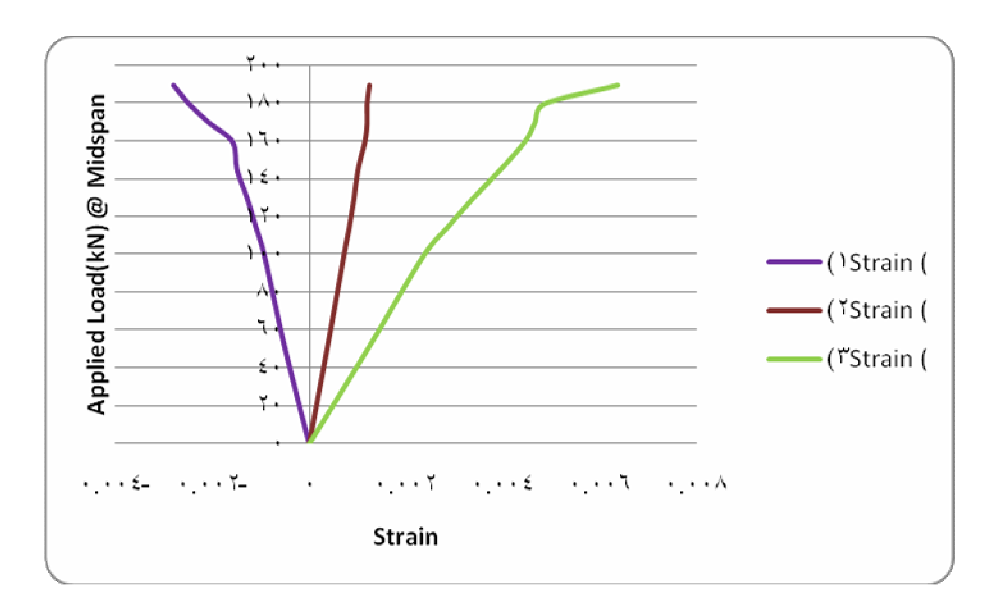


Figure 5.36 Test specimens (CFR 02) – showing strain gauges (1), (2) and (3)

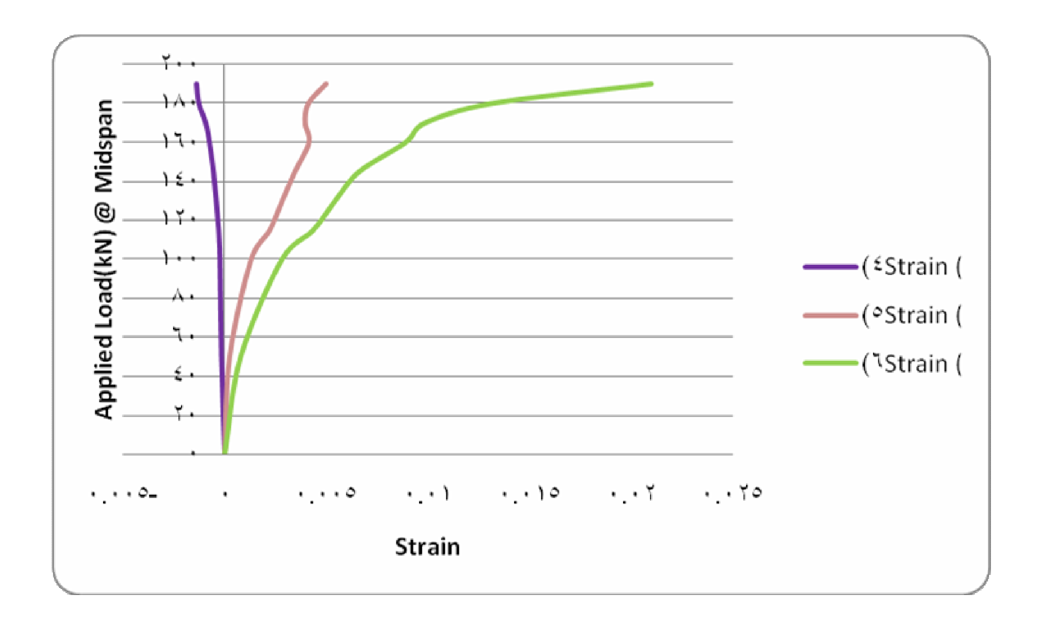


Figure 5.37 Test specimens (CFR02) – showing strain gauges (4), (5) and (6)

Figure 5.37 shows the load – strain curves on the surface of the concrete at middle of span of specimen CFR 03. Compressive strain (strain 1) at failure load, approximately, equals 190 kN is -0.003, while the strain at tension side (strain 3) at failure load is 0.004.

Figure 5.38 shows the load – strain curves on the surface of the concrete at right side of span of specimen CFR 03. Compressive strain (strain 4) at failure load is -0.001, while tensile strain (strain 6) is 0.0112.

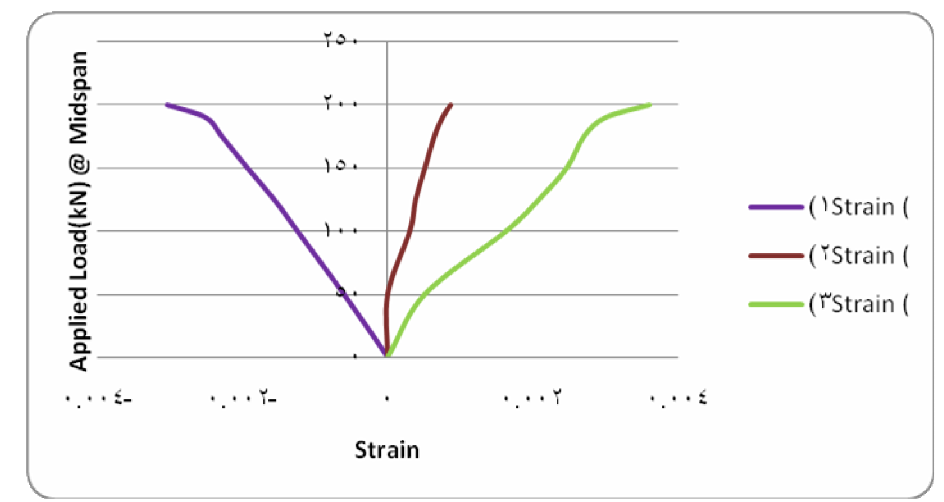


Figure 5.38 Test specimens (CFR 03) – showing strain gauges (1), (2) and (3)

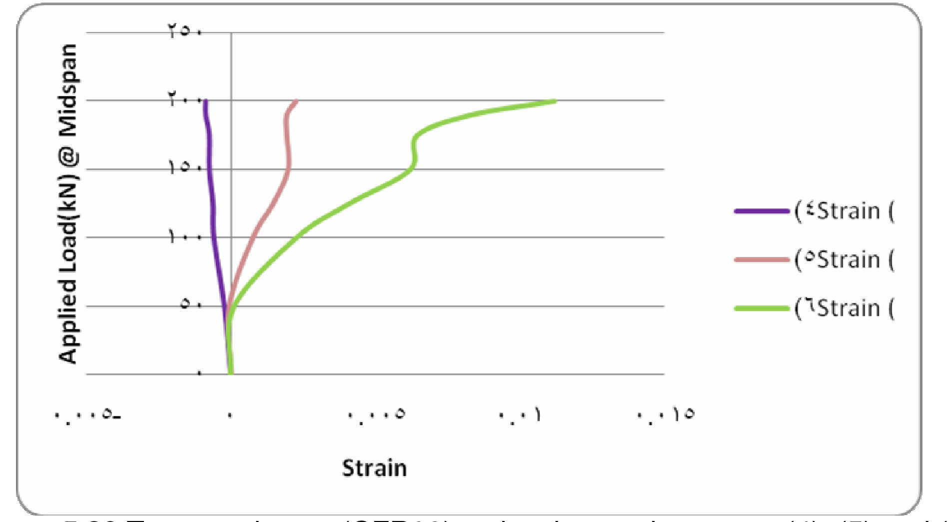


Figure 5.39 Test specimens (CFR03) – showing strain gauges (4), (5) and (6)

Figures (5.39 and 5.40) show the strain profiles distribution with depth for the ST 01, ST 02, ST 03 and ST 04 beams at middle right side of span respectively.

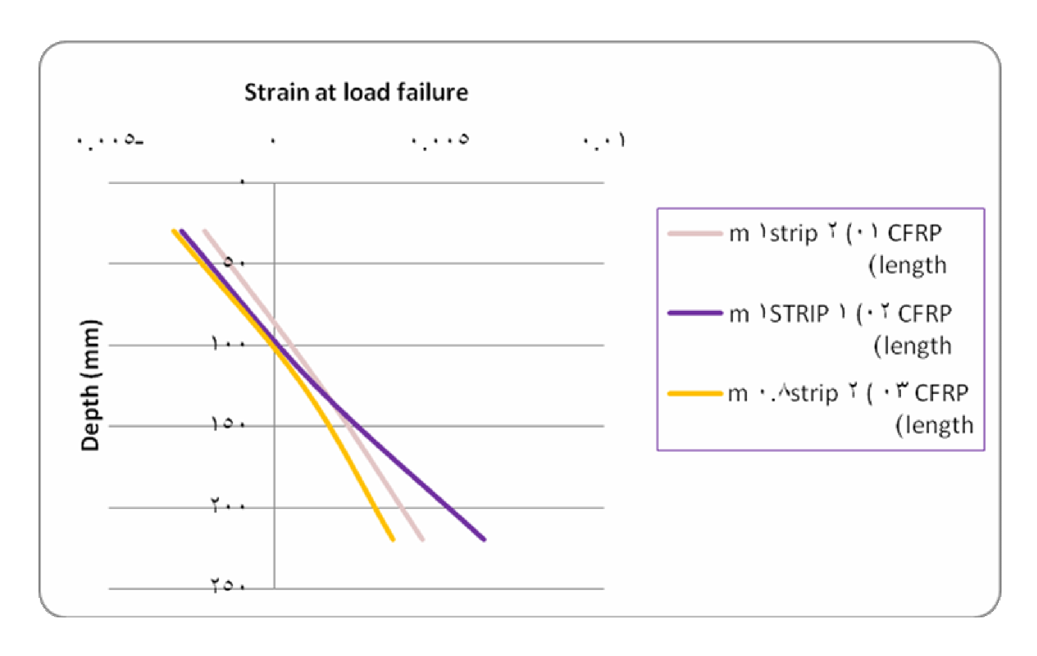


Figure 5.40 Strain profile for CFR 01, CFR 02 and CFR 03 at middle of span

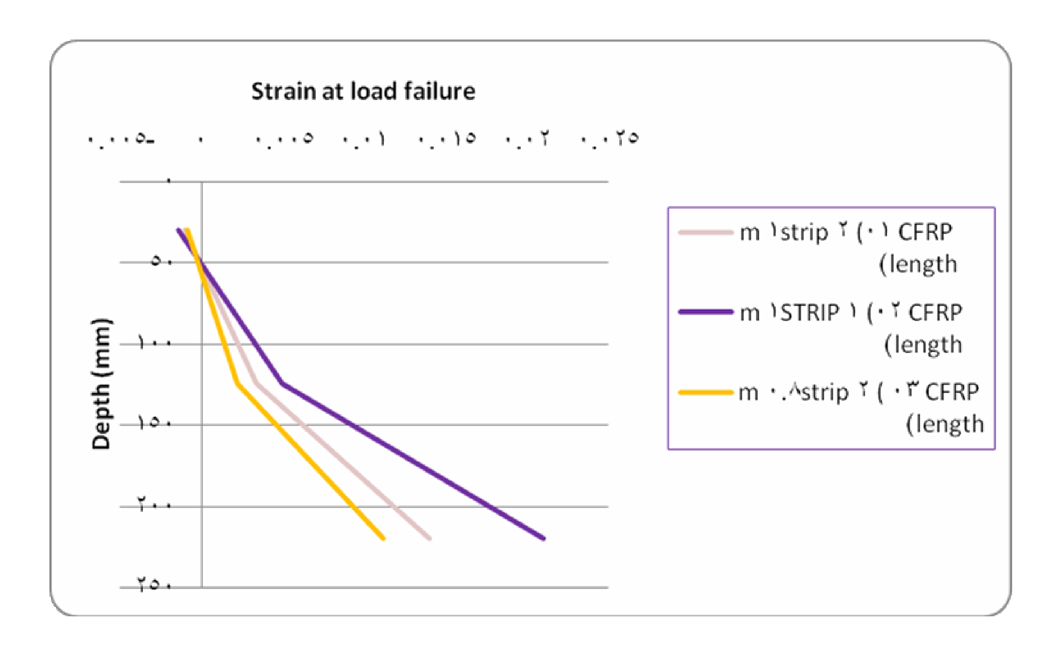


Figure 5.41 Strain profile for CFR 01, CFR 02 and CFR 03 at right side of span

All the load – strain curves and strain profiles were an indication of failure mode of beams strengthened by carbon fiber polymer CFR 01 and CFR 03 were shear failure, while beam CFR 02 flexural failure.

The Figures (5.41, 5.42 and 5.43) show the failure mode of beams strengthened by laminate carbon fiber reinforced polymer.





Figure 5.42 Beam CFR 01 at failure



Figure 5.43 Beam CFR 02 at failure



Figure 5.44 Beam CFR 03 at failure

5.4.3.2 Reinforced concrete beam (1500mm X 200mm X 250mm) strengthened by CFRP wrap system.

Properties of CFRP				
Beam	t(mm)	Ultimate tensile strength	Modulus of elasticity	Rupture strain
CFW01	0.65	650	38600	0.0168
CFW02	0.65	650	38600	0.0168

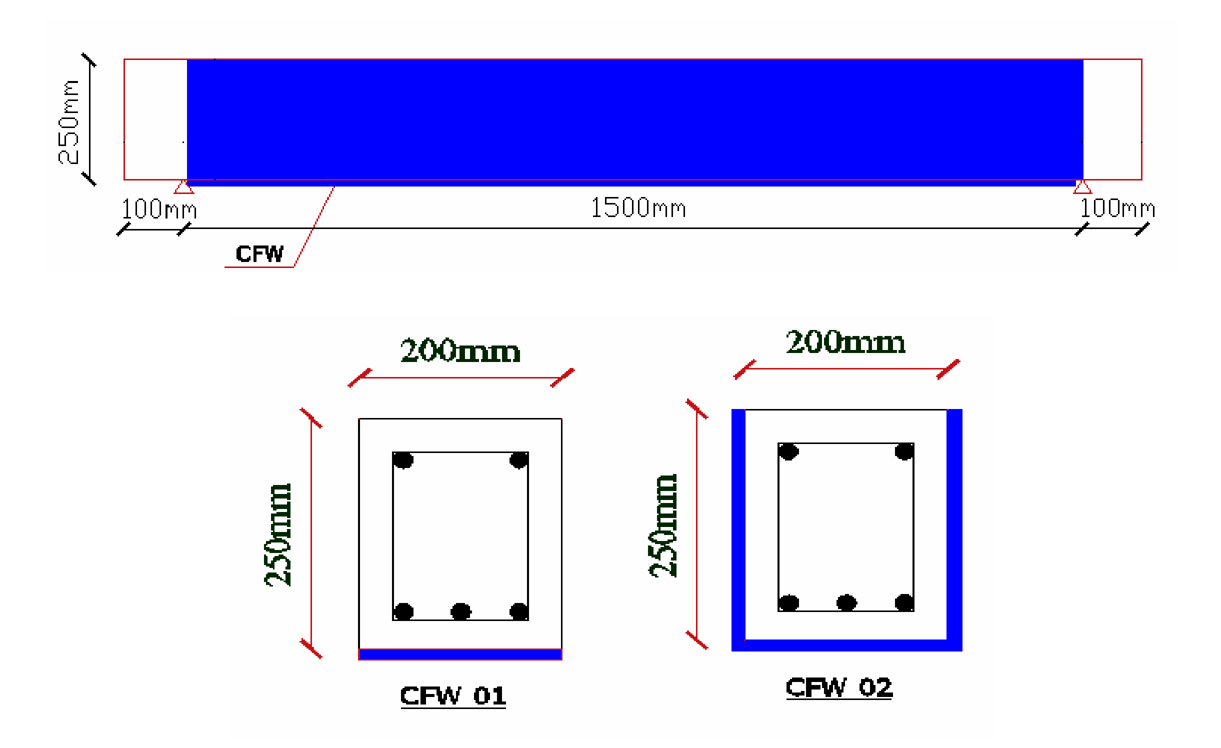


Figure 5.45 beam specimen strengthened by CFRP wrap system

Figure 5.45 shows load – strain curves of specimens CFW01and CFW 02 with control Beam. The slope in the load - deflection curves of the strengthened specimens indicating that stiffness of the beams were increased significantly, by the carbon fiber reinforced polymer composite material.

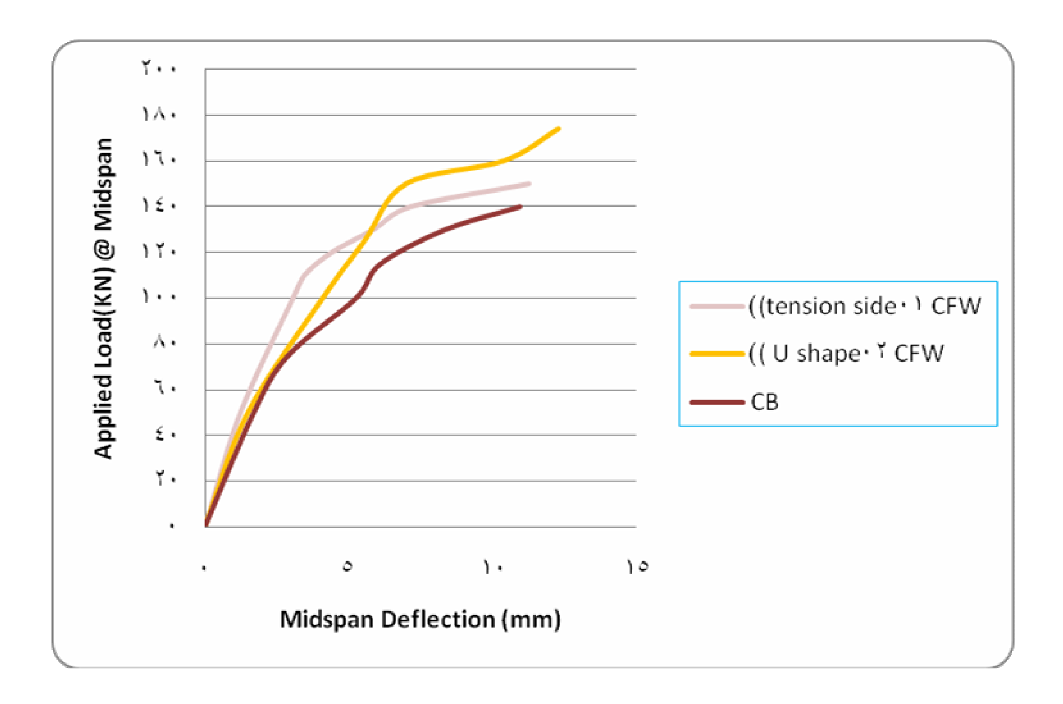


Figure 5.46 Load – versus – midspan deflection for CFRP Wrap system with control beam

Figure 5.46 shows the load – strain curves on the surface of the concrete at middle of span of specimen CFW 01. Compressive strain (strain 1) at failure load, approximately, equals 170 kN is -0.0023, while the strain at tension side (strain 3) at failure load is 0.0061.

Figure 5.47 shows the load – strain curves on the surface of the concrete at right side of span of specimen CFW 01. Compressive strain (strain 4) at failure load is -0.0011, while tensile strain (strain 6) is 0.008.

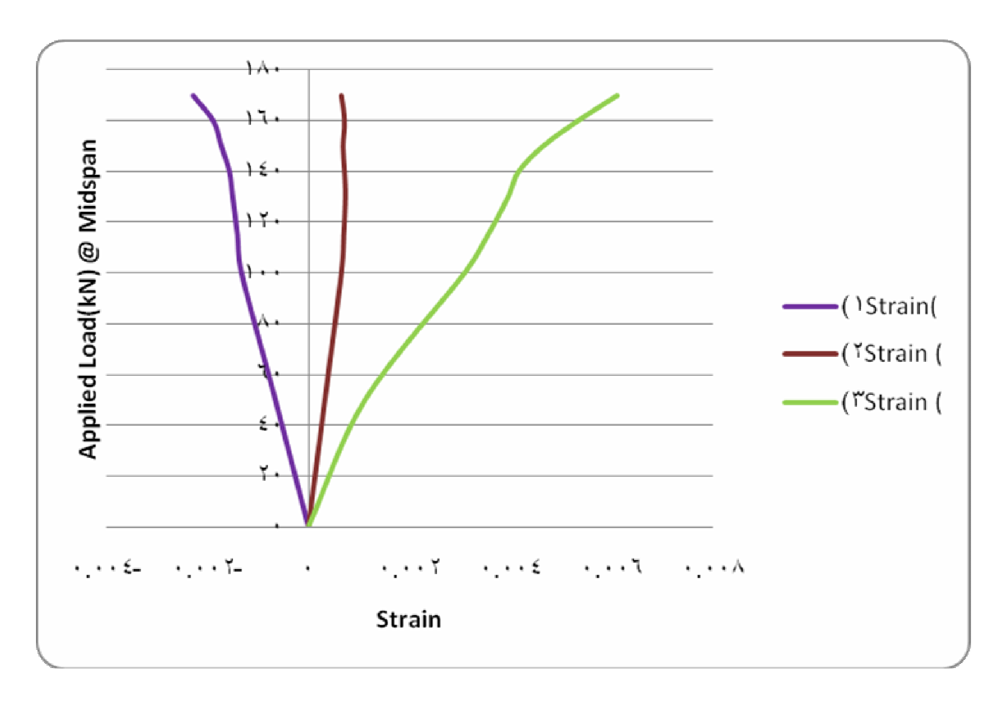


Figure 5.47 Test specimens (CFW 01) – showing strain gauges (1), (2) and (3)

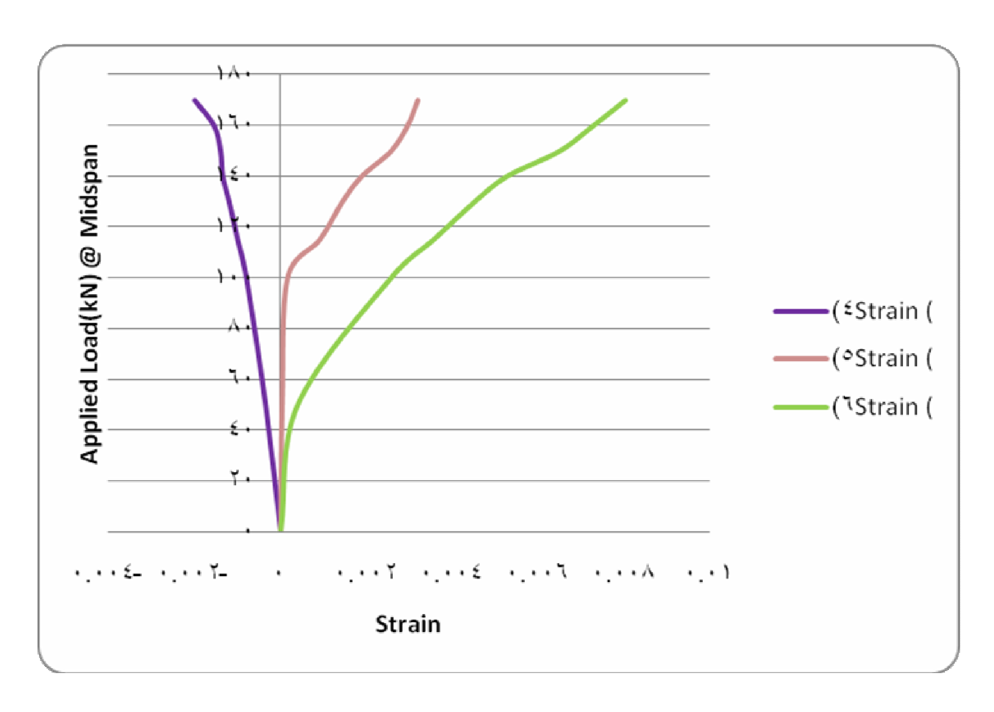


Figure 5.48 Test specimens (CFW01) – showing strain gauges (4), (5) and (6)

Figure 5.48 shows the strain profile distribution with depth for the CFW 01 beam at middle of span, while Figure 5.49 shows the strain profile distribution at the right side of beam.

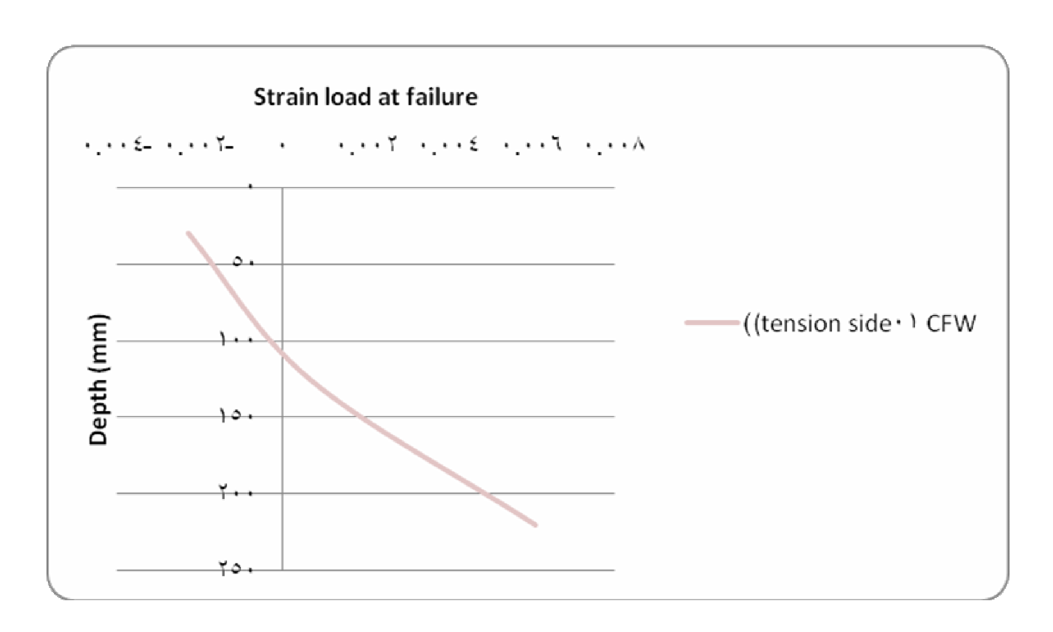


Figure 5.49 Strain profile for CFW 01 at middle of span

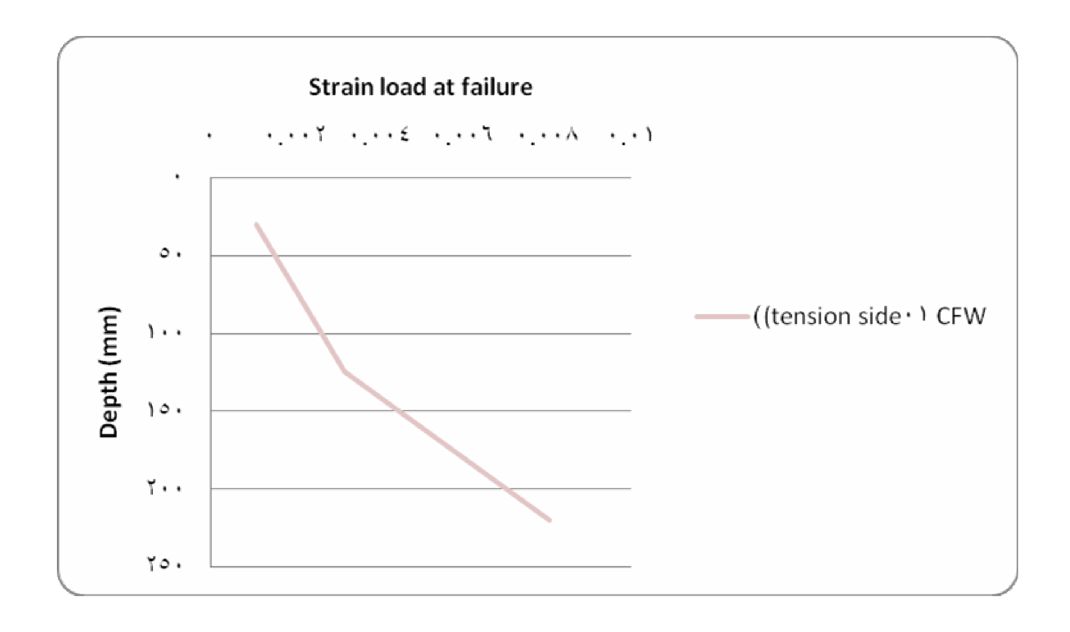


Figure 5.50 Strain profile for CFW 01 at right side of span

5.4 Rectangular beam with light gauge high tensile steel strengthening materials.

Properties of Steel Plate					
Beam	L(mm)	b(mm)	t(mm)	Ultimate tensile strength (MPa)	Modulus of elasticity (GPa)
LG01	1500	150	0.89	550	204
LG02	1500	120	0.89	550	204
LG03	1500	100	0.89	550	204
LG04	1500	2X50	0.89	550	204

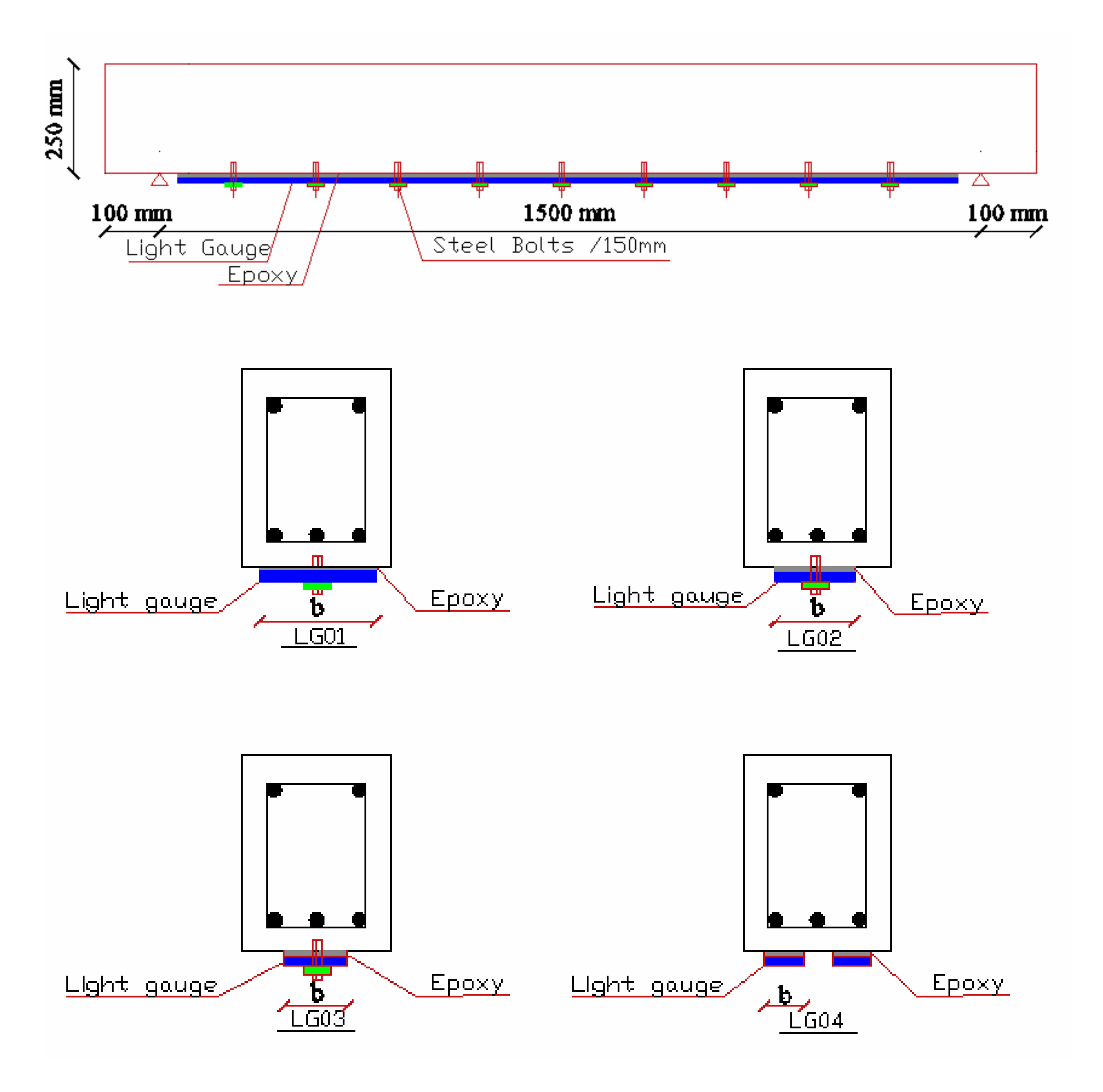


Figure 5.51 Details of beams strengthened by light gauge steel

Load – deflection curves of specimens LG 01, LG 02, LG 03 and LG 04 are compared with load – deflection curves of control Beam in Figure 5.51.

Load - deflection curves of the strengthened specimens indicating that the beams were strengthened by light gauge high tensile steel stiffer than control beam (without composite materials).

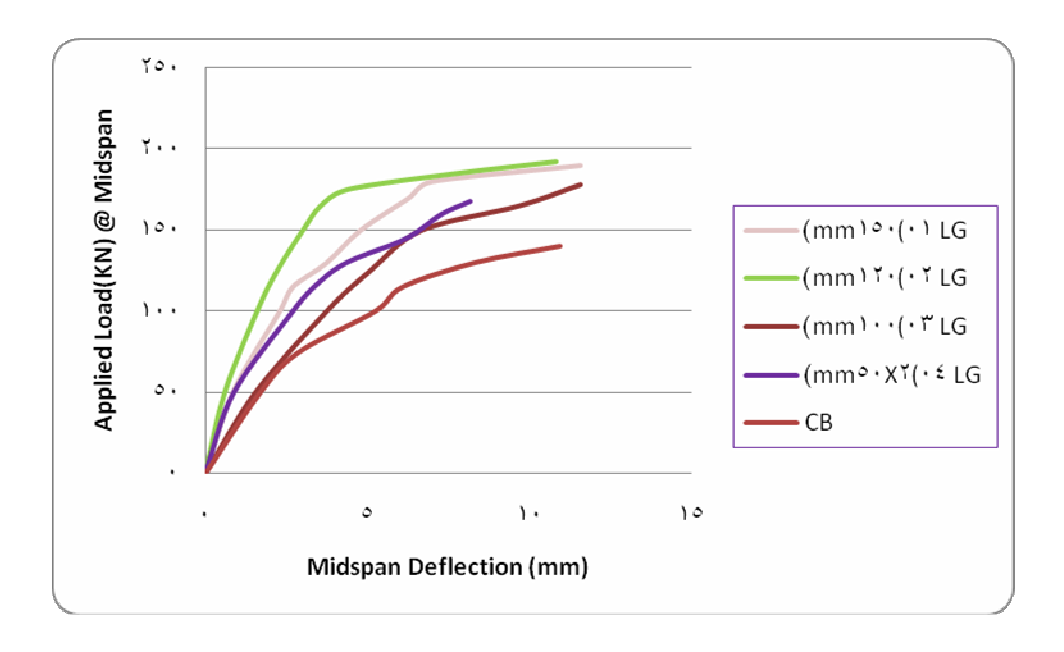


Figure 5.52 Load – versus – midspan deflection for light gauge high tensile steel system

Figure 5.52 shows the load – strain curves on the surface of the concrete at middle of span of specimen LG 01. Compressive strain (strain 1) at failure load, approximately, equal 190 kN was -0.0047, while the strain at tension side (strain 3) at failure load was 0.008.

Figure 5.53 shows the load – strain curves on the surface of the concrete at right side of span of specimen LG 01. Compressive strain (strain 4) at failure load is -0.0019, while tensile strain (strain 6) is 0.0148.

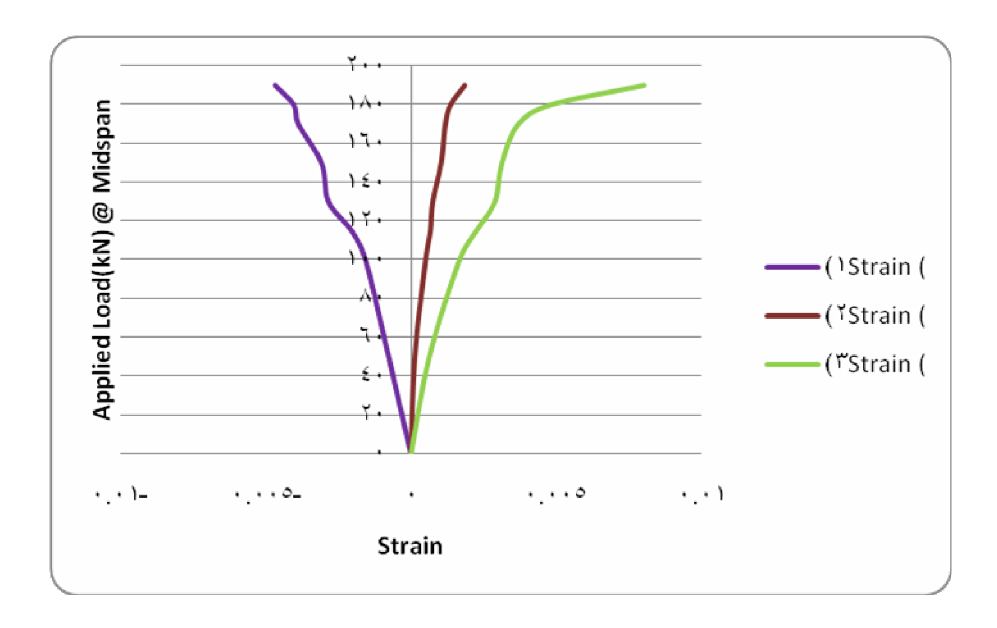


Figure 5.53 Test specimens (LG 01) – showing strain gauges (1), (2) and (3)

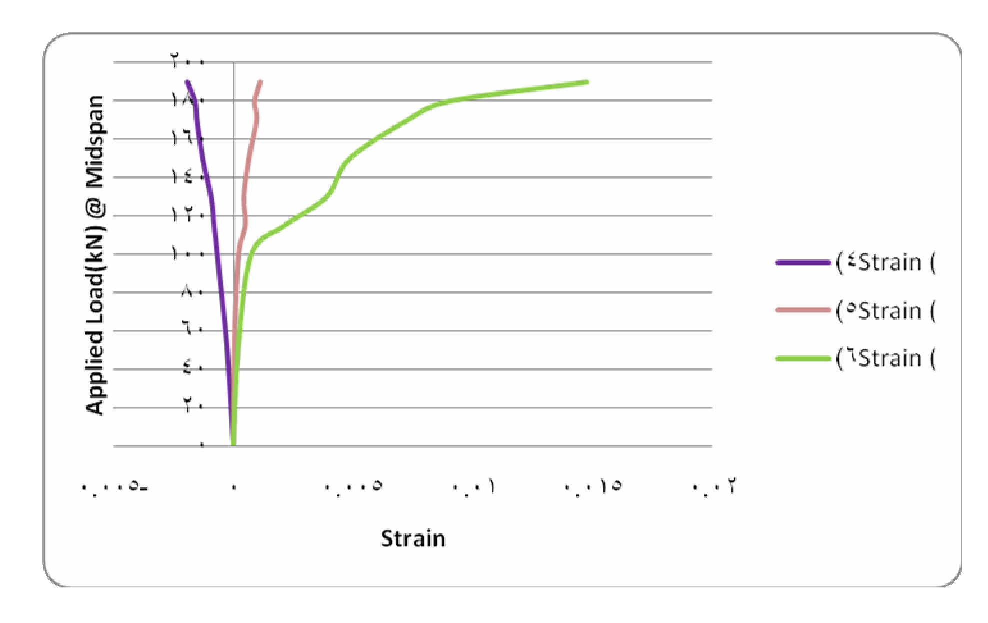


Figure 5.54 Test specimen (LG 01) – showing strain gauges (4), (5) and (6)

Figure 5.54 shows the load – strain curves on the surface of the concrete at middle of span of specimen LG 02. Compressive strain (strain 1) at failure load, approximately, equals 192 kN is -0.0022, while the strain at tension side (strain 3) at failure load is 0.0257.

Figure 5.55 shows the load – strain curves on the surface of the concrete at right side of span of specimen LG 02. Compressive strain (strain 4) at failure load is -0.0016, while tensile strain (strain 6) is 0.0158.

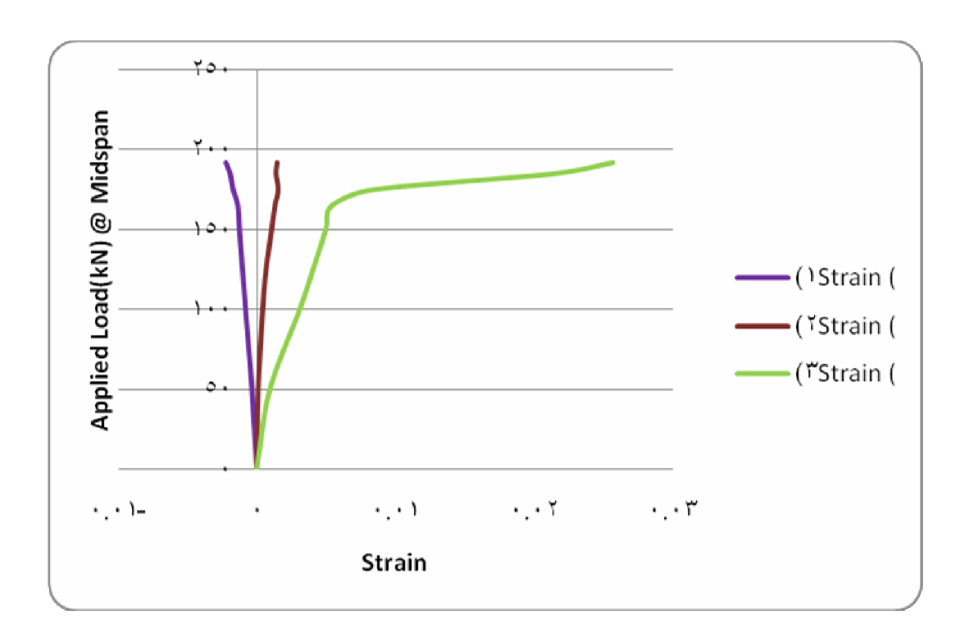


Figure 5.55 Test specimens (LG 02) – showing strain gauges (1), (2) and (3)

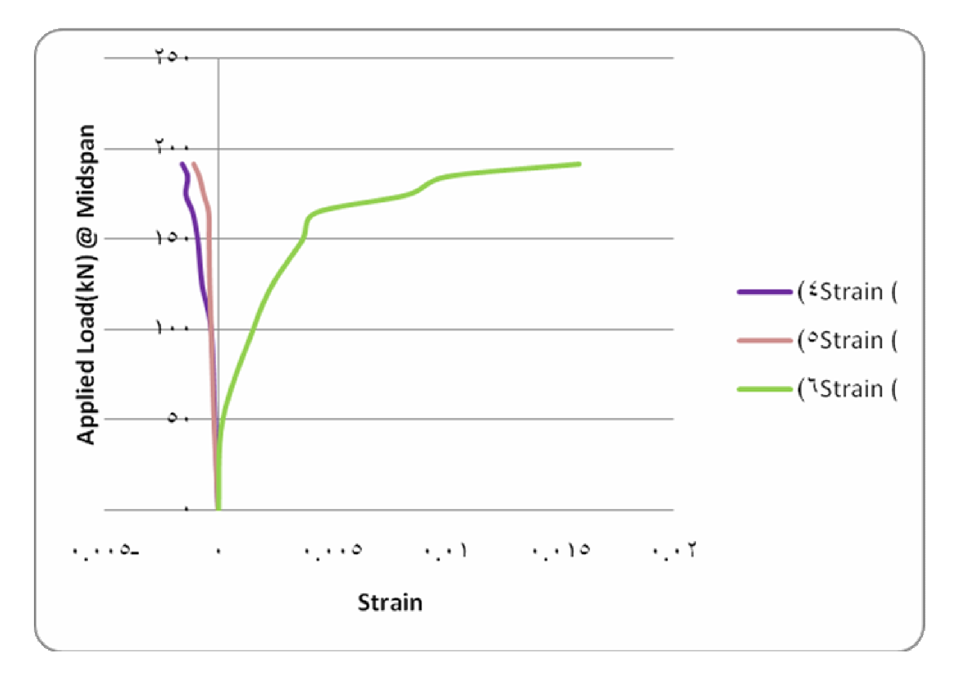


Figure 5.56 Test specimen (LG 02) – showing strain gauges (4), (5) and (6)

Figure 5.56 shows the load – strain curves on the surface of the concrete at middle of span of specimen LG 03. Compressive strain (strain 1) at failure load, approximately, equals 178 kN is -0.0033, while the strain at tension side (strain 3) at failure load is 0.0047.

Figure 5.57 shows the load – strain curves on the surface of the concrete at right side of span of specimen LG 03. Compressive strain (strain 4) at failure load is -0.0015, while tensile strain (strain 6) is 0.0179.

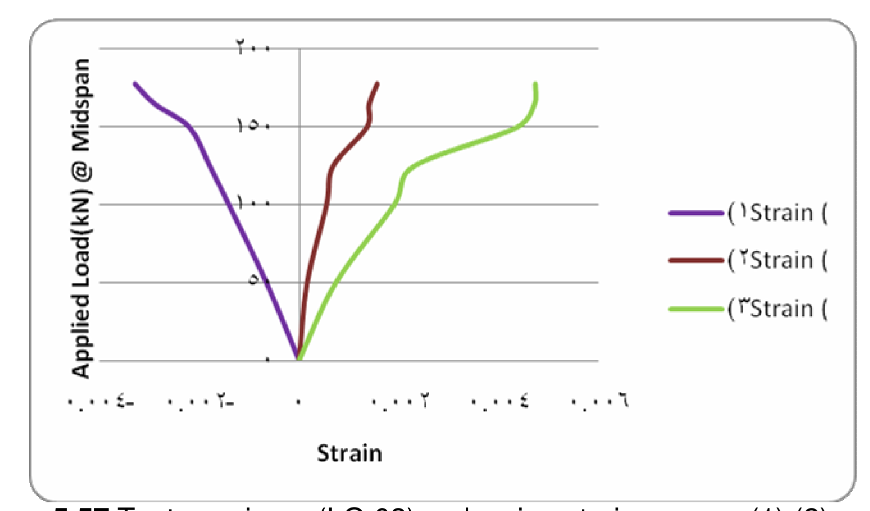


Figure 5.57 Test specimen (LG 03) – showing strain gauges (1),(2) and (3)

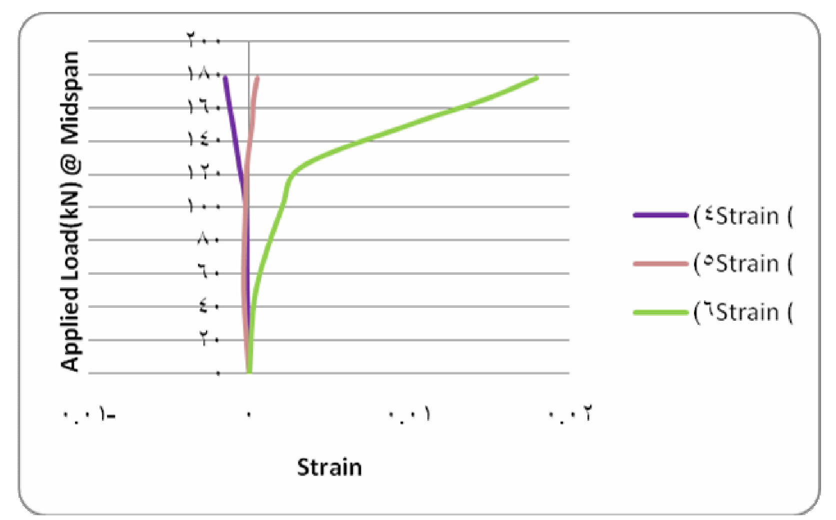


Figure 5.58 Test specimen (LG 03) – showing strain gauges (4),(5) and (6)

Figure 5.58 shows the load – strain curves on the surface of the concrete at middle of span of specimen LG 04. Compressive strain (strain 1) at failure load, approximately, equals 168 kN is -0.0013, while the strain at tension side (strain 3) at failure load is 0.0064.

Figure 5.59 shows the load – strain curves on the surface of the concrete at right side of span of specimen LG 01. Compressive strain (strain 4) at failure load is -0.0005, while tensile strain (strain 6) is 0.0112.

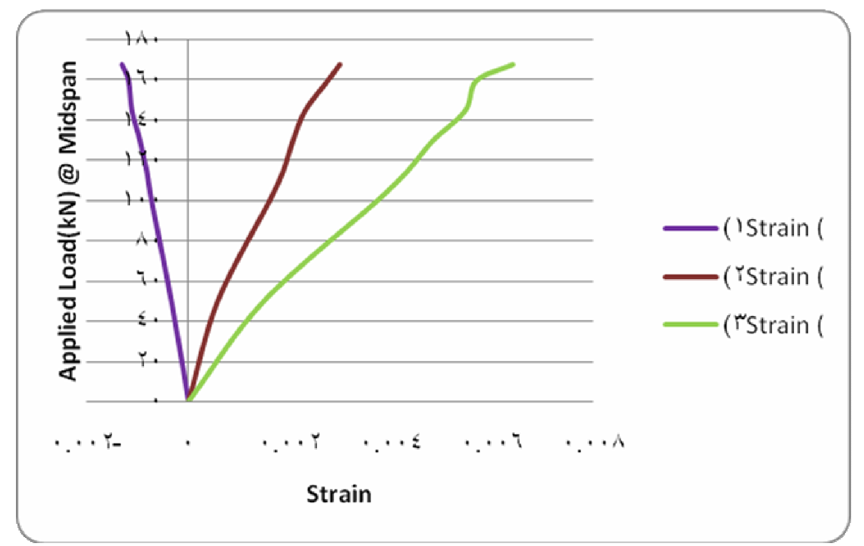


Figure 5.59 Test specimens (LG 04) – showing strain gauges (1), (2) and (3)

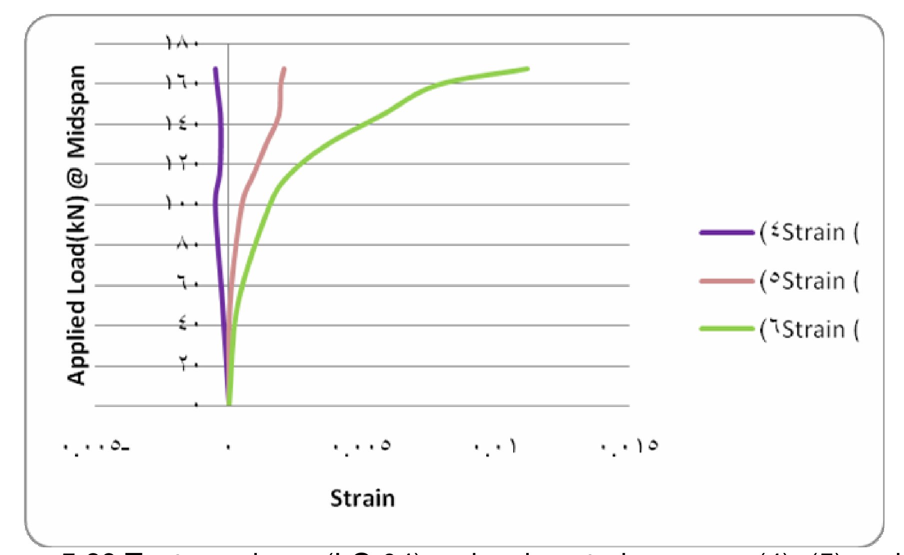


Figure 5.60 Test specimen (LG 04) – showing strain gauges (4), (5) and (6)

Figure 5.60 shows the strain profiles distribution with depth for the LG beam at middle of span of span, while Figure 5.61 shows the strain profiles distribution at the right side of beam.

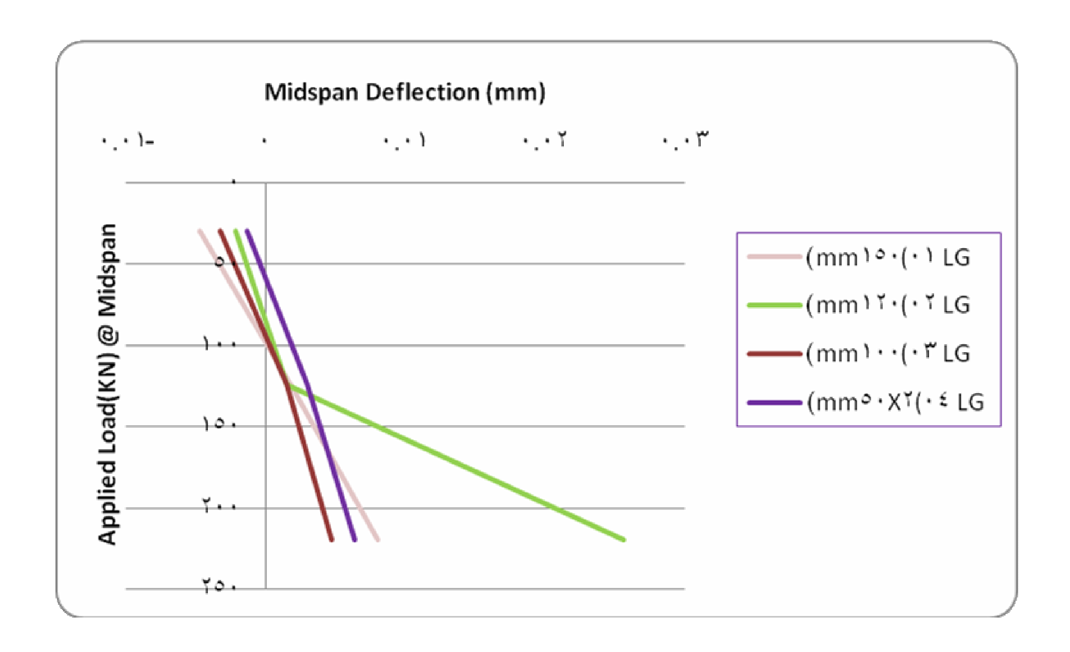


Figure 5.61 Strain profile for LG 01, LG 02, LG 03 and LG 04 at middle of span

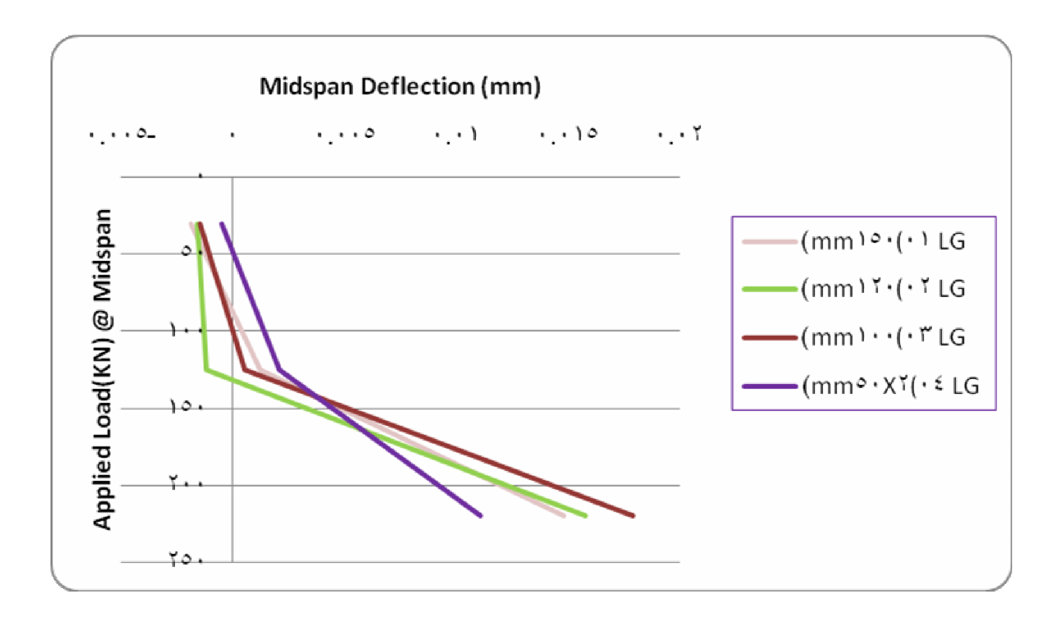


Figure 5.62 Strain profile for LG 01, LG 02, LG 03 and LG 04 at right side

All load – strain curves and strain profiles were an indication of failure mode of beams strengthened by light gauge high tensile steel (LG01, LG02, LG03 and LG04).

Figures (5.62,5.63,5.64 and 5.65) show (LG 01 and LG 02) failure, the failure happened after occurrence many cracks which caused shear crack failure while LG 02 failure mode was flexural cracks failure, but the failure mode of specimen LG 04 was cover delimitation.





Figure 5.63 Beam LG 01 at failure



Figure 5.64 Beam LG 03 at failure



Figure 5.65 Beam LG 04 at failure

5.5 Result and Discussion

The measured load-deflection was compared within the different groups of strengthening composite materials (Carbon Fiber Polymer, Steel Plate and Light Gauge High Tensile Steel) along with unstrengthened beams (control beams).

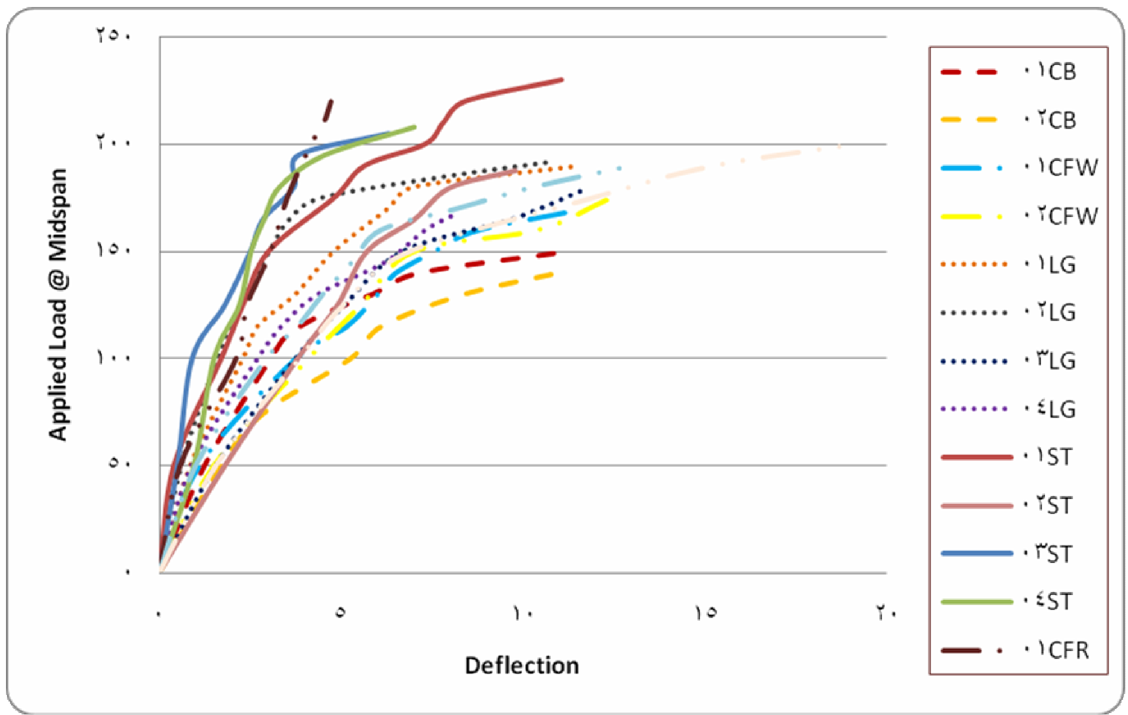


Figure 5.66 Load – versus – midspan deflection for CFRP, steel plate, light gauge high tensile steel and Control beams

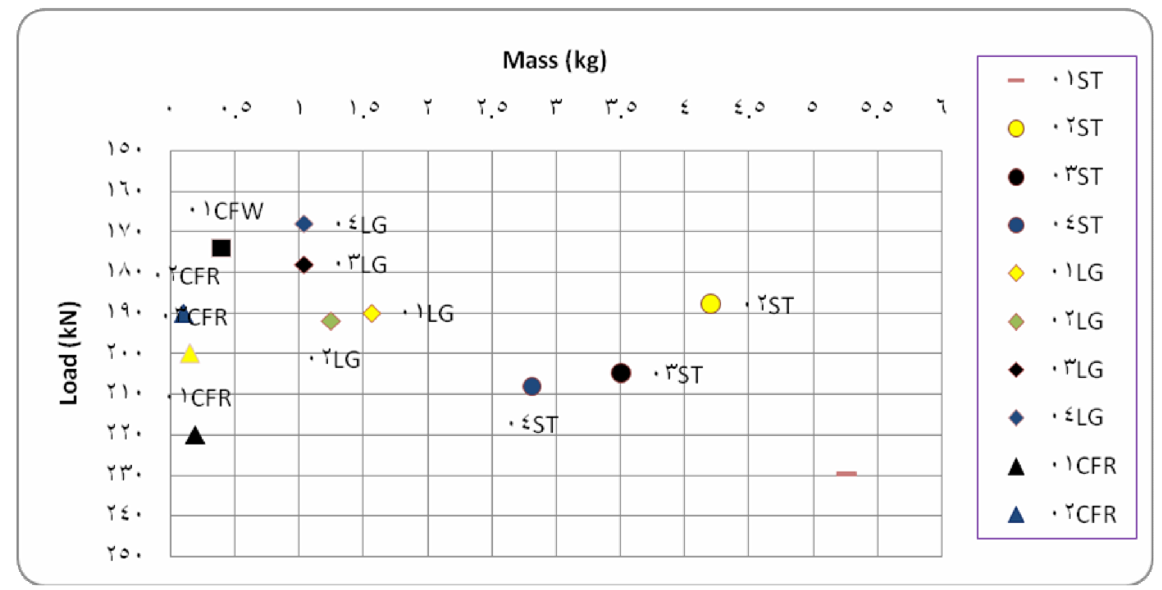


Figure 5.67 Load – versus – Mass for composite materials

Table (5.1) Theoretical and Experimental Results

Beam	Theoretical	Experimental	Failure Mode
	Mu	Mu	
CB01	28.9	37.5	Flexural Crack
CB02	28.9	35	Flexural Crack
ST01	57.8	57.5	Cover delimitation
ST02	55.37	47	Plate end shear
ST03	50.83	51.25	Concrete Crushing
ST04	46.13	52	Cover delimitation
CFR01	45.83	55	Debonding of strengthening material
CFR02	45.83	47.5	Cover delimitation
CFR03	40.52	50	Debonding from flexural crack
CFW01	41.75	42.5	Debonding from flexural crack
CFW02	41.75	43.5	Concrete Crushing
LG01	40.89	47.5	Plate end shear
LG02	38	48	Debonding from shear crack
LG03	36.07	44.5	Plate end shear
LG04	36.07	42	Cover delimitation

Table 5.1 Summarizes the test results and failure modes of all tested beams, failures in reinforced concrete beams strengthened by composite materials were occurred by flexural failures of critical sections, such as rupture and crushing of concrete, or by debonding of plate from the RC beams. Debonding in strengthened reinforced concrete beams occurs in regions of high stress concentrations, which are associated with material discontinuities and with the presence of cracks.

The failure mechanisms of ST01, ST04, CFR02 and LG04 were cover delimitation which usually associated with high stresses, low concrete strength or with extensive shear cracking but the mechanism failure of ST02, LG01 and LG03 were end plate shear, which associated with insufficient shear capacities, to prevent debonding from plate ends we need an anchor bolts or mechanics clamping. On other hand the failure of LG02 was debonding from shear crack due to large flexure-shear cracks.

Chapter 6 Summary, Conclusions and Recommendations

This chapter reports and discusses conclusions of the experimental program and a summary of the test procedure in addition to recommendations for future researches.

6.1 Summary

The objective of this research was to investigate composite material for the purpose of strengthening reinforced concrete beams.

The research divided into four phases included 15 rectangular reinforced concrete beams. The first phase of the research project included testing 2 rectangular concrete beam specimens without strengthening material, Second stage included 4 rectangular concrete beams strengthened by using steel plates with length 1500mm, with different widths (150, 120, 100, and 80mm) and thickness 3mm, Third stage included 5 rectangular beams strengthened by CFRP (laminate and wrap system) three of them strengthened by laminate carbon fiber with length (1000 and 800mm), width 50mm and 1.21mm thickness and last stage included 4 rectangular concrete beams strengthened by light gauge high tensile steel with 1500mm length, width (150, 120, 100 and 2X50mm) and 0.89mm thickness.

The flexural strength of reinforced concrete beams strengthened by carbon fiber reinforced polymer are increased up to 57% while the flexural strength of beams strengthened by steel plates and light gauge high tensile steel plates are increased up to 48% and 37%, respectively.

All specimens were tested monotonically to failure by debonding of the composite materials from the surface of concrete.

6.2 Conclusions

This thesis presents a theoretical and experimental approach for the strengthening of reinforced concrete beams with externally bonded steel plates, CFRP and light gauge high tensile steel plates.

1- The application of carbon fiber reinforced polymer (CFRP) and steel plates were very effective for flexural strengthening of reinforced concrete beams, but the thickness of steel plates was 3mm and the density was $7.8 g/cm^3$, while the thickness of CFRP was 1.21mm and the density was $1.6 g/cm^3$, so the strength to weight ratio was a very effective for CFRP.

2- Compared with the deflection of beams strengthened by carbon fiber reinforced polymer, steel plate and light gauge high tensile steel along with the control beams. The beams strengthened by carbon fiber reinforced polymer have adequate deformation capacity, in spite of their brittle modes.

3- To achieve full capacity of strengthened beams and prevent end plate, peeling and cover delimitation failures, the design of end anchorage is very important. One of the most anchorage systems common is mechanical anchorage by clamping or CFRP wrapping system.

6.3 Recommendations

It is recommended that future research should include:

- Mechanical clamping combined with adhesion is effective in anchoring the external composite materials and increases the anchorage capacity above that expected for adhesive bond only.

- It would be worth to extend this research study to other types of composite materials, as glass fiber reinforced polymer (GFRP) and aramid fiber reinforced polymer (AFRP).

- Determine the feasibility of using the external composite materials to strengthen beams in compression (continuous or cantilever beams).

REFERANCES

ACI Committee 318 (2005), **"Building Code Requirements for Structural Concrete (ACI 318-05) and Commentary (318R-05)"**, American Concrete Institute, Farmington Hills

ACI 440 (2002). **"Guide for the design and construction of externally bonded FRP systems for strengthening concrete structures"**, ACI 440.2R-02, American Concrete Institute.

Anders Carolin (2003), "**Carbon Fiber Reinforced polymers for Strengthening of Structural Elements**", PhD Thesis, Department of Civil and Mining Engineering Division of Structural Engineering.

ASCE (1984), **"Structural Plastic Design Manual "**, ASCE Manual and Report on Engineering Practice No. 63, ASCE, Reston, USA.

Barros, J. and Fortes, A. (2005), "**Flexural Strengthening of Concrete Beams with CFRP Laminates Bonded Into Slits**", Cement & Concrete Composites

Beber, A. J., Filho, A. C., and Campagnolo (2001), "**CFRP in the Strengthening of Reinforced Concrete Beams**", Proceedings of the International Conference on FRP Composites in Civil Engineering, Hong Kong, China.

Büyüköztürk, O., O. Gunes, and E. Karaca (2004), "**Progress on understanding debonding problems in reinforced concrete and steel members strengthened using FRP composites**", Construction and Building Materials, Vol. 18, pp.9-19.

Dat Duthinh & Monica Stranes (2001), "**Strengthening of Reinforced Concrete Beams with Carbon FRP**", National Institute of Standards and Technology, ISBN 90 2651 858 7.

De Lorenzis, L. and Teng, J. (2006), "**Near-Surface Mounted FRP Reinforcement: An Emerging Technique for Strengthening Structures**", Composites Part B: Engineering.

Diego L. Vasquez Rayo (2008), " **Plate-End Debonding of longitudinal Near Surface Mounted Fiber Reinforced Polymer Strips on Reinforced Concrete Flexural Members**", MSc Thesis, North Carolina State University.

Emmanuelle David, Chafika Djelal, Francios Buyle (1998), "**Repair and Strengthening of Reinforced Concrete Beams Using Composite Material**", 2ND Int. PhD Symposium in Civil Engineering Budapest.

Foster DC, Richards D, Boqner BR., (2000), **"Design and installation of fiber-reinforced polymer composite bridge,"** Journal of Composites for Construction, ASCE 4(1), pp. 33-37.

Gunes, O. (2004), **"A Fracture Based Approach to Understanding Debonding in FRP Bonded Structural Members"**, Ph.D. Thesis, Massachusetts Institute of Technology, Cambridge, MA.

Han Tae Choi (2008), " **Flexural Behaviour of Partially Bonded CFRP Strengthened Concrete T-Beams "**, PhD thesis, Civil and Environmental Engineering Waterloo, Canada.

Leung, C.K.Y. (2001), "**Delimitation Failure in Concrete Beams Retrofitted with a Bonded Plate**", Journal of Materials in Civil Engineering, Vol. 13, No. 2, pp.106-113.

Meier, U., Deuring, M., Meier, H., and Schwegler, G. (1992). **"Strengthening of structures with CFRP laminates: Research and applications in Switzerland."** Advanced Compos. Mat. in Bridges and Struct., K. W. Neale and P. Labossiere, eds. Canadian Society for Civil Engineers, Montreal.

Meier, U. and Winistörfer, A., (1995), **"Retrofitting of Structures through External Bonding of CFRP Sheets,"** Non-metallic (FRP) Reinforcement for Concrete Structures, Ed. L. Taerwe, pp. 465-472.

Miller, B. (1999), "**Bond Between Carbon Fiber Reinforced Polymer Sheets and Concrete**", MSc. Thesis, Department of Civil Engineering, University of Missouri.

Mohd Zamin Jumaat and Md. Ashraful Alam (2008), **"Strengthening of R.C. Beams Using Externally Bonded Plates and Anchorages"**, Australian Journal of Basic and Applied Sciences, 3(3): 2207-2211.

Nanni, A. (1999), **" Composites: Coming on Strong "** Concrete Construction, Vol. 44.

O. Gunes, E. Karaca, and B. Gunes(2006), "**Design of FRP Retrofit Flexural Members Against Debonding Failures**", Proceedings of the 8th U.S. National Conference on Earthquake Engineering April 18-22, 2006, San Francisco, California, USA, Paper No. 1205.

Oral Büyüköztürk, Tzu-Yang Yu (2006), "**Understanding and Assessment of Debonding Failures in FRP-Concrete Systems**" Yildiz Technical University, Istanbul, Turkey.

Shin, Y.S., Lee, C., (2003), "**Flexural Behavior of RC Beams Strengthened with Carbon Fiber-Reinforced Polymer Laminates at Different Levels of Sustaining Load**". ACI Structural Journal, 100(2):231-239.

Shouping Shang, Patrick X.W. Zou, Hui Peng1, and Haidong Wang (2005), "**Avoiding DE-Bonding in FRP Strengthened Reinforced Concrete Beams Using Prestressing Techniques**", Proceedings of the International Symposium on Bond Behaviour of FRP in Structures.

Tang B. (1997), **"Fiber Reinforced Polymer Composites Applications"** First Korea/U.S.A. Road Workshop Proceedings.

Teng, J., De Lorenzis, L., Wang, B., Rong, L., Wong, T. and Lam, L. (2006), "**Debonding Failures of RC Beams Strengthened with Near Surface Mounted CFRP Strips**", ASCE Journal of Composites for Construction.

Tom Norris and Hamid Saadatmanesh (1997), "**Shear and Flexural Strengthening of RC Beams with Carbon Fiber Sheets**", ASCE.

Yung-Chih Wang *, Kai Hsu (2008), "**Design Recommendations for the Strengthening of Reinforced Concrete Beams with Externally Bonded Composite Plates**", Composite Structure.

Ziraba, Y.N., Baluch, M.H., Basunbul, I.A., Sharif, A.M., Azad, A.K., Sulaimani, G.J. (1994), "**Guidelines Toward The Design of Reinforced Concrete Beams with External Plate**", ACI Structural Journal ;91(6):639-646.

ZHANG Ai-hui, JIN Wei-liang, LI Gui-bing (2006) , "**Behavior of Preloaded RC Beams Strengthened with CFRP Laminates**", Journal of Zhejiang University SCIENCE A, ISSN 1009-3095.

Appendix A: Theoretical Flexural Design

A.1 Control Beams.

Calculations

Equilibrium:

$$a = \frac{A_s f_y}{0.85 f_c' b}$$

Where

A_s = 339 mm²
f_y = 420 Mpa
f_c '= 25 Mpa

$$a = 33.5mm$$

$$c = a/\beta = 33.5/0.85 = 39.41mm$$

Compatibility

$$\varepsilon_s = 0.003 \frac{(d-c)}{c}$$

$$\varepsilon_s = 0.0129 > \varepsilon_y\ (0.005)$$

Flexural Capacity

$$\square M_n = \square\ (A_s f_y (d - \frac{a}{2})$$

$$\square M_n = 26.05 \text{ kN.m}$$

A.2 Carbon Fiber Reinforced Polymer (Wrap System)

From (section 8.1)

a = 33.5mm
c = 39.41mm
$\varepsilon_s = 0.0129 > \varepsilon_y$ (0.005)
$\square M_n$ = 24.76 kN.m

Properties of RC beam

$E_c = 4750\sqrt{25} = 23750$ MPa

$\rho_s = \frac{A_s}{b \times d} = 0.008$

$n_s = \frac{E_s}{E_C} = 8.42$

$\rho_s \ n_s = 0.0674$

Properties of CFRP material

We assume that the beam is interior so the environmental reduction factor C_E from Table 4.1 = 0.95

$$A_f = 0.89\ (200) = 178 mm^2$$

$$f_{fu} = C_E f_{fu}^* = 0.95\ (650) = 617.5 \text{ MPa}$$

$$\varepsilon_{fu} = C_E\ \varepsilon_{fu}^* = 0.95\ (0.0168) = 0.016$$

$$\rho_f = \frac{A_f}{b X d} = 0.0042$$

$$n_f = \frac{E_f}{E_C} = 1.62$$

$$\rho_f \ n_f = 0.0068$$

Strain in CFRP due to dead load

$$k = \sqrt{(\rho_s\ n_s)^2 + 2(\rho_s\ n_s)} \ - \ (\rho_s\ n_s)$$

$$k = \sqrt{(0.0674)^2 + 2(0.0674)} \ - \ (0.0674)$$

$$k = 0.30588$$

$$c = kd$$

$$c = 0.30588\ (220) = 67.29 mm$$

$$Icr = \frac{bc^3}{3} + n_s A_s (d - c)^2$$

$$I_{cr} = 86877481.024 mm^4$$

$$\varepsilon_{bi} = \frac{Md(h - kd)}{Icr\ E_C}$$

Where bond – dependent coefficient for CFRP system K_m

$$n_f E_f t_f = 1.0\,(38600)(0.89) < 180{,}000$$

$$K_m = \begin{cases} \frac{1}{60\varepsilon_{fu}}\left(1 - \frac{n E_f t_f}{360{,}000}\right) \le 0.9 & \text{for } n E_f t_f \le 180{,}000 \text{ N/mm} \\ \frac{1}{60\varepsilon_{fu}}\left(1 - \frac{90{,}000}{n E_f t_f}\right) \le 0.9 & \text{for } n E_f t_f > 180{,}000 \text{ N/mm} \end{cases}$$

$$K_m = \frac{1}{60\varepsilon_{fu}}\left(1 - \frac{n E_f t_f}{360{,}000}\right) \le 0.9 \quad \text{for } n E_f t_f \le 180{,}000 \text{ N/mm}$$

$$K_m = 0.88 \le 0.9$$

$$\varepsilon_{fe} = \varepsilon_{cu} \frac{(h-c)}{c} \le K_m \varepsilon_{fu}$$

<u>Where:</u>

$c = 0.2d$ (suggested by ACI 440.2R-02)

$$c = 44\text{mm}$$

$$\varepsilon_{fe} = 0.014 \le 0.88(0.016) \text{ (not satisfied)}$$

$$f_{fe} = E_f\, \varepsilon_{fe}$$

$$f_{fe} = 38600\,(0.014) = 540 \text{ MPa}$$

Strain in the reinforcing steel of the beam

$$\varepsilon_s = (\varepsilon_{fe} + \varepsilon_{bi})\frac{(d-c)}{(h-c)} = 0.0119$$

$$f_s = E_s\,\varepsilon_s$$

$$f_s = 2427\text{MPa} \le (f_y) \quad \text{So } (f_s = 420 \text{ MPa})$$

We check suggested "c" by checking equilibrium equation

$$a = \frac{A_s f_y + A_f f_{fe}}{0.85\, f_c' b}$$

$$a = 56.11$$

$$c = a/\beta = 56.11/0.85 = 66 \text{ mm}$$

We revise the calculation and use c = 66 and repeat iteration until equilibrium is achieved

$$\varepsilon_{fe} = \varepsilon_{cu} \frac{(h-c)}{c} \leq K_m\ \varepsilon_{fu}$$

$$\varepsilon_{fe} = 0.008 \leq 0.88(0.016)$$

$$f_{fe} = 38600\ (0.008) = 323 \text{ MPa}$$

$$a = \frac{A_s f_y + A_f f_{fe}}{0.85\, f_c' b}$$

$$a = 47.03$$

$$c = a/\beta = 47.03/0.85 = 55.32 \text{ mm}$$

.

.

.

.

.

.

$$a = 49.50$$

$$c = a/\beta = 49.05/0.85 = 58.27 \text{ mm}$$

$$\varepsilon_{fe} = 0.0098 \leq 0.88(0.016)$$

$$f_{fe} = 38600\ (0.0098) = 381 \text{ MPa}$$

$$\Box M_n = \Box(A_s\, f_y(d - \frac{a}{2}) + \psi_f\, A_{cfrp}\ E_{cfrp}\ \varepsilon_{cfrp}\ (h - \frac{a}{2}))$$

$$\Box M_n = 41.27 \text{ MPa}$$

A.3 Carbon Fiber Reinforced Polymer (Laminate System)

We assume that the beam is interior so the environmental reduction factor C_E form Table 4.1 = 0.95

$$A_f = 1.21\ (100) = 121.0\text{mm}^2$$

$$f_{fu} = C_E f_{fu}^* = 0.95\ (3100) = 2945 \text{ MPa}$$

$$\varepsilon_{fu} = C_E\, \varepsilon_{fu}^* = 0.95\ (0.0085) = 0.00808$$

$$\rho_f = \frac{A_f}{b \times d} = 0.0043$$

$$n_f = \frac{E_f}{E_C} = 6.95$$

$$\rho_f\ n_f = 0.030$$

Where bond – dependent coefficient for CFRP system K_m

$$n_f E_f t_f = 1\ (16500)(1.21) > 180{,}000$$

$$K_m = \begin{cases} \frac{1}{60\varepsilon_{fu}}\left(1 - \frac{n E_f t_f}{360{,}000}\right) \le 0.9 & \text{for } n E_f t_f \le 180{,}000 \text{ N/mm} \\ \frac{1}{60\varepsilon_{fu}}\left(1 - \frac{90{,}000}{n E_f t_f}\right) \le 0.9 & \text{for } n E_f t_f > 180{,}000 \text{ N/mm} \end{cases}$$

$$K_m = \frac{1}{60\varepsilon_{fu}}\left(1 - \frac{90{,}000}{n E_f t_f}\right) \le 0.9 \quad \text{for } n E_f t_f > 180{,}000 \text{ N/mm}$$

$$K_m = 1.133 \ge 0.9 \text{ (Use 0.9)}$$

$$\varepsilon_{fe} = \varepsilon_{cu} \frac{(h - c)}{c} \le K_m\ \varepsilon_{fu}$$

<u>Where:</u>

c = 0.2d (suggested by ACI440.2R-02)

$$c = 44\text{mm}$$

$$\varepsilon_{fe} = 0.014 \leq 0.9(0.00808) \text{ (not satisfied)}$$

$$f_{fe} = E_f \, \varepsilon_{fe}$$

$$f_{fe} = 165000\ (0.014) = 2310 \text{ MPa}$$

Strain in the reinforcing steel of the beam

$$\varepsilon_s = (\varepsilon_{fe} + \varepsilon_{bi}) \frac{(d-c)}{(h-c)} = 0.0119$$

$$f_s = E_s \, \varepsilon_s$$

$$f_s = 2427\text{MPa} \leq (f_y) \text{ So } (f_s = 420)$$

We check suggested "c" by checking equilibrium equation

$$a = \frac{As\, fy + Af\, ffe}{0.85\, fc'b}$$

$$a = 99.26$$

$$c = a/\beta = 99.26/0.85 = 116.78 \text{ mm}$$

We revise the calculation and use c = 116.78 and repeat iteration until equilibrium is achieved

$$\varepsilon_{fe} = \varepsilon_{cu} \frac{(h-c)}{c} \leq K_m \ \varepsilon_{fu}$$

$$\varepsilon_{fe} = 0.0034 \leq 0.9(0.00808)$$

$$f_{fe} = 165000\ (0.0034) = 564.7 \text{ MPa}$$

a = 49.58
c = a/β = 49.58/0.85 = 58.3mm

.
.
.

c = 76.94
$\varepsilon_{fe} = 0.00675 \leq 0.9(0.00808)$
$f_{fe} = 165000\ (0.00675) = 1113$ MPa

$$\phi M_n = \phi(A_s\, f_y(d - \frac{a}{2}) + \psi_f\, A_{cfrp}\, f_{fe}\ (h - \frac{a}{2}))$$

$$\phi M_n = 45.83 \text{ MPa}$$

A.4 Steel Plate

NOMINAL FLEXURAL STRENGTH

A_s = 339 mm²
A_s' = 150 X 3 = 450mm²

$$a = \frac{As\ fy + As'\ fy}{0.85\ fc'b}$$

$$a = 77.97$$

$$c = a/\beta = 77.97/0.85 = 91.73 \text{ mm}$$

$$\square M_n = \square\ (A_s\ f_y\ (d - \frac{a}{2}) + \square\ (A_{sp}\ f_y'(h - \frac{a}{2}))$$

$$\square M_n = \mathbf{57.8\ MPa}$$

A.5 Light Gauge High Tensile Steel

NOMINAL FLEXURAL STRENGTH

A_s = 339 mm²
A_s' = 150 X 0.89 = 133.5 mm²

$$a = \frac{As\ fy + As'\ fy'}{0.85\ fc'b}$$

$$a = 50.77$$

$$c = a/\beta = 50.77/0.85 = 59.73\text{mm}$$

$$\square M_n = \square\ (A_s\ f_y\ (d - \frac{a}{2}) + \square\ (A_{sp}\ f_y'(h - \frac{a}{2}))$$

$$\square M_n = 38.3 \text{ MPa}$$

تقوية الجسور (الكمرات) باستخدام الألياف الكربونية, الحديد الخفيف عالي الشد والحديد الصلب

إعداد
عمر محمد علي ملكاوي

المشرف
الأستاذ الدكتور دياسر حنيطي

ملخص

ما زال تقوية المنشىءات يشكل تحديا كبيرا, ولتجاوز هذه المشكلة تم استخدام أنواع مختلفة من مواد التقوية, الهدف من هذا البحث التأكد من أداء ثلاث مواد من مواد التقوية الخارجية (الألياف الكربونية, حديد الخفيف عالي الشد والحديد الصلب), بالإضافة الى تحسين وتطوير الجزء النظري من نظام التقوية.

البحث يتكون من 15 جسر (كمرة) قسمت الى أربع مجموعات, المجموعة الأولى تتكون من جسرين بدون أي تقوية خارجية وتسمى كمرة التحكم والجزء الثاني يتكون من خمسة كمرات بتقوية خارجية من الألياف الكربونبة بالإضافة إلى أربع كمرات بتقوية خارجية من الحديد الخفيف عالي الشد وأخيرا أربع كمرات مقوية باستخدلم الحديد الصلب.

وتبين أن استخدام الألياف الكربونية في التقوية الخارجية للكمرات أعطى نتائج جيدة مقارنة مع وزن المادة.